

Cropland abandonment is largely fleeting, limiting its potential environmental benefits

Christopher L. Crawford^{a,1}, He Yin^b, Volker C. Radeloff^c, and David S. Wilcove^{a,d}

^aPrinceton School of Public and International Affairs, Princeton University, Princeton, NJ; ^bDepartment of Geography, Kent State University, Kent, OH; ^cSILVIS Lab, Department of Forest & Wildlife Ecology, University of Wisconsin - Madison, Madison, WI; ^dDepartment of Ecology & Evolutionary Biology, Princeton University, Princeton, NJ

This manuscript was compiled on September 2, 2021

1 Agricultural expansion is a major cause of land-use change globally,
2 yet tens of millions of hectares of cropland have been abandoned since 1950 due to demographic, economic, and environmental
3 changes. These abandoned croplands could be valuable for carbon
4 sequestration and biodiversity restoration. However, their environmental
5 value depends on the duration and persistence of abandonment, which is poorly known.
6 Here, we quantify the duration and persistence of cropland abandonment at eleven sites on four continents using 30-m annual land cover maps for the years 1987 through
7 2017. We find that abandonment is generally fleeting, lasting on average only 14.42 years (SD = 1.52). At most sites, we project that
8 >50% of abandoned croplands will be recultivated within 25 years,
9 and sites in Eastern Europe, Russia, and the US show accelerating
10 rates of recultivation. If current rates of abandonment and recultivation continue,
11 the mean duration of abandonment at most sites will plateau between 10 and 22.3 years by 2040. Counter to optimistic
12 assumptions, most abandonment is unlikely to be permanent and will
13 produce limited benefits for carbon sequestration and biodiversity
14 conservation. New policies and incentives are needed to lengthen the
15 period of abandonment in order to generate such benefits. Until then,
16 abandoned croplands will remain an untapped opportunity.

Agriculture | Cropland abandonment | Rural land abandonment | Biodiversity conservation | Secondary succession | Carbon sequestration | Land-cover mapping

1 Human populations are in flux around the world, as people seek new economic opportunities in cities and flee changing environments and conflicts (1). Coupled with environmental degradation and changing agricultural technologies, urbanization and rural outmigration have contributed to decreasing economic viability of many agricultural lands and a growing global trend of cropland abandonment (2, 3). Given increasing competition for land, these abandoned croplands have been targeted for diverse goals such as biofuel production (4), carbon sequestration (5, 6), biodiversity and ecosystem restoration (7–9), or simply recultivation (10).

11 Millions of hectares of agricultural lands have been abandoned since 1950 (11), with abandonment predicted to continue in many places (1, 12), but for how long and to what end remains unclear. Understanding the environmental effects of agricultural abandonment requires detailed information on not only where and when abandonment takes place, but also on what happens to croplands after they are abandoned. In order for abandoned lands to yield environmental benefits, these lands must stay abandoned long enough to acquire appreciable gains in both plant biomass and the species that make up intact ecological communities. It can take many decades to approach the levels of carbon sequestration or biodiversity typical of many intact ecosystems, with species recolonizing at different successional stages (13–19). Knowing how long aban-

donment persists is thus critical to understanding its potential to help mitigate the ongoing climate and biodiversity crises.

Until recently, it has been difficult to gather detailed information on abandonment. Many estimates of abandonment are inferred by aggregating regional estimates of cultivation, such as country-level FAO data on cultivated areas (15, 20). When derived from satellite imagery, abandonment is most frequently estimated by simply taking the difference in cultivated area between land cover maps for two time points (e.g., 1992 and 2015, ref. 4). Annual land-cover time series are becoming more common, but are typically limited to a few years (e.g., 2–12 years, refs. 21–23) or are coarse in resolution (e.g., ≥ 250-m, refs. 4 and 22), and most analyses are restricted to a single region (24). These approaches all lack the spatial and temporal detail needed to understand long-term outcomes for individual croplands. By failing to capture the dynamic patterns of abandonment and recultivation, scientists may substantially overestimate abandonment and the potential for associated benefits (25).

Empirical evidence for secondary forests in the Neotropics shows that forest regeneration is often short-lived (26–29). For example, in the Brazilian Amazon, half of secondary forests were recleared in 5 to 8 years (6, 27, 30), and in southern Costa Rica in ≤ 20 years (26). However, estimates based on the growth of woody vegetation miss abandonment in earlier stages of regeneration and in biomes where succession does

Significance Statement

Demographic, economic, and environmental changes often cause cropland abandonment. While sometimes a threat to food security and cultural landscapes, abandonment also provides a vast opportunity for carbon sequestration and habitat restoration. However, those environmental benefits depend on how long ecosystems are allowed to regenerate and accumulate carbon and biodiversity following abandonment. Existing studies have often relied on single snapshots in time to estimate abandonment, and ignore recultivation. Using annual land-cover maps, we tracked abandonment and recultivation at eleven sites across four continents. Abandonment was short-lived, with most abandoned croplands being recultivated within three decades. Unless policymakers take steps to reduce recultivation or provide incentives for regeneration, abandonment will remain a missed opportunity to reduce biodiversity loss and climate change.

Please provide details of author contributions here.

The authors declare no conflicts of interest.

¹ To whom correspondence should be addressed. E-mail: ccrawford@princeton.edu

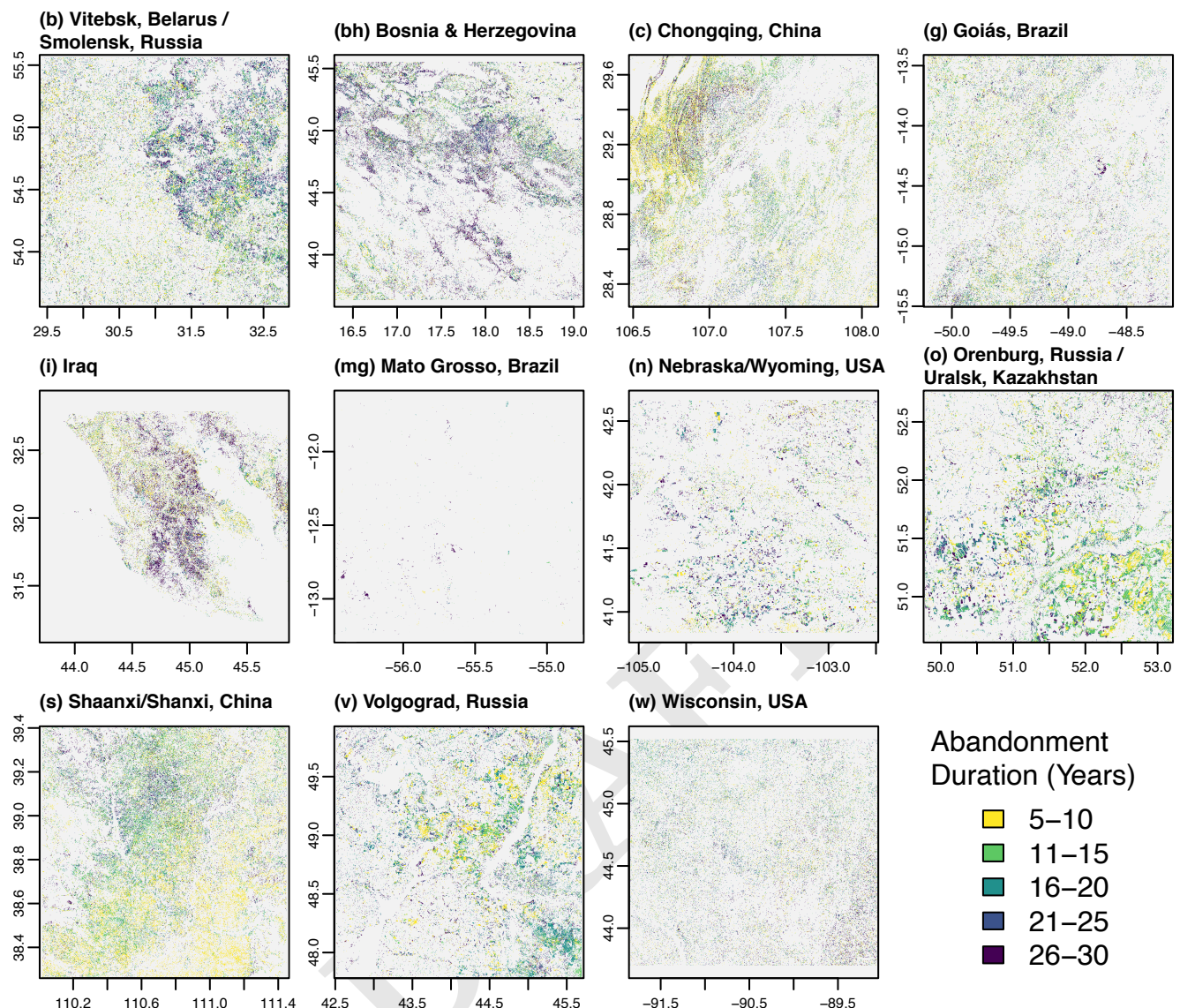


Fig. 1. Observed duration of cropland abandonment (in years) as of 2017 in our eleven study sites. Site locations are shown in Figure S1, and maps of maximum abandonment duration are shown in Figure S7.

not lead to woody vegetation (25).

Recent advances in remote sensing have made it possible to produce maps of cropland abandonment at both high spatial and temporal resolution. Yin et al. (25) used a trajectory-based approach to produce accurate maps of annual cropland abandonment at 30-m resolution from 1987 to 2017 without relying on woody revegetation as a proxy of abandonment, thereby allowing for a direct measurement of abandonment in both forest and non-forest biomes. Here, we utilize these new annual time-series of cropland abandonment (25) to investigate the duration and persistence of abandonment at eleven sites across four continents, including in Brazil, the United States, Eastern Europe, Russia, the Middle East, and China (Figure 1).

We address three questions: How long does abandoned cropland stay abandoned (i.e., duration of abandonment), and how does this vary geographically? How quickly is abandoned land recultivated (i.e., persistence of abandonment), and do

recultivation (or “decay”) rates vary through time? Finally, if abandonment and recultivation continue at current rates, what will ultimately be the mean age of abandoned croplands?

By making use of new, more accurate, and finer resolution abandonment maps for eleven sites across the globe, and by covering a longer period and a broader set of sites than previous studies, we provide the most detailed analysis to date of the duration and persistence of cropland abandonment. Given that some abandonment periods are inherently limited by the length of our time series (and may remain abandoned beyond the three decades covered by our data), tracking recultivation rates for each year provides a more accurate understanding of persistence. Our results reveal the temporal nature of cropland abandonment and its potential to sequester carbon and conserve biodiversity.

Results

Abandonment duration. Cropland abandonment was widespread across our eleven study sites. We detected 8.36 million ha (Mha) of croplands that were abandoned at least once between 1987 and 2017 across our eleven sites. (To exclude normal fallow periods, we only classify croplands as “abandoned” when they have not been cultivated for at least five contiguous years; see Materials and Methods.) This corresponds to 35.22% of the total cropland extent of 23.74 Mha (i.e., all lands that were cultivated at some point during the time series). At individual sites, the area of cropland abandoned at least once ranged from 25.25% (Wisconsin, USA) to 56.16% (Vitebsk, Belarus/Smolensk, Russia) of the total cropland extent (Figures S2 and S3), except for Mato Grosso, Brazil, where only 0.98% was abandoned at least once (see Section S1.A.).

However, we also found that many of these abandoned croplands were recultivated: 37.77% of abandoned area had been recultivated as of 2017, on average across sites ($SD = 8.9\%$; Figure S11). In fact, only 5.73 Mha of croplands remained abandoned as of 2017 across our sites (Figure 1). This corresponded to 24.15% of the total cropland extent overall, ranging from 17.86% (Nebraska, USA) to 41.06% (Bosnia & Herzegovina) at individual sites. Accordingly, the mean duration of abandonment across all sites was short: 14.42 years ($SD = 1.52$), ranging from 12.86 years (Orenburg, Russia/Uralsk, Kazakhstan) to 17.7 years (Bosnia & Herzegovina; Figure 2). Abandonment duration also varied substantially within sites, with individual site standard deviations ranging between 6.95 (Orenburg/Uralsk) and 9.21 years (Mato Grosso) (for an average of 7.78 years across all sites).

Modeling abandonment decay & recultivation. We developed models to predict how long a given pixel of abandoned cropland will remain abandoned before it is recultivated, regardless of when it was abandoned during the time series. These models also allow us to calculate the mean recultivation (or “decay”) trajectory at each site (Figure 3). To do so, we defined a cohort of abandoned cropland as all cropland abandoned in a given year at a given site. We modeled the proportion of each cohort remaining abandoned as a function of time since initial abandonment (see Figure 4, Materials and Methods).

Recultivation occurred quickly: we predict that >50% of abandoned croplands will be recultivated within 25 years of initial abandonment at almost all sites (Figure 4). At individual sites, the half-life (defined as the time required for half of the croplands abandoned in a given year to be recultivated) ranged from 12 years (Orenburg/Uralsk) to 24 years (Wisconsin). Shaanxi/Shanxi (China) was a notable exception; here our models predicted a half-life of 48 years, and 137 years for complete turnover (defined as the time required for all abandonment in a given cohort to be recultivated; Figure 3). For comparison, complete turnover took 21 and 61 years respectively in Orenburg/Uralsk and Wisconsin. The mean decay trajectories also display wide variation in the percentage of abandoned croplands that persist beyond 20 years: as little as 7.46% in Orenburg/Uralsk, while up to 70.9% in Shaanxi/Shanxi.

By modeling recultivation for each abandonment cohort, we investigated whether recultivation of abandoned cropland accelerated. Most sites showed a negative trend in the time until recultivation, indicating that abandoned croplands were being recultivated more quickly in recent years (Figure S18).

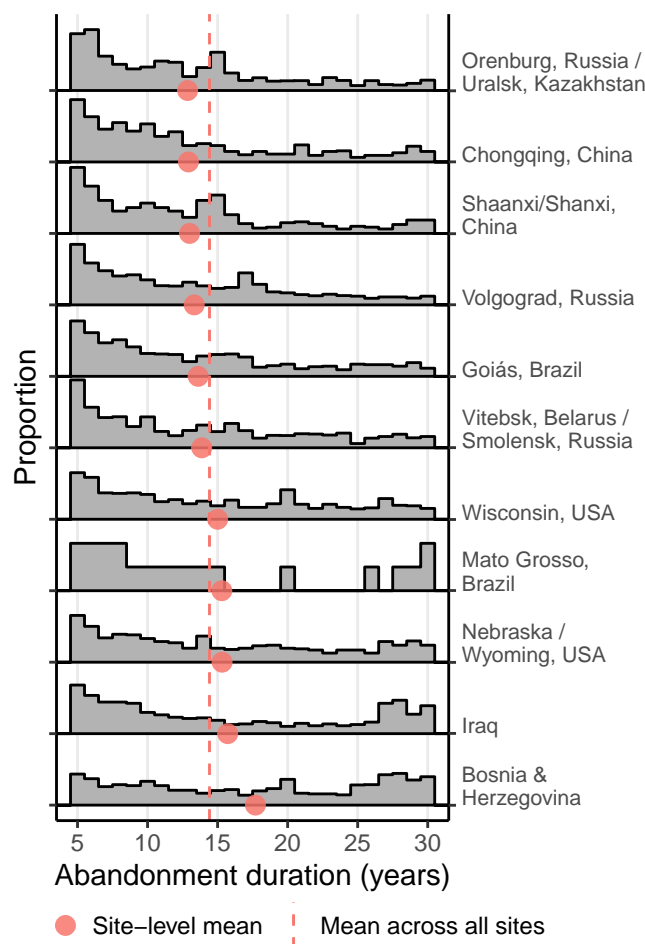


Fig. 2. The distribution of abandonment duration (in years) for all periods of abandonment from 1987 to 2017. The y-scale shows the proportion of abandonment periods of a given duration at each site. The red points represent the mean abandonment duration (in years) at each site, and the red vertical dashed line represents the mean of these site-level mean duration values across all sites. Note that these distributions include multiple periods of abandonment for those pixels that experienced abandonment and recultivation multiple times during the time series. See Figure S6 to view distributions of the maximum abandonment duration for each pixel.

Based on a linear regression on the half-life (the time required for 50% recultivation), over half of our sites had rates of change that were significantly different from zero and negative, corresponding to recultivation accelerating through time: Bosnia & Herzegovina, Volgograd (Russia), Wisconsin, Nebraska, Orenburg/Uralsk, and Iraq (Figure S18). The remaining sites had trends that were not significantly different from zero.

Projecting future abandonment and recultivation. Assuming that abandonment rates and recultivation rates remain constant at each site, our projection suggests that the impermanence of abandonment we observe is not an artifact of our time series being only 30 years long. We project the mean duration of abandonment to plateau at 20 years or less at most sites (Figure S22), with the notable exception of Shaanxi/Shanxi, which is projected to plateau at a mean duration of 46 years. The time required to plateau depends on the time required for complete turnover, ranging from 21 to 61 years for all sites except Mato Grosso (110 years) and Shaanxi/Shanxi (137 years).

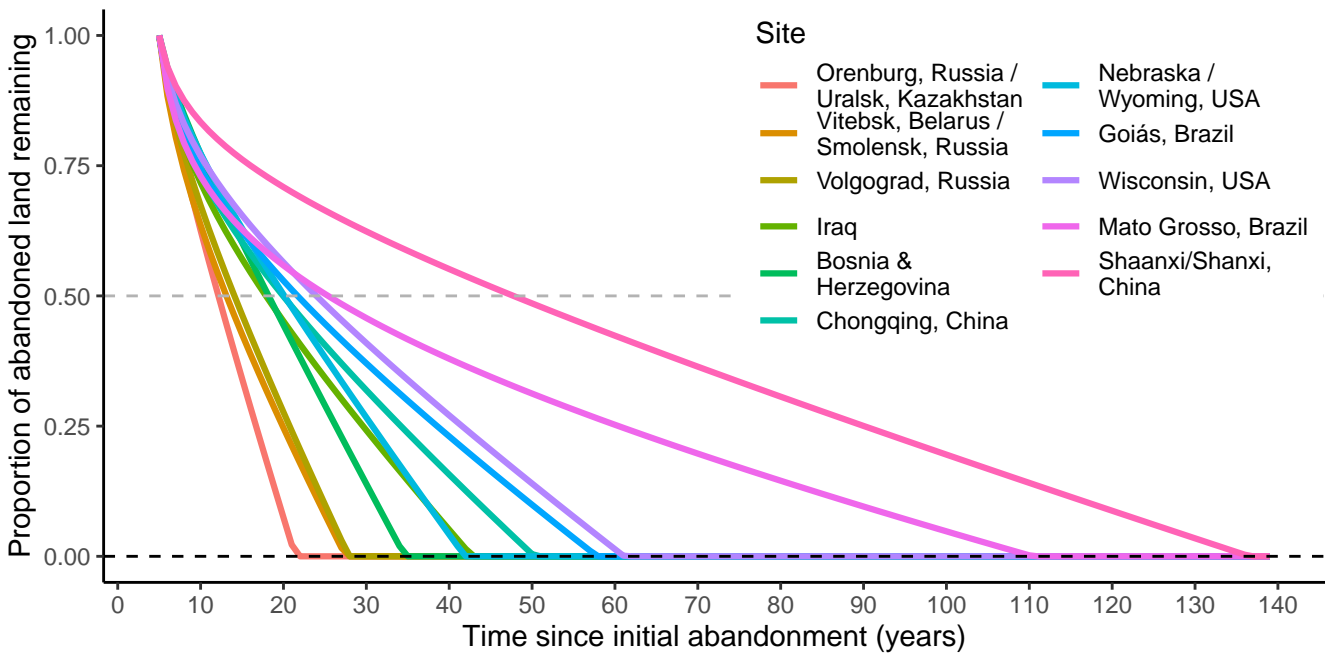


Fig. 3. Mean decay trajectories for each site, based on a linear model predicting the proportion of abandoned land remaining abandoned as a function of time (including a linear and a logarithmic term of time). The function describing each site's mean trajectory is calculated by taking the mean of each time coefficient across all cohorts of abandonment at each site. The light gray dashed line at a proportion of 0.50 indicates the half-life at each site, defined as the time required for half of the croplands abandoned in a given year to be recultivated.

165 years).

166 Furthermore, we project that only a relatively small pro-
167 portion of abandoned croplands will persist beyond 30 years
168 (<27% at most sites; Figure S23). Even in Shaanxi/Shanxi,
169 the site we project will have the most long-lasting abandon-
170 ment, only 40% of abandoned land will remain so for longer
171 than 50 years.

172 Discussion

173 Using a new detailed, annual land-cover time series, we found
174 substantial amounts of cropland abandonment from 1987 to
175 2017 in eleven sites on four continents: 35.22% of all lands
176 that were cultivated during our time series were abandoned
177 at least once between 1987 and 2017. However, we also found
178 substantial levels of recultivation, so that only 24.15% of total
179 cropland remained in an abandoned state as of 2017. On aver-
180 age abandonment lasted only 15 years, and 37% of abandoned
181 croplands had been recultivated by 2017. Furthermore, some
182 sites had accelerating rates of recultivation, and even the sites
183 with the most persistent abandonment are unlikely to remain
184 uncultivated for ≥ 50 years. Our modeled decay rates portray
185 a dynamic process, where abandonment is rarely an endpoint
186 but rather part of a cycle of turnover on decadal timescales
(20).

187 By tracking cohorts of abandoned croplands based on the
188 year of abandonment, we developed a much more detailed and
189 nuanced picture of abandonment persistence than previous
190 studies. For example, while Shaanxi/Shanxi had one of the
191 shortest mean abandonment durations (because most aban-
192 donment took place towards the end of the time series), current
193 recultivation trajectories indicate more persistent aban-
194 donment than we can observe during the time series. Our models

195 revealed Shaanxi/Shanxi to have the longest half-life and com-
196 plete turnover time, due to a decrease in recultivation rates
197 over time. In contrast, Bosnia & Herzegovina, which had the
198 longest mean abandonment duration, experienced accelerat-
199 ing recultivation in recent years, limiting future persistence.
200

201 Furthermore, estimates of abandonment based on short
202 time series or two points in time (e.g., 83 Mha estimated in ref.
203 4) likely overestimate the amount of persistent abandonment,
204 due to both a failure to exclude short-term fallow periods,
205 and, as our analysis shows, high rates of recultivation. When
206 estimating abandonment at our sites based on cultivation
207 in two points in time (1987 and 2017), we find 5 Mha of
208 “abandonment,” a 12.74% underestimate compared to the
209 5.73 Mha of abandonment as of 2017 identified using our full
210 annual time series. This corresponds to site-level estimates that
211 ranged from 39.75% less (Goiás, Brazil) to 83.29% more (Mato
212 Grosso) area abandoned than the area identified using the
213 full time series. Moreover, the two-year assessments identify
214 different areas of abandonment from those derived from our
215 full annual time series, with spatial agreement ranging from
216 28.08% (Mato Grosso) to 66.3% (Bosnia & Herzegovina) (see
217 Table S2, Section S1.D.).

218 The abandonment and impermanence that we found gener-
219 ally matches that observed in the few other comparable case
220 studies (6). To the best of our knowledge, the only other study
221 that uses an annual time series to investigate agricultural
222 abandonment (in a grassland region of northern Kazakhstan
223 between 1991–2017; ref. 24), observed abandonment of about
224 40% of cultivated areas, and the subsequent recultivation of
225 about 20% of that abandonment. This recultivation rate was
226 similar to our most persistent site (Shaanxi/Shanxi), but lower
227 than both our average recultivation rate across sites (37.77%),

228 and in our sites closest to Kazakhstan: Orenburg/Uralsk and
229 Volgograd, which had higher recultivation rates of 43.34% and
230 45.52% respectively (Figure S11).

231 Our projected half-lives of 12-24 years at most sites were
232 similar to those found in Costa Rica (20 years, ref. 26), but
233 slightly longer than in other parts of the Neotropics (6, 27, 28).
234 Secondary forests were recleared more quickly in the Brazilian
235 Amazon (50% within 5 to 8 years), where 80% of secondary
236 forests were \leq 20 years old (6, 27, 28). Across the tropics,
237 only 33% of forests regenerating after recent deforestation
238 were \geq 10 years (31). However, these differences may be the
239 result of 1) a time delay between abandonment and sufficient
240 regrowth of secondary woody vegetation to be detected by
241 satellites, 2) our exclusion of abandonment of less than five
242 years, or 3) our models of recultivation for each cohort, which
243 eliminate the influence of the time series length, and lengthen
244 abandonment estimates.

245 **Implications for biodiversity recovery and carbon sequestra-**
246 **tion.** Our results show that most cropland abandonment is
247 unlikely to be long-lasting, contrary to optimistic assumptions
248 (4, 32). The high recultivation rate we observed will dramatically
249 limit the scope for abandoned croplands to play a major
250 role in carbon sequestration or the recovery of biodiversity.

251 There is, of course, substantial variability in how quickly
252 and how completely ecosystems recover following disturbances
253 and abandonment (33–35). Natural regeneration can be a viable
254 restoration strategy under the right conditions, especially
255 after low-intensity disturbances (e.g., selective logging) and
256 when there are relatively undisturbed or mature ecosystems
257 nearby to act as propagule sources. Under such conditions,
258 plant and animal dispersal can result in secondary growth that
259 can approach the habitat and carbon values of undisturbed
260 ecosystems (17, 34, 35).

261 However, even under optimal conditions, recovery requires
262 time, typically multiple decades, in order to recover species
263 richness to values approximating those in reference systems (7,
264 14–16, 36). Species richness values for rarer, forest-adapted,
265 and old-growth dependent species recover even more slowly.
266 Importantly, when recovery towards old-growth ecosystems is
267 measured in terms of community composition, species similarity,
268 and vegetation structure, it can take much longer than
269 when measured simply by the recovery of total species richness
270 or abundance (which can be dominated by widespread
271 generalist species) (34–37).

272 In some cases species-rich tropical ecosystems can regenerate
273 quickly, but never on a time scale as short as the abandonment
274 durations we observe here. Chronosequences show that lowland
275 Neotropical forests recover quickly in terms of tree species
276 richness (reaching 80% of old-growth levels after
277 20 years, 90% after 31 years), but much more slowly in terms
278 of tree species composition (34% of old-growth levels after
279 20 years, requiring 487 years to reach 90%) (13). The area
280 around these sites retained relatively high forest cover (76%
281 on average), however, and recovery is likely to be slower in
282 more deforested landscapes (13).

283 Recovery can be rapid for certain animal groups in specific
284 cases (e.g., birds and dung beetles in the Colombian Andes;
285 ref. 17), but typically takes a long time for most types of
286 vertebrate species. Across tropical forests, amphibian, bird,
287 mammal, and reptile species richness largely recovers within 40
288 years, but species compositional similarity for these vertebrate

289 groups takes much longer to recover (if at all), particularly for
290 late-successional species, insectivorous birds, and forest specialists (14).
291 No vertebrate groups reach species compositional similarity to reference old-growth forests, even in the oldest
292 secondary forests (30–65 years) (14).

293 Grassland ecosystems can sometimes recover more quickly
294 following disturbances than forests (38), but not often (15,
295 16). On average, secondary grasslands distributed around the
296 world that are between 1–251 years old contain only 53–76%
297 of the plant species richness of never-cultivated (i.e., undisturbed)
298 grasslands (16). Even after full recovery of species
299 richness (with minimum estimated recovery times of >100
300 years), compositional similarity of secondary grasslands to
301 undisturbed grasslands remains low (43%). Similarly, Minnesota
302 (USA) grasslands showed quick initial gains in bio-
303 diversity following abandonment, but both biodiversity and
304 productivity increased slowly after the first year, reaching only
305 73% of the diversity and 53% of the productivity levels of the
306 reference ecosystem after 91 years (15). Eurasian grasslands,
307 where widespread abandonment has occurred, had not fully
308 recovered with respect to either plant species richness or com-
309 munity composition after 24 years of observation (39), nor
310 with respect to bird species richness and diversity after 18
311 years of observation (40).

312 Abandoned croplands also only achieve a small fraction of
313 their carbon storage potential if abandonment lasts only a couple
314 of decades. Despite relatively quick accumulation of carbon
315 in aboveground biomass in forests over the first few decades of
316 regeneration, it can take between 50–100 years for secondary
317 forests to achieve similar levels of biomass as old-growth forests
318 (19, 41). For example, Neotropical aboveground forest biomass
319 reaches 90% of old-growth forest biomass after a median of
320 66 years, but <50% biomass after 20 years. Furthermore,
321 carbon accumulation estimates vary by biome and by prior
322 land use. Based on estimates of potential aboveground carbon
323 accumulation rates during the first 30 years of natural regenera-
324 tion in different biomes (18), we predict that the abandoned
325 cropland areas that we studied could accumulate 30–70 Mg
326 C/ha in aboveground biomass total over 20 years, or 18%–45%
327 of the 110–250 Mg C/ha total that could be accumulated in
328 aboveground biomass over 100 years (18).

329 Grassland biomes, where much of the abandonment we
330 observed occurred, can also harbor substantial amounts of
331 carbon sequestered in soils (42). However, grassland soil
332 carbon may accumulate even more slowly than aboveground
333 forest biomass, taking a century or longer to return to reference
334 levels (43). For example, while abandoned croplands across
335 Russia accumulated a total of 13.2 Mg C/ha in the top 5
336 cm of soil during the first 20 years following abandonment,
337 these fields still had significantly less carbon sequestered than
338 reference grasslands after 24 years of observation, and were
339 expected to take >60 years to recover to reference levels (44).

340 Moreover, beyond the issue of the duration of aban-
341 donment, the very fact that these lands were used for agriculture
342 can impede full achievement of carbon or biodiversity goals.
343 The degradation and slow recovery of soils, a lack of nearby
344 source populations, a lack of natural disturbance regimes, and
345 climate change all pose obstacles to successful recovery of
346 stored carbon or biodiversity (34, 45, 46). While natural re-
347 generation is typically cheaper and sometimes more successful
348 than active restoration, more heavily altered systems typically
349

require more active approaches such as invasive species control or translocation of plants and animals, along with longer recovery times (17, 36, 43, 47). Grassland regeneration is particularly challenging, because many grasslands require natural disturbance regimes (e.g., grazing or fire), which may be absent following abandonment (16). Without such disturbances, grassland biodiversity can be lost if low-intensity farmlands are abandoned, particularly in historically unforested ecosystems (2, 16, 48, 49).

Conclusions

We found strong evidence that abandoned croplands did not remain uncultivated for long periods of time at eleven sites across the globe. Without new policies and incentives to discourage recultivation, abandoned areas are unlikely to provide meaningful biodiversity and carbon benefits. Our results reinforce growing calls for enhanced monitoring of regeneration after abandonment (50), and the development of a stronger policy framework for managing such lands (7). In some cases, active management of abandoned sites will be needed to achieve biodiversity and carbon goals.

There are a range of socioeconomic and political barriers hindering habitat regeneration in abandoned croplands. These include policies that obligate farmers to cultivate land, a lack of incentives to protect and foster regenerating habitats, and perhaps most importantly, negative cultural perceptions of “abandonment” and the “messy” landscapes that result (7). Agricultural abandonment is a consequence of complex societal changes, and the emotional distress associated with the loss of certain types of landscapes and rural ways of life can be substantial (2, 10, 11, 20). Behavioral research into farmer decisions to recultivate abandoned croplands highlights the importance of addressing factors such as corruption, political and institutional support for agriculture, and demographics, alongside biophysical and environmental conditions, when managing abandonment (51).

In order for abandoned croplands to provide environmental benefits through habitat regeneration or carbon sequestration, they must persist for longer periods than we observed. This could be achieved by designating abandoned fields as protected areas, incorporating natural regeneration into payments for ecosystem service programs to allow landowners to benefit economically, or by taking steps to support sustainable long-term cultivation of some sites, thereby reducing turnover among fields that have previously been part of long-term fallowing cycles. As a case in point, the relative durability of abandonment at Shaanxi/Shanxi may be due to large-scale ecosystem restoration programs that began in the late 1990s and created economic incentives to reforest croplands. This is encouraging, even though there continues to be a need to improve the biodiversity outcomes of such programs (52). We stress that any policies should be developed jointly with local communities to address trade-offs between biodiversity, carbon storage, and livelihoods.

Our results make one thing clear: if cropland abandonment continues to be as short-lived as we show here, the large potential benefits of regenerating habitats to both store carbon and sustain biodiversity will remain an untapped opportunity.

Materials and Methods

Abandonment maps. We use annual land cover maps with 30-m resolution from 1987-2017 (25), derived from publicly available Landsat satellite imagery, mapping four land cover classes: 1) cropland, 2) herbaceous vegetation (e.g., grassland), 3) woody vegetation (e.g., forests), and 4) non-vegetation (e.g., water, urban, or barren land). Our eleven sites were mapped with high accuracy (average overall accuracy $85 \pm 4\%$) and provide broad coverage of different continents and ecosystems (Figure 1). We focused exclusively on cropland abandonment, because pasture abandonment is very difficult to discern from satellite imagery and is not captured in our data. Yin et al. (25) selected sites where recent abandonment was documented and likely given socioeconomic, political, or environmental conditions. Thus, while our results are likely representative of those areas that have recently experienced abandonment, they are not a representative sample for the globe, and overestimate the overall prevalence of abandonment.

Defining abandonment. Differentiating abandonment from short-term fallowing or crop rotations is difficult because agricultural practices can vary widely by region, and studies use many different definitions (25). Here, in order to exclude short-term fallowing, we define “abandonment” as cropland that is no longer under active cultivation, is left free of direct human influence (e.g., is not converted to urban land use), and remains so for at least five subsequent years, following FAO (53). Recognizing that longer abandonment thresholds may be more appropriate in certain contexts, we performed a sensitivity analysis by varying our abandonment definition (Section S1.C.) and found that, as expected, longer definitions resulted in less abandonment over all, longer average abandonment durations (Figure S10), and lower recultivation rates (Figure S11). However, even when only considering abandonment ≥ 10 years, we still observed between 11.61% and 30.37% recultivation across our sites (in Shaanxi/Shanxi and Volgograd respectively), suggesting the reliability of our abandonment definition.

Data processing. We processed and analyzed abandonment map data in RStudio version 1.4.1717 (54), using R version 4.1.0 (2021-05-18), primarily with the `raster` (55), `data.table` (56), and `tidyverse` (57) packages.

We identified periods of cropland abandonment by tracking each pixel’s land cover through time and looking for land-cover changes that indicated transitions between cultivation and abandonment. We first implemented five- and eight-year moving window temporal filters to smooth land-cover trajectories and remove land-cover changes that are temporally unlikely (Section S2). Together with our five-year abandonment threshold, these temporal filters address very short-term misclassifications that might otherwise appear like recultivation.

We classified a pixel as “abandoned” anytime it transitioned from cropland to either herbaceous or woody vegetation (collectively referred to as “non-cropland”) and subsequently remained classified as non-cropland for five or more consecutive years. We considered an abandoned pixel to be “recultivated” when it transitioned from abandoned to cropland. Pixels that transitioned from cropland to the non-vegetation class were not considered “abandoned,” and were excluded from our analysis. Non-vegetated land consisted of <10% of total site area in all sites except Shaanxi (12.7%) and Iraq (52.8%), and remained

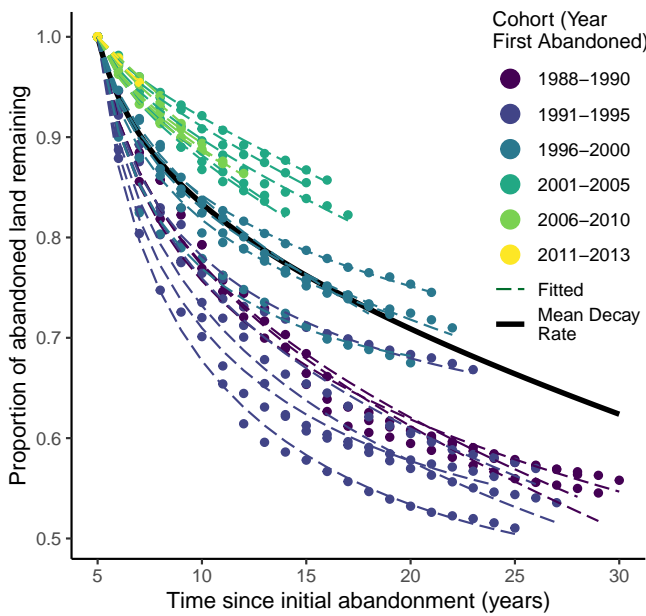


Fig. 4. Recultivation (decay) of abandoned land in Shaanxi/Shanxi (China), showing the proportion of each cohort of abandoned land (i.e., all pixels abandoned in a given year) remaining abandoned over time. Points represent actual observations by cohort, dashed lines represent linear model predictions (fitted values) for each cohort as a function of time (including a linear and logarithmic term of time), and the solid black line represents the mean trend across all cohorts (calculated by taking the mean of each time coefficient value across all cohorts). Colors of both points and dashed lines correspond to roughly five-year group of cohorts, ranging from dark purple (oldest cohorts) to green and yellow (most recent cohorts). See Figure S12 for model results for all sites.

Information Criterion values (AIC; Figure S13). For cohorts of abandonment initially abandoned in years $y = 1988, \dots, 2013$, our model predicted the proportion p of each cohort y remaining abandoned as a function of time t (i.e., the number of years following initial abandonment), with one log-transformed and one linear term of time (Equation Eq. (1)).

$$p_y = 1 + \beta_{1,y} \log(t + 1) + \beta_{2,y} t \quad [1]$$

Where $\beta_{1,y}$ and $\beta_{2,y}$ represent the regression coefficients on the log and linear terms of time t , respectively, for cohort y . Model assumptions were tested through visual inspection of diagnostic plots (Figures S14 and S15, full details in Section S2.C.). We calculated each site's mean recultivation trend by taking the mean of the model coefficients across all cohorts (Figure 2). Modeled decay trajectories are shown for one example site, Shaanxi/Shanxi (China), in Figure 4, and model coefficients for all sites in Figure S16.

To estimate changes in persistence over time, we calculated the time required for half of a given cohort to be recultivated based on the modeled recultivation trajectory of each cohort. We parameterized a linear model on this value for each cohort to identify temporal changes in recultivation patterns at each site (Section S2.D.). Trends were considered statistically significant when the 95% confidence interval for model coefficients did not include zero (Figure S18).

Projecting future abandonment and recultivation. Based on our modeled decay rates, we project abandonment and recultivation in the future based on two assumptions: (1) a constant amount of cropland is newly abandoned each year, based on the mean area of cropland abandoned each year at each site (Figure S5); and (2) all abandoned croplands are recultivated at the mean predicted rate for each site (Figure 3). Total abandonment in our projection remained below the total cropland extent at each site. We also considered an alternative assumption in which annual abandonment linearly declined to 0 between 2017 and 2050, but found similarly short mean abandonment durations (below 37 years at all sites by 2050; see Figures S24 and S25). While mean age of abandoned land increased through time after 2017 (and most dramatically after 2050), it remained below 37 years at all sites by 2050. Increases in mean abandonment duration were offset by recultivation, and total area abandoned declined quickly after 2020 at most sites. See details in Section S2.E.

Data Availability Statement

The annual land cover maps that underly our analysis are archived at Zenodo (URL TBD), along with other datasets generated and analyzed for this article (including maps of abandonment age and datasets summarizing area, persistence, and turnover). Code to replicate these analyses is available on GitHub at https://github.com/chriscra/abandonment_trajectories, and is archived at Zenodo (URL TBD).

Supporting Information

Supporting Information for this manuscript can be found [here](#).

ACKNOWLEDGMENTS. We thank the following researchers at the University of Wisconsin-Madison, whose land cover maps made our analysis possible, and who generously shared their data: Amintas Brandão, Johanna Buchner, David Helmers, Benjamin

stable or declined over time in all eleven sites.

Calculating abandonment duration. We calculated abandonment duration as the number of years that elapsed between the initial transition from cropland to non-cropland, and either recultivation or the end of the time series. Because our abandonment definition only considers croplands that have been abandoned for five or more contiguous years, the minimum abandonment duration is five years. Because a pixel may be abandoned and recultivated multiple times throughout the time series, we calculated the mean abandonment duration in two ways: 1) across all periods of abandonment (Figure 2), and 2) across only the longest period of abandonment experienced by each pixel (Figures S6 and S7).

Modeling abandonment decay. Because some abandonment periods are limited by the length of the time series, we modeled recultivation of abandoned croplands as a function of time since initial abandonment. We tracked recultivation (“decay”) by calculating the proportion of each cohort of pixels abandoned in a given year that remain abandoned in each year following abandonment. We parameterized linear models predicting the proportion of abandoned cropland in each cohort remaining abandoned as a function of time since initial abandonment. We tested a range of model specifications, including linear and log transformations of both proportion and time, and multiple time predictor terms. Importantly, we included cohort level fixed effects, fitting unique coefficients for each cohort at each site.

We selected the highest performing model based on Akaike

- 552 G. Iuliano, Niwaeli E. Kimambo, Katarzyna E. Lewińska, Elena
 553 Razenkova, Afag Rizayeva, Natalia Rogova, Seth A. Spawn, and
 554 Yanhua Xie. We are deeply indebted to Alex Wiebe, whose sta-
 555 tistical advice significantly improved our models of abandonment
 556 decay and recultivation. We also thank the Drongos research group
 557 for advice and companionship. This work was supported by the
 558 High Meadows Foundation and the NASA Land Cover and Land
 559 Use Change Program (Grant no. 80NSSC18K0343) and analyses
 560 were performed using Princeton Research Computing resources at
 561 Princeton University. This research contributes to the Global Land
 562 Programme (<https://glp.earth/>). 598
- 563 **References**
- 564 1. Sanderson EW, Walston J, Robinson JG (2018) From Bot-
 565 tleneck to Breakthrough: Urbanization and the Future of
 566 Biodiversity Conservation. *BioScience* 68(6):412–426. 599
- 567 2. Rey Benayas J, Martins A, Nicolau JM, Schulz J (2007) Abandonment of agricultural land: an overview of drivers
 568 and consequences. *CAB Reviews: Perspectives in Agriculture, Veterinary Science, Nutrition and Natural Resources* 2(057). doi:[10.1079/PAVSNNR20072057](https://doi.org/10.1079/PAVSNNR20072057). 600
- 569 3. Prishchepov AV, Schierhorn F, Löw F (2021) Unraveling the Diversity of Trajectories and Drivers of Global Agricultural Land Abandonment. *Land* 10(2):97. 601
- 570 4. Næss JS, Cavalett O, Cherubini F (2021) The land–energy–water nexus of global bioenergy potentials from abandoned cropland. *Nature Sustainability*. doi:[10.1038/s41893-020-00680-5](https://doi.org/10.1038/s41893-020-00680-5). 602
- 571 5. Griscom BW, et al. (2017) Natural climate solutions. *Proceedings of the National Academy of Sciences* 114(44):11645–11650. 603
- 572 6. Chazdon RL, et al. (2016) Carbon sequestration potential of second-growth forest regeneration in the Latin American tropics. *Science Advances* 2(5):e1501639. 604
- 573 7. Chazdon RL, et al. (2020) Fostering natural forest regeneration on former agricultural land through economic and policy interventions. *Environmental Research Letters* 15(4):043002. 605
- 574 8. Xie Z, et al. (2019) Conservation opportunities on uncontested lands. *Nature Sustainability*. doi:[10.1038/s41893-019-0433-9](https://doi.org/10.1038/s41893-019-0433-9). 606
- 575 9. Navarro LM, Pereira HM (2012) Rewilding abandoned landscapes in Europe. *Ecosystems* 15:900–912. 607
- 576 10. Meyfroidt P, Schierhorn F, Prishchepov AV, Müller D, Kuemmerle T (2016) Drivers, constraints and trade-offs associated with recultivating abandoned cropland in Russia, Ukraine and Kazakhstan. *Global Environmental Change* 37:1–15. 608
- 577 11. Li S, Li X (2017) Global understanding of farmland abandonment: A review and prospects. *Journal of Geographical Sciences* 27(9):1123–1150. 609
- 578 12. Popp A, et al. (2017) Land-use futures in the shared socio-economic pathways. *Global Environmental Change* 42:331–345. 610
- 579 13. Rozendaal DMA, et al. (2019) Biodiversity recovery of Neotropical secondary forests. *Science Advances* 5(3):eaau3114. 611
- 580 14. Acevedo-Charry O, Aide TM (2019) Recovery of amphibian, reptile, bird and mammal diversity during secondary forest succession in the tropics. *Oikos* 128(8):1065–1078. 612
- 581 15. Isbell F, Tilman D, Reich PB, Clark AT (2019) Deficits of biodiversity and productivity linger a century after agricultural abandonment. *Nature Ecology & Evolution* 3(11):1533–1538. 613
- 582 16. Nerlekar AN, Veldman JW (2020) High plant diversity and slow assembly of old-growth grasslands. *Proceedings of the National Academy of Sciences* 117(31):18550–18556. 614
- 583 17. Gilroy JJ, et al. (2014) Cheap carbon and biodiversity co-benefits from forest regeneration in a hotspot of endemism. *Nature Climate Change* 4(6):503–507. 615
- 584 18. Cook-Patton SC, et al. (2020) Mapping carbon accumulation potential from global natural forest regrowth. *Nature* 585(7826):545–550. 616
- 585 19. Poorter L, et al. (2016) Biomass resilience of Neotropical secondary forests. *Nature* 530(7589):211–214. 617
- 586 20. Munroe DK, Berkel DB van, Verburg PH, Olson JL (2013) Alternative trajectories of land abandonment: Causes, consequences and research challenges. *Current Opinion in Environmental Sustainability* 5(5):471–476. 618
- 587 21. Alcantara C, et al. (2013) Mapping the extent of abandoned farmland in Central and Eastern Europe using MODIS time series satellite data. *Environmental Research Letters* 8(3). doi:[10.1088/1748-9326/8/3/035035](https://doi.org/10.1088/1748-9326/8/3/035035). 619
- 588 22. Estel S, et al. (2015) Mapping farmland abandonment and recultivation across Europe using MODIS NDVI time series. *Remote Sensing of Environment* 163:312–325. 620
- 589 23. Lark TJ, Salmon JM, Gibbs HK (2015) Cropland expansion outpaces agricultural and biofuel policies in the United States. *Environmental Research Letters* 10(4):044003. 621
- 590 24. Dara A, et al. (2018) Mapping the timing of cropland abandonment and recultivation in northern Kazakhstan using annual Landsat time series. *Remote Sensing of Environment* 213:49–60. 622
- 591 25. Yin H, et al. (2020) Monitoring cropland abandonment with Landsat time series. *Remote Sensing of Environment* 246:111873. 623
- 592 26. Reid JL, Fagan ME, Lucas J, Slaughter J, Zahawi RA (2019) The ephemerality of secondary forests in southern Costa Rica. *Conservation Letters* 12(2):e12607. 624
- 593 27. Nunes S, Oliveira L, Siqueira J, Morton DC, Souza CM (2020) Unmasking secondary vegetation dynamics in the Brazilian Amazon. *Environmental Research Letters* 15(3):034057. 625
- 594 28. Smith CC, et al. (2020) Secondary forests offset less than 10% of deforestation-mediated carbon emissions in the Brazilian Amazon. *Global Change Biology* 6:gcb.15352. 626
- 595 29. Schwartz NB, Aide TM, Graesser J, Grau HR, Uriarte M (2020) Reversals of Reforestation Across Latin America Limit Climate Mitigation Potential of Tropical Forests. *Frontiers in Forests and Global Change* 3(July):1–10. 627
- 596 30. Aguiar APD, et al. (2016) Land use change emission scenarios: Anticipating a forest transition process in the Brazilian Amazon. *Global Change Biology* 22(5):1821–1840. 628
- 597 31. Vancutsem C, et al. (2021) Long-term (1990–2019) monitoring of forest cover changes in the humid tropics. *Science Advances* 7(10):1–22. 629
- 598 32. Campbell JE, Lobell DB, Genova RC, Field CB (2008) The global potential of bioenergy on abandoned agriculture lands. *Environmental Science and Technology* 42(15):5791–5794. 630
- 599 33. Norden N, et al. (2015) Successional dynamics in Neotropical forests are as uncertain as they are predictable. *Proceedings of the National Academy of Sciences* 112(26):8013–8018. 631
- 600 34. Crouzeilles R, et al. (2016) A global meta-analysis on the ecological drivers of forest restoration success. *Nature Communications* 7(1):11666. 632
- 601 35. Arroyo-Rodríguez V, et al. (2017) Multiple successional pathways in human-modified tropical landscapes: new insights from forest succession, forest fragmentation and landscape ecology research. *Biological Reviews* 92(1):326–340. 633
- 602 36. Meli P, et al. (2017) A global review of past land use, climate, and active vs. passive restoration effects on forest recovery. *PLOS ONE* 12(2):e0171368. 634
- 603 37. Rydgren K, et al. (2020) Assessing restoration success by predicting time to recovery—But by which metric? *Journal of Applied Ecology* 57(2):390–401. 635
- 604 38. Jones HP, Schmitz OJ (2009) Rapid recovery of damaged ecosystems. *PLoS ONE* 4(5). doi:[10.1371/journal.pone.0005653](https://doi.org/10.1371/journal.pone.0005653). 636

- 640 39. Kämpf I, Mathar W, Kuzmin I, Hözel N, Kiehl K (2016) Post-Soviet recovery of grassland vegetation on abandoned fields in the forest steppe zone of Western Siberia. *Biodiversity and Conservation* 25(12):2563–2580.
- 641 40. Kamp J, Urazaliev R, Donald PF, Hözel N (2011) Post-Soviet agricultural change predicts future declines after recent recovery in Eurasian steppe bird populations. *Biological Conservation* 144(11):2607–2614.
- 642 41. Martin PA, Newton AC, Bullock JM (2013) Carbon pools recover more quickly than plant biodiversity in tropical secondary forests. *Proceedings of the Royal Society B: Biological Sciences* 280(1773). doi:[10.1098/rspb.2013.2236](https://doi.org/10.1098/rspb.2013.2236).
- 643 42. Lal R (2004) Soil carbon sequestration impacts on global climate change and food security. *Science* 304(5677):1623–1627.
- 644 43. Yang Y, Tilman D, Furey G, Lehman C (2019) Soil carbon sequestration accelerated by restoration of grassland biodiversity. *Nature Communications* 10(718):1–7.
- 645 44. Wetterbach T-M, et al. (2017) Soil carbon sequestration due to post-Soviet cropland abandonment: estimates from a large-scale soil organic carbon field inventory. *Global Change Biology* 23(9):3729–3741.
- 646 45. Crouzeilles R, et al. (2019) A new approach to map landscape variation in forest restoration success in tropical and temperate forest biomes. *Journal of Applied Ecology* (August):1365–2664.13501.
- 647 46. Parkhurst T, Prober SM, Hobbs RJ, Standish RJ (2021) Global meta-analysis reveals incomplete recovery of soil conditions and invertebrate assemblages after ecological restoration in agricultural landscapes. *Journal of Applied Ecology* (April 2020):1–15.
- 648 47. Crouzeilles R, et al. (2017) Ecological restoration success is higher for natural regeneration than for active restoration in tropical forests. *Science Advances* 3(11):1–8.
- 649 48. Queiroz C, Beilin R, Folke C, Lindborg R (2014) Farmland abandonment: Threat or opportunity for biodiversity conservation? A global review. *Frontiers in Ecology and the Environment* 12(5):288–296.
- 650 49. Sirami C, Brotons L, Burfield I, Fonderlick J, Martin JL (2008) Is land abandonment having an impact on biodiversity? A meta-analytical approach to bird distribution changes in the north-western Mediterranean. *Biological Conservation* 141(2):450–459.
- 651 50. Cook-Patton SC, Shoch D, Ellis PW (2021) Dynamic global monitoring needed to use restoration of forest cover as a climate solution. *Nature Climate Change* 11(5):366–368.
- 652 51. Prishchepov AV, Ponkina EV, Sun Z, Bavorova M, Yekimovskaja OA (2021) Revealing the intentions of farmers to recultivate abandoned farmland: A case study of the Buryat Republic in Russia. *Land Use Policy* 107(July 2020):105513.
- 653 52. Hua F, et al. (2016) Opportunities for biodiversity gains under the world's largest reforestation programme. *Nature Communications* 7:12717.
- 654 53. Food and Agriculture Organization of the United Nations (FAO) (2016) FAOSTAT Statistical Database: Methods & Standards. Available at: <http://www.fao.org/ag/agn/nutrition/Indicatorsfiles/Agriculture.pdf>.
- 655 54. RStudio Team (2020) RStudio: Integrated Development Environment for R. Available at: <http://www.rstudio.com/>.
- 656 55. Hijmans RJ (2021) *Raster: Geographic data analysis and modeling*. Available at: <https://r-spatial.org/raster>.
- 657 56. Dowle M, Srinivasan A (2021) *Data.table: Extension of ‘data.frame’*. Available at: <https://CRAN.R-project.org/package=data.table>.
- 658 57. Wickham H (2021) *Tidyverse: Easily install and load the tidyverse*. Available at: <https://CRAN.R-project.org/package=tidyverse>.

678 **Supporting Information**

679 **Contents**

680 Results	2
681 Abandonment duration	2
682 Modeling abandonment decay & recultivation	3
683 Projecting future abandonment and recultivation	3
684 Discussion	4
685 Implications for biodiversity recovery and carbon sequestration	5
686 Conclusions	6
687 Materials and Methods	6
688 Abandonment maps	6
689 Defining abandonment	6
690 Data processing	6
691 Calculating abandonment duration	7
692 Modeling abandonment decay	7
693 Projecting future abandonment and recultivation	7
694 Data Availability Statement	7
695 Supporting Information	7
696 References	8
697 Supporting Information	10
698 S1 Extended Results	13
699 A Limited abandonment in Mato Grosso	13
700 B Biomes	13
701 C The effect of varying abandonment definitions	13
702 D Comparing annual and two-year estimates of abandonment	13
703 E Maps of abandonment duration as of 2017 and maximum duration during time series	14
704 S2 Extended Methods	14
705 A Classifying abandonment	14
706 B Temporal filters	14
707 C Modeling abandonment decay	14
708 C.1 Model selection and diagnostics	14
709 C.2 Recultivation (“decay”) model results	14
710 D Change in recultivation rates over time	15
711 E Projecting abandonment duration into the future	15
712 S3 Supporting Tables & Figures	16
713 List of Tables	
714 S2 Cropland abandonment (in Mha) as of 2017 as identified using a) our annual time series and a five-year abandonment definition and b) a two year method taking the difference between land cover in 1987 and 2017.	16
715 S1 Summary statistics describing the duration of abandonment (in years) at our eleven sites between 1987 and 2017, using a five year abandonment definition, and incorporating all periods of abandonment (allowing for multiple per pixel).	16
718 List of Figures	
719 1 Observed duration of cropland abandonment (in years) as of 2017 in our eleven study sites. Site locations are shown in Figure S1, and maps of maximum abandonment duration are shown in Figure S7.	2
720 2 The distribution of abandonment duration (in years) for all periods of abandonment from 1987 to 2017. The y-scale shows the proportion of abandonment periods of a given duration at each site. The red points represent the mean abandonment duration (in years) at each site, and the red vertical dashed line represents the mean of these site-level mean duration values across all sites. Note that these distributions include multiple periods of abandonment for those pixels that experienced abandonment and recultivation multiple times during the time series. See Figure S6 to view distributions of the maximum abandonment duration for each pixel.	3
721 3 Mean decay trajectories for each site, based on a linear model predicting the proportion of abandoned land remaining abandoned as a function of time (including a linear and a logarithmic term of time). The function describing each site’s mean trajectory is calculated by taking the mean of each time coefficient across all cohorts of abandonment at each site. The light gray dashed line at a proportion of 0.50 indicates the half-life at each site, defined as the time required for half of the croplands abandoned in a given year to be recultivated.	4

4	Recultivation (decay) of abandoned land in Shaanxi/Shanxi (China), showing the proportion of each cohort of abandoned land (i.e., all pixels abandoned in a given year) remaining abandoned over time. Points represent actual observations by cohort, dashed lines represent linear model predictions (fitted values) for each cohort as a function of time (including a linear and logarithmic term of time), and the solid black line represents the mean trend across all cohorts (calculated by taking the mean of each time coefficient value across all cohorts). Colors of both points and dashed lines correspond to roughly five-year group of cohorts, ranging from dark purple (oldest cohorts) to green and yellow (most recent cohorts). See Figure S12 for model results for all sites.	732 733 734 735 736 737 738
S1	The locations of our 11 sites, from Yin et al. (25). Sites are labeled as follows: (b) Vitebsk, Belarus / Smolensk, Russia; (bh) Bosnia & Herzegovina; (c) Chongqing, China; (g) Goiás, Brazil; (i) Iraq; (mg) Mato Grosso, Brazil; (n) Nebraska/Wyoming, USA; (o) Orenburg, Russia / Uralsk, Kazakhstan; (s) Shaanxi/Shanxi, China; (v) Volgograd, Russia; (w) Wisconsin, USA.	739 740 741 742 743 744 745 746 747 748 749
S2	Area abandoned a) as of 2017, b) at any point between 1987-2017, c) as of 2017 as a proportion of the total cropland extent (i.e., the area of all lands that were cultivated at some point during the time series). Note that sites are shown in ascending order of area abandoned as of 2017 as a proportion of total cropland extent.	740 741 742 743 744 745 746 747 748 749
S3	Cumulative area abandoned at each site through time, according to age class (in years).	745
S4	Area in each land cover class at each site through time. Land cover classes are cropland, grassland, woody vegetation, non-vegetation, and abandoned (for at least 5 years).	746
S5	Annual turnover of abandoned croplands at each site, showing the annual gain (dark green) and annual loss (i.e., recultivation, light green) and net change (black line) of abandoned croplands.	747
S6	The distribution of the maximum abandonment duration (in years) for each pixel at each site from 1987 to 2017. The y-scale shows the proportion of pixels with maximum duration values of a given duration at each site. As previously noted, abandonment and recultivation can occur multiple times at a single pixel during our time series, and this figure serves as a companion to the distribution of all abandonment values shown in Figure 2. Site-level mean duration values are shown in the red and blue dots, corresponding to mean values calculated across all periods of abandonment (in red, including multiple periods per pixel) and mean values calculated across only the maximum duration of abandonment at each pixel (in blue). The vertical dashed lines represent the mean of these site-level mean duration values, for all abandonment periods (red) and only the maximum duration at each pixel (blue), respectively.	748 749 750 751 752 753 754 755 756 757
S7	Maximum duration of cropland abandonment (in years) observed at each pixel between 1987 and 2017 in our eleven study sites. This serves as a companion to maps of the abandonment duration as of 2017 shown in Figure 1. Site locations are shown in Figure S1.	758 759
S8	Proportion of abandoned cropland in each land cover class as of 2017.	760
S9	Site biomes, using biome classifications from The Nature Conservancy's Terrestrial Ecoregions of The World (TEOW) database, derived from Olson et al. (61) and Olson and Dinerstein (62).	761
S10	Mean abandonment lengths shown for various abandonment thresholds.	762
S11	Recultivation rates shown for various abandonment thresholds.	763
S12	Decay model results for all sites, showing the proportion of each cohort of abandoned land (i.e., all pixels abandoned in a given year) remaining abandoned over time for each of our eleven sites. Points represent actual observations by cohort, dashed lines represent linear model predictions (fitted values) for each cohort as a function of time (including a linear and logarithmic term of time), and the solid black line represents the site-level mean trend across all cohorts (calculated by taking the mean of each time coefficient values across all cohorts, respectively, and using those two mean values to plot a mean trend). Colors of both points and dashed lines correspond to roughly five-year group of cohorts, ranging from dark purple (oldest cohorts) to green and yellow (most recent cohorts). The horizontal black dashed line shows a proportion of 0.5, indicating the point where half of a cohort has been recultivated. Model diagnostic plots are shown in Figures S14 and S15.	764 765 766 767 768 769 770 771 772 773 774
S13	Akaike Information Criterion (AIC) values for various recultivation ("decay") model specifications for each site. More negative AIC values indicate a better model fit.	775 776
S14	Residuals vs. fitted diagnostic plots for our linear models of the recultivation ("decay") of abandonment at each site. These models take the form shown in Equation Eq. (S2), and are shown in Figure S12.	777
S15	QQ plots calculated using the <code>car</code> package (63) for our linear models of the recultivation ("decay") of abandonment at each site. These models take the form shown in Equation Eq. (S2), and are shown in Figure S12.	778
S16	Mean decay model coefficients across cohorts at each site. The left panel shows the mean coefficient on the log(time) terms and the right shows the site mean coefficient on the linear time terms. These mean coefficients are used to plot the mean decay trajectories shown in Figure 3.	779 780 781 782
S17	An alternative representation of the mean decay rate for each site (also shown in Figure 3). The color of each point corresponds to the proportion remaining after a given amount of time.	783 784 785
S18	The rate of change of decay rates (measured as the half-life, or the time required for 50% of each cohort to be recultivated) at each site over the course of the time series. Individual site trends are shown in panel a. Solid lines show simple linear regressions, the slopes of which are shown in panel b. Gray bands around the linear trends in panel a and the error bars on slope estimates in panel b both represent 95% confidence intervals. These models are described by Eq. Eq. (S3). Model diagnostic plots are shown in Figures S19 and S20.	786 787 788 789 790
S19	Residuals vs. fitted diagnostic plots for each site, for a simple <code>lm</code> call corresponding to Eq. Eq. (S3), in which the half-life (i.e., the time required for half (50%) of a given cohort of abandoned cropland to be recultivated) is modeled as a function of the year of initial abandonment at each site.	791 792 793
S20	QQ plots calculated using the <code>car</code> package ((63)), for a simple <code>lm</code> call corresponding to Eq. Eq. (S3), in which the half-life (i.e., the time required for half (50%) of a given cohort of abandoned cropland to be recultivated) is modeled as a function of the year of initial abandonment at each site.	794 795 796
S21	Annual gain in newly abandoned cropland at our eleven sites. Panel a shows the trend in annual abandonment over time at each site (in 10^3 ha), and Panel b shows the mean annual abandonment (in 10^3 ha) at each site. The mean values in panel b feed into the extrapolations. Note that the annual gain in abandonment corresponds to the dark green bars in Figure S5.	797 798 799
S22	The results of our simple extrapolation, including a) the mean age of abandonment, and b) the total area abandoned into the future. Colors corresponding to each site are consistent across the three panels. These extrapolation assume recultivation based on the mean decay trend for each site Figure 3 and annual new abandonment based on the mean annual gain in abandonment shown in Figure S5 (dark green bars).	800 801 802
S23	Extrapolating area by age bin, assuming a 1) each site follows the mean recultivation ("decay") rate, and 2) a constant area abandoned each year (based on the mean annual area abandoned at each site).	803 804 805

806	S24	The results of our second extrapolation, including a) the mean age of abandonment, and b) the total area abandoned 807 into the future. Colors corresponding to each site are consistent across the three panels. These extrapolations assume 808 recultivation based on the mean decay trend for each site Figure 3 and annual new abandonment based on the mean annual 809 gain in abandonment shown in Figure S5 (dark green bars).	37
810	S25	Extrapolating area by age bin, assuming a 1) each site follows the mean recultivation (“decay”) rate, and 2) a constant area 811 abandoned each year until 2017 (based on the mean annual area abandoned at each site), followed by a linearly declining 812 area abandoned each year until reaching 0 in 2050.	38
813	S26	Comparing the mean duration of abandonment at our 11 sites observed between 1987 and 2017 with the extrapolated mean 814 duration as of 2050 for our two extrapolations.	39
815	S27	Abandonment patterns for Vitebsk, Belarus / Smolensk, Russia, showing a) accumulation of abandoned land by age class, 816 b) decay of abandoned land by year abandoned, c) the area in each land cover class through time (including both land that 817 has been abandoned for five or more years, as well as any land abandoned for 1 or more years, therefore including short-term 818 fallows), d) the annual turnover of abandoned land through time, and e) the distribution of abandonment duration for all 819 periods of cropland abandonment (top) and the maximum duration of abandonment at each pixel (bottom).	40
820	S28	Abandonment patterns for Bosnia & Herzegovina, following Figure S27.	41
821	S29	Abandonment patterns for Chongqing, China, following Figure S27.	42
822	S30	Abandonment patterns for Goiás, Brazil, following Figure S27.	43
823	S31	Abandonment patterns for Iraq, following Figure S27.	44
824	S32	Abandonment patterns for Mato Grosso, Brazil, following Figure S27.	45
825	S33	Abandonment patterns for Nebraska/Wyoming, USA, following Figure S27.	46
826	S34	Abandonment patterns for Orenburg, Russia / Uralsk, Kazakhstan, following Figure S27.	47
827	S35	Abandonment patterns for Shaanxi/Shanxi, China, following Figure S27.	48
828	S36	Abandonment patterns for Volgograd, Russia, following Figure S27.	49
829	S37	Abandonment patterns for Wisconsin, USA, following Figure S27.	50

S1. Extended Results

Cropland abandonment at individual sites (excluding Mato Grosso, see Section S1.A.) ranged between 314,374.8 ha (Shaanxi) and 930,424 ha (Orenburg) as of 2017 (Figure S3), and because our sites varied in size, this corresponded to between 7.91% (Nebraska) and 19.91% (Shaanxi) of the total area of each site (Figure S2).

On average, we found that cropland abandonment lasted for only 14.42 years ($SD = 1.52$ years) across our time series at our eleven sites. Note, however, that these summary statistics are calculated based on the mean abandonment duration at each site, to account for different site sizes. The summary statistics reported are therefore the mean of the mean abandonment duration at each of our eleven sites, and the standard deviation of the mean abandonment duration at each of our eleven sites.

We also calculated the mean standard deviation of abandonment duration across our sites, which was 7.78 years. The former is a measure of the spread of mean abandonment lengths across the 11 sites, whereas the latter is a measure of the average spread of abandonment lengths at each site. See Table S1.

The area abandoned at each site is shown in Figure S2 (see also Table S2). The area abandoned at each site, by age class, is shown in Figure S3, and the area in each land cover class at each site is shown in Figure S4. Figure S3 shows that the timing of abandonment varied across sites; some sites showed more abandonment earlier in the time series (e.g., Iraq; Bosnia & Herzegovina; Volgograd, Russia; Nebraska/Wyoming, USA; & Mato Grosso, Brazil), some showed consistent abandonment over time (e.g., Vitebsk, Belarus/Smolensk, Russia; Goiás, Brazil; and Wisconsin, USA), and others showed increasing abandonment later on in the time series (e.g., sites in Shaanxi/Shanxi and Chongqing, China). Furthermore, Figure S5 shows the annual gain, loss, and net change in the area of abandoned croplands abandoned at each site.

A. Limited abandonment in Mato Grosso. Mato Grosso, Brazil, was the only site that did not experience significant amounts of cropland abandonment during our time series. This is unsurprising given the recent history of agriculturally-driven land-use change over the last few decades. That being said, the abandonment that did take place in Mato Grosso was relatively more durable, requiring 25 years to decline by half and 110 years for complete turnover. However, because Mato Grosso showed large amounts of new cultivation over the source of our time series and relatively little abandonment (9,006 ha, or 0.47% of the total cropland extent, as of 2017), these results should be interpreted with care.

B. Biomes. Some ecosystems and biomes seem to recover more quickly than others, namely in relatively higher latitudes, relatively colder climates, and in relatively more humid biomes (58). Our sites cover a range of biomes (Figure S9), including:

- Temperate Broadleaf and Mixed Forests (Vitebsk Belarus/Smolensk, Russia; Bosnia & Herzegovina; Wisconsin, USA),
- Temperate Grasslands, Savannas, and Shrublands (Nebraska/Wyoming, USA; Orenburg, Russia/Uralsk, Kazakhstan; Volgograd, Russia),
- Tropical Grassland (Goiás and Mato Grosso, Brazil),
- Tropical Moist Broadleaf Forests (Chongqing, China; Mato Grosso, Brazil),
- Montane Grassland and Shrublands (Shaanxi/Shanxi, China), and
- Deserts & Xeric Shrublands (Iraq).

The long-term land-cover outcomes for abandoned croplands are shown (as of 2017) in Figure S8. Land cover outcomes for abandoned croplands showed wide variation across sites, with most abandonment in Wisconsin being classified as forest by 2017 (60% forest, 40% grassland), but remaining mostly in grassland elsewhere (Figure S8). This limited woody vegetation regrowth may be a product of the biome, but it may simply be a result of insufficient time for woody biomass to develop. Land cover alone cannot confidently serve as a proxy for ecosystem recovery.

C. The effect of varying abandonment definitions. A relatively short-term definition of abandonment might result in an overestimation of recultivation, because short-term abandonment may be better understood as cyclical fallow periods, not true abandonment (20). Because typical fallow period length may vary around the world, we tested multiple abandonment thresholds in order to test the sensitivity of our results to our choice of a five-year abandonment definition, following the FAO (53). As our abandonment threshold increased in length, the mean abandonment duration across our sites increased accordingly, ranging between 7 years (no threshold) and 19 years (10-year threshold). As expected, using a longer abandonment definition reduced the amount of cropland abandonment we detected, which is also shown in the area in the different colored age classes in Figure S3.

The proportion of abandoned croplands that were recultivated by the end of the time series also responded to our abandonment threshold, with less recultivation for longer abandonment thresholds (Figure S11). However, even at the longest abandonment definition (10 years), we still saw that between 10% and 30% of abandoned croplands were recultivated by the end of the time series. We find that the mean area of abandoned croplands that get recultivated by the end of the time series declines from 37.77% with a 5 year threshold to 30.93% with a 7 year threshold, and 22.83% with a 10 year threshold. This indicates that the abandonment and recultivation we observe is not merely a function of our five-year abandonment definition.

D. Comparing annual and two-year estimates of abandonment. Some studies estimate cropland abandonment by simply looking for areas where land cover is classified as “cultivated” in one year, but not in a later year (e.g., 1992 and 2015 in ref. 4). In order to understand the magnitude of the differences that could result from using this two-year approach, we estimated cropland abandonment by simply identifying areas that were classified as “cropland” in 1987 and classified as either “woody vegetation” or “herbaceous vegetation” in 2017 (i.e., excluding “non-vegetation”).

Table S2 shows the area of abandoned croplands as identified using a five-year abandonment definition and the full annual time series (Column 2), and the area of abandoned croplands identified using only the difference between 2017 and 1987 (Column 3). These two methods produced abandonment area estimates that ranged between 39.75% lower (Goiás, Brazil) and 83.29% higher (Mato Grosso, Brazil) than the abandoned area identified using the full time series.

Not only do these methods produce different area estimates, but they also differ in the location of the abandonment they identify, with spatial agreement of only 28.08% (Mato Grosso, Brazil) to 66.3% (Bosnia & Herzegovina) (see Table S2). We measure spatial agreement using the Jaccard similarity index [Legendre2012], a measure of overlap between two sets, defined as the proportion of shared elements, or the intersection divided by the union (Equation Eq. (S1)) (59):

$$J(a, b) = \frac{a \cap b}{a \cup b} \quad [S1] \quad 894$$

995 **E. Maps of abandonment duration as of 2017 and maximum duration during time series.** As described in the main text, because a pixel may
996 be abandoned and recultivated multiple times throughout the time series, we calculated the mean abandonment duration in two ways: 1)
997 across all periods of abandonment (as shown in Figure 2), and 2) across only the longest period of abandonment experienced by each
998 pixel. Maps of the maximum abandonment duration at each pixel at each site is shown in Figure S7 (serving as a companion to Figure 1).
999 The distribution of maximum duration values, and the corresponding mean maximum duration value at each site, is shown in Figure S6
999 (serving as a companion to Figure 2).

999 Expanded site-specific results are shown in Figures S27-S37.

999 **S2. Extended Methods**

999 As noted in our main text, we build on annual land cover maps for 1987-2017 developed by Yin et al. (25). The following section outlines
999 our data processing and analytical methods in more specific detail than was possible in the main text. We processed and analyzed our
999 abandonment map data in RStudio version 1.4.1717 (54), using R version 4.1.0 (2021-05-18), relying heavily on the {raster} (55), {terra}
999 (60), {data.table} (56), and {tidyverse} (57) packages.

999 **A. Classifying abandonment.** Pixels that remained in cropland or non-cropland classes throughout the entire time series were excluded,
999 as were periods of non-cropland that began in the first year of the time series, even if that pixel was later classified as cropland and
999 subsequently abandoned. In effect, we only counted periods of abandonment that we could verify had followed agricultural activity during
999 our time series.

999 As noted, pixels that transitioned from cropland to the non-vegetation land cover class were not considered “abandoned,” and therefore
999 we excluded all non-vegetation pixels from our entire analysis. These pixels accounted for <10% of total site area at all sites except
999 Shaanxi (12.7%) and Iraq (52.8%), and remained stable or declined over time at all eleven sites (see Figure S4).

999 All area calculations were performed using the {terra} package’s `cellSize()` function, which calculates the spherical area of each cell
999 as defined by its four corners (60).

999 **B. Temporal filters.** In order to address potential classification errors in a single year, we implemented a series of temporal filters designed
999 to smooth trajectories by looking for short-term land-cover changes that are temporally unlikely. We applied five-year and eight-year
999 moving-window filters that searched for short periods of land cover classifications that do not match those immediately before and after,
999 and subsequently updated them to match the surrounding classifications. Specifically, the five-year filter searched for one year periods
999 that did not match the two years immediately before and after (i.e., patterns of 11011, where 1 represents non-cropland and 0 represents
999 cropland), and our eight-year filter searched for two year periods that did not match the three years before and after (i.e., 11100111). The
999 central classifications were then updated to match the classes on either end.

999 **C. Modeling abandonment decay.** Our mean abandonment duration metric tells us about the general persistence of abandoned croplands
999 throughout the time series. However, this value is limited by the time series length, and does not account for when the majority of
999 the abandonment took place at a site, nor whether a period of abandonment ends as a result of recultivation or the end of the time
999 series. As a result, the mean abandonment duration does not tell us how long to expect a piece of land to remain abandoned, nor how
999 abandonment length varies through time. To address this constraint, we track the trajectory of each pixel through time following its
999 initial abandonment, grouping pixels abandoned in a given year into “cohorts.” Decay rates provide information about how long it takes
999 for land to be recultivated, complementing the mean abandonment length and providing a more nuanced story about how long to expect
999 abandonment to last.

999 For example, a site may have a relatively short mean length of abandonment (e.g., Shaanxi/Shanxi [China], with a mean abandonment
999 length of 13 years; see Figure 1), but also have a gradual decay rate, indicating that land should stay abandoned for a relatively longer
999 amount of time. This may result from more abandonment occurring towards the end of the time series; this land simply does not have as
999 long to age and shows up as younger in our data, regardless of how long it may last. Looking at abandonment decay rates for each cohort
999 individually allows us to produce a decay rate for each site in general in a way that accounts for when during the time series a piece of
999 land was abandoned (i.e., giving us a sense of how long to expect a given piece of land to remain abandoned, even into the future).

999 **C.1. Model selection and diagnostics.** We fit linear models using the `lm()` function in R’s core statistics package {stats}, predicting the
999 proportion of abandoned cropland in each cohort remaining abandoned as a function of time since initial abandonment at each site. The
999 proportion of abandoned cropland remaining abandoned is measured relative to the area abandoned 5 years following the year of initial
999 abandonment, as dictated by our five year abandonment definition.

999 We tested a range of model specifications, including linear and log transformations of both *proportion* and *time*. Due to a linear
999 relationship between model residuals and time when including only one term for *time*, we also tested models containing multiple *time*
999 predictor terms, including both log and linear terms.

999 We chose a model with the following specifications shown in Equation 1 and reproduced here in Equation Eq. (S2). For cohorts of
999 abandonment initially abandoned in years $y = 1988, \dots, 2013$, we estimate the proportion p of each cohort y remaining abandoned as a
999 function of time t (i.e., based on the number of years after initial abandonment).

$$p_y = 1 + \beta_{1,y} \log(t+1) + \beta_{2,y} t \quad [\text{S2}]$$

999 Where $\beta_{1,y}$ represents the regression coefficient on the log term of time t for cohort y , and $\beta_{2,y}$ represents the regression coefficient
999 on the linear term of time t for cohort y . We allow for cohort level fixed effects, fitting unique coefficients for each cohort at each site.
999 We ran individual models for each site, using a `stats::lm()` call of `lm(formula = I(proportion - 1) ~ 0 + log(time + 1):cohort
999 + I(time):cohort)` on data for only that site. Taken together, these 11 models correspond to a `stats::lm()` call of `lm(formula =
999 I(proportion - 1) ~ 0 + log(time + 1):cohort:site + I(time):cohort:site)`.

999 Model selection was performed based on Akaike Information Criterion (AIC) values (Figure S13), selecting the model with the lowest
999 (i.e., more negative) AIC value. We confirmed that linear model assumptions were not violated through visual inspection of both residuals
999 vs. fitted plots (Figure S14) and Q-Q plots (Figure S15).

999 **C.2. Recultivation (“decay”) model results.** The observed data, fitted values from these linear models, and mean decay rates for each site,
999 are shown in Figure S12.

999 In order to calculate the mean decay trajectory at each site (as shown in Figure 3), we took the mean of the log coefficients ($\beta_{1,\bar{y}}$) and
999 the linear coefficients ($\beta_{2,\bar{y}}$) respectively across all cohorts y at each site. These mean values are shown in Figure S16. We then used these
999 mean coefficient values ($\beta_{1,\bar{y}}$ and $\beta_{2,\bar{y}}$) to define a new function describing the mean recultivation (or decay) trajectory at each site, using
999 the same form as Equation Eq. (S2).

999 An alternative representation of the mean recultivation rate is shown in Figure S17.

D. Change in recultivation rates over time. We examined the rate of change of recultivation rates by calculating the half-life, $t_{half,s}$, defined as the time required for half (50%) of a given cohort of abandoned cropland to be recultivated, and parameterizing a simple linear model on these half-life values as a function of time, using the `stats::lm()` function in R's core statistics package `{stats}`. We estimate the half-life, $t_{half,s}$, as a function of the year of initial abandonment ($yearabn_s$), at each site s , as shown in Equation Eq. (S3). 963
964
965
966

$$t_{half,s} = \beta_{0,s} + \beta_{1,s} yearabn_s \quad [S3] \quad 967$$

Where $\beta_{1,s}$ represents the regression slope on the year abandoned (cohort) for site s ($yearabn_s$), and $\beta_{0,s}$ represents the intercept. This corresponds to a `stats:::lm()` call of `lm(formula = t_half ~ year_abandoned)`, run for each site individually. Results are shown in Figure S18. 968
969
970
971
972

We confirmed that model assumptions were met through visual inspection of residuals vs. fitted plots (Figure S19) and Q-Q plots (Figure S20). 973
974
975
976
977
978
979
980
981
982
983
984
985
986

E. Projecting abandonment duration into the future. The results of the projection highlighted in the main text (referred to here as “Extrapolation 1”) are shown in Figure S22 and Figure S23. As noted in the main text, we make two simple assumptions in our projection of abandonment and recultivation into the future: specifically, that 1) recultivation rates remain the same (based on mean recultivation trends at each site, shown in Figure 3, and that 2) a constant amount of cropland is newly abandoned each year, based on the mean annual gain in abandonment shown in Figure S21b (note: the annual gain in abandonment in Figure S21a corresponds to the dark green bars in Figure S5).

Given that abandonment may not continue indefinitely, we also explore an alternative to our second assumption about the amount of additional abandonment each year. In this alternative assumption (“Extrapolation 2”), the area abandoned each year is the same as “Extrapolation 1” from 1987-2017, based on the mean annual gain in abandonment (Figure S21b), but linearly declines between 2017-2050, reaching 0 ha at each site in 2050 (see Figures S24 and S25).

While mean age of abandoned land increased through time after 2017 (and most dramatically after 2050), it remained below 37 years at all sites by 2050. Increases in mean abandonment duration were offset by recultivation, and total area abandoned declined quickly after 2020 at most sites. The mean abandonment duration increases as annual abandonment declines, as the total pool of abandoned land grows older and is gradually recultivated. 973
974
975
976
977
978
979
980
981
982
983
984
985
986

Table S2. Cropland abandonment (in Mha) as of 2017 as identified using a) our annual time series and a five-year abandonment definition and b) a two year method taking the difference between land cover in 1987 and 2017.

Site	Area (annual, as of 2017)	Area (two year: 2017-1987)	Percent Difference	Jaccard Similarity
Goiás, Brazil	530,252	319,499	-39.75%	0.29
Vitebsk, Belarus / Smolensk, Russia	917,934	655,689	-28.57%	0.51
Chongqing, China	382,125	273,839	-28.34%	0.43
Nebraska/Wyoming, USA	351,006	274,133	-21.9%	0.50
Bosnia & Herzegovina	690,376	569,091	-17.57%	0.66
Wisconsin, USA	411,833	358,420	-12.97%	0.48
Iraq	368,103	348,152	-5.42%	0.54
Volgograd, Russia	828,276	857,989	3.59%	0.47
Orenburg, Russia / Uralsk, Kazakhstan	930,424	975,131	4.8%	0.52
Shaanxi/Shanxi, China	314,375	355,581	13.11%	0.49
Mato Grosso, Brazil	9,006	16,507	83.29%	0.28

987 S3. Supporting Tables & Figures

Table S1. Summary statistics describing the duration of abandonment (in years) at our eleven sites between 1987 and 2017, using a five year abandonment definition, and incorporating all periods of abandonment (allowing for multiple per pixel).

Site	Mean	Median	Standard Deviation
Vitebsk, Belarus / Smolensk, Russia	13.87	12	7.60
Bosnia & Herzegovina	17.70	18	8.36
Chongqing, China	12.92	11	7.32
Goiás, Brazil	13.61	12	7.42
Iraq	15.72	13	8.78
Mato Grosso, Brazil	15.30	11	9.21
Nebraska/Wyoming, USA	15.32	14	8.04
Orenburg, Russia / Uralsk, Kazakhstan	12.86	11	6.95
Shaanxi/Shanxi, China	13.00	11	7.15
Volgograd, Russia	13.33	12	7.01
Wisconsin, USA	15.00	14	7.78

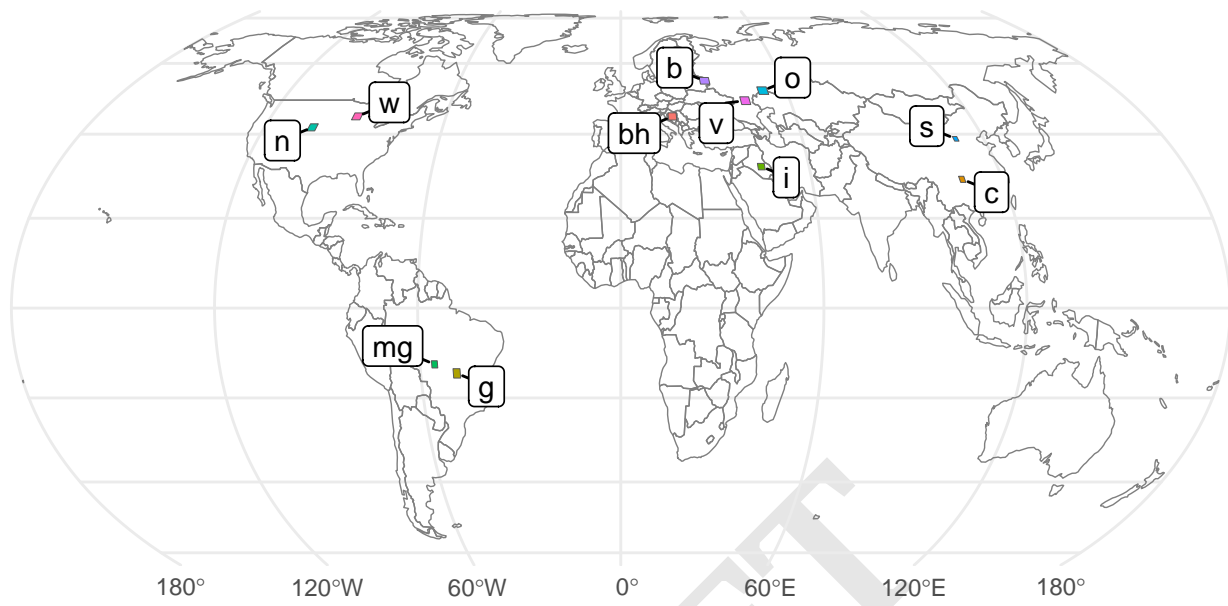


Fig. S1. The locations of our 11 sites, from Yin et al. (25). Sites are labeled as follows: (b) Vitebsk, Belarus / Smolensk, Russia; (bh) Bosnia & Herzegovina; (c) Chongqing, China; (g) Goiás, Brazil; (i) Iraq; (mg) Mato Grosso, Brazil; (n) Nebraska/Wyoming, USA; (o) Orenburg, Russia / Uralsk, Kazakhstan; (s) Shaanxi/Shanxi, China; (v) Volgograd, Russia; (w) Wisconsin, USA.

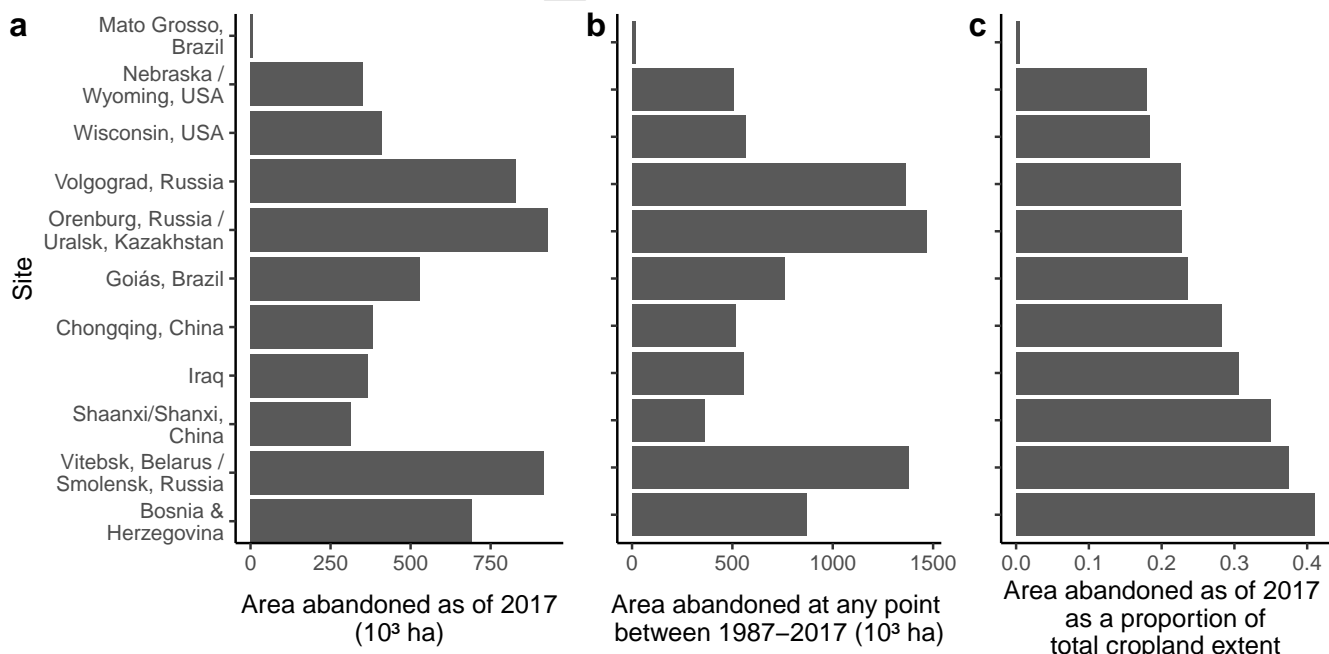


Fig. S2. Area abandoned a) as of 2017, b) at any point between 1987–2017, c) as of 2017 as a proportion of the total cropland extent (i.e., the area of all lands that were cultivated at some point during the time series). Note that sites are shown in ascending order of area abandoned as of 2017 as a proportion of total cropland extent.

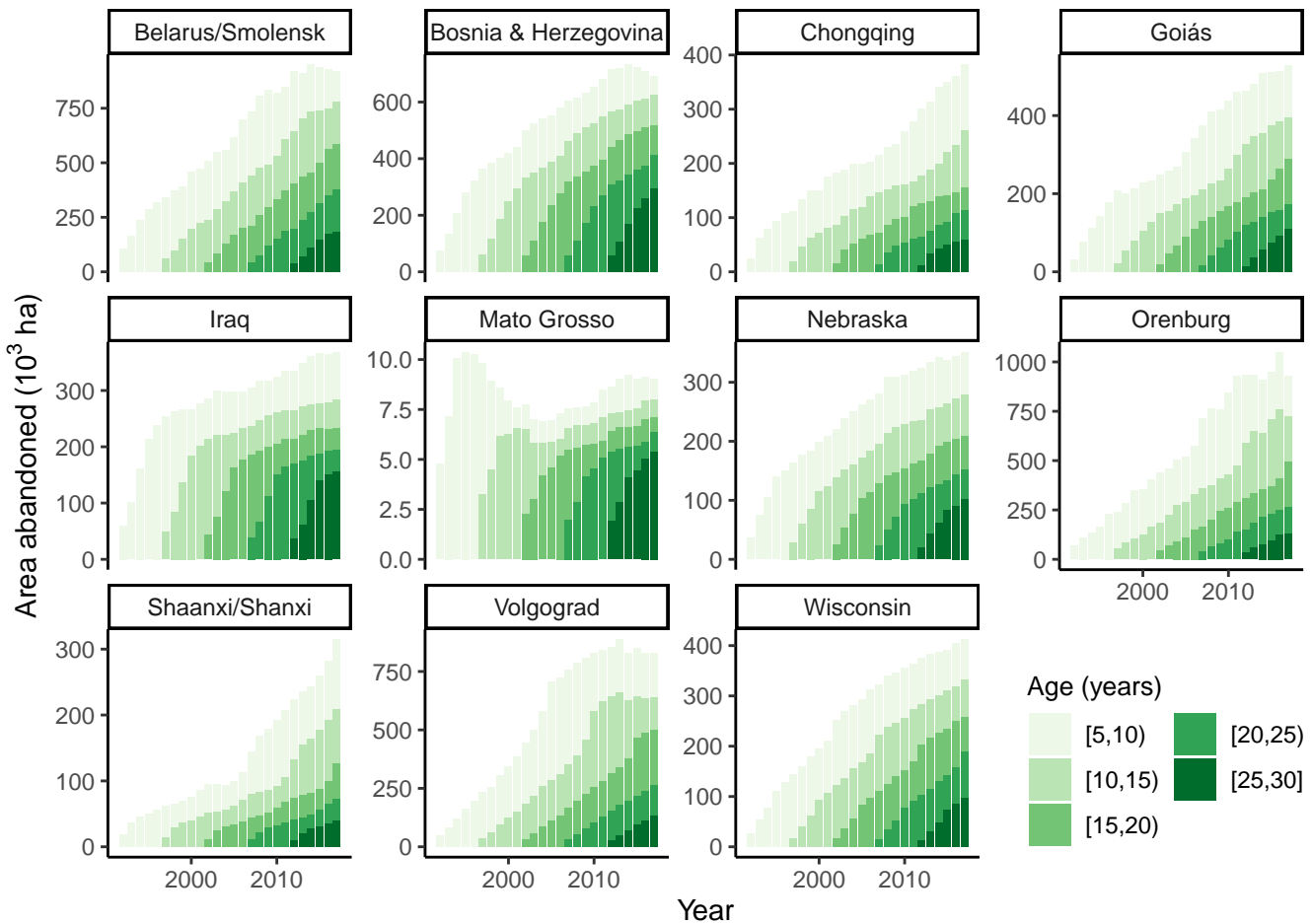


Fig. S3. Cumulative area abandoned at each site through time, according to age class (in years).

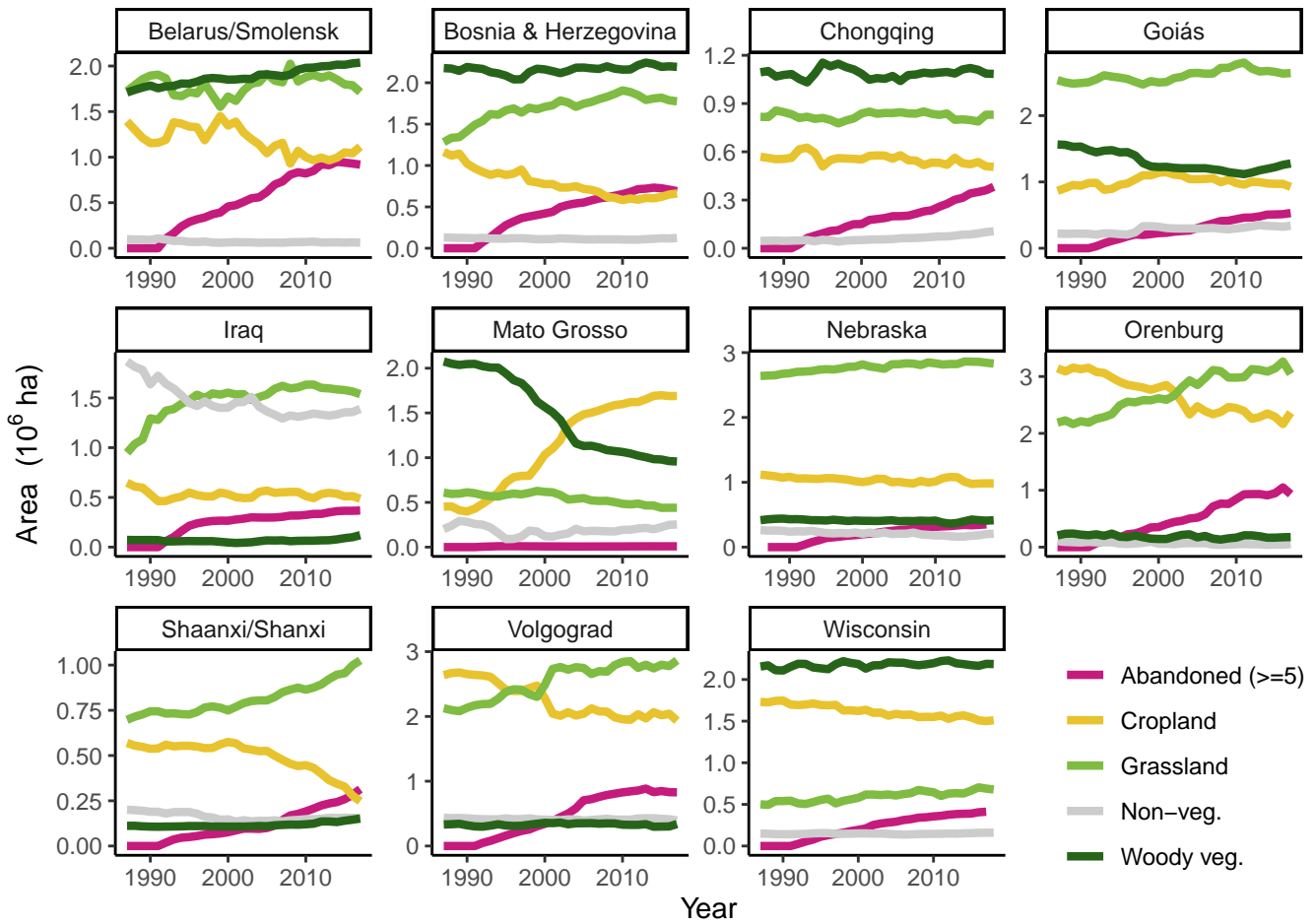


Fig. S4. Area in each land cover class at each site through time. Land cover classes are cropland, grassland, woody vegetation, non-vegetation, and abandoned (for at least 5 years).

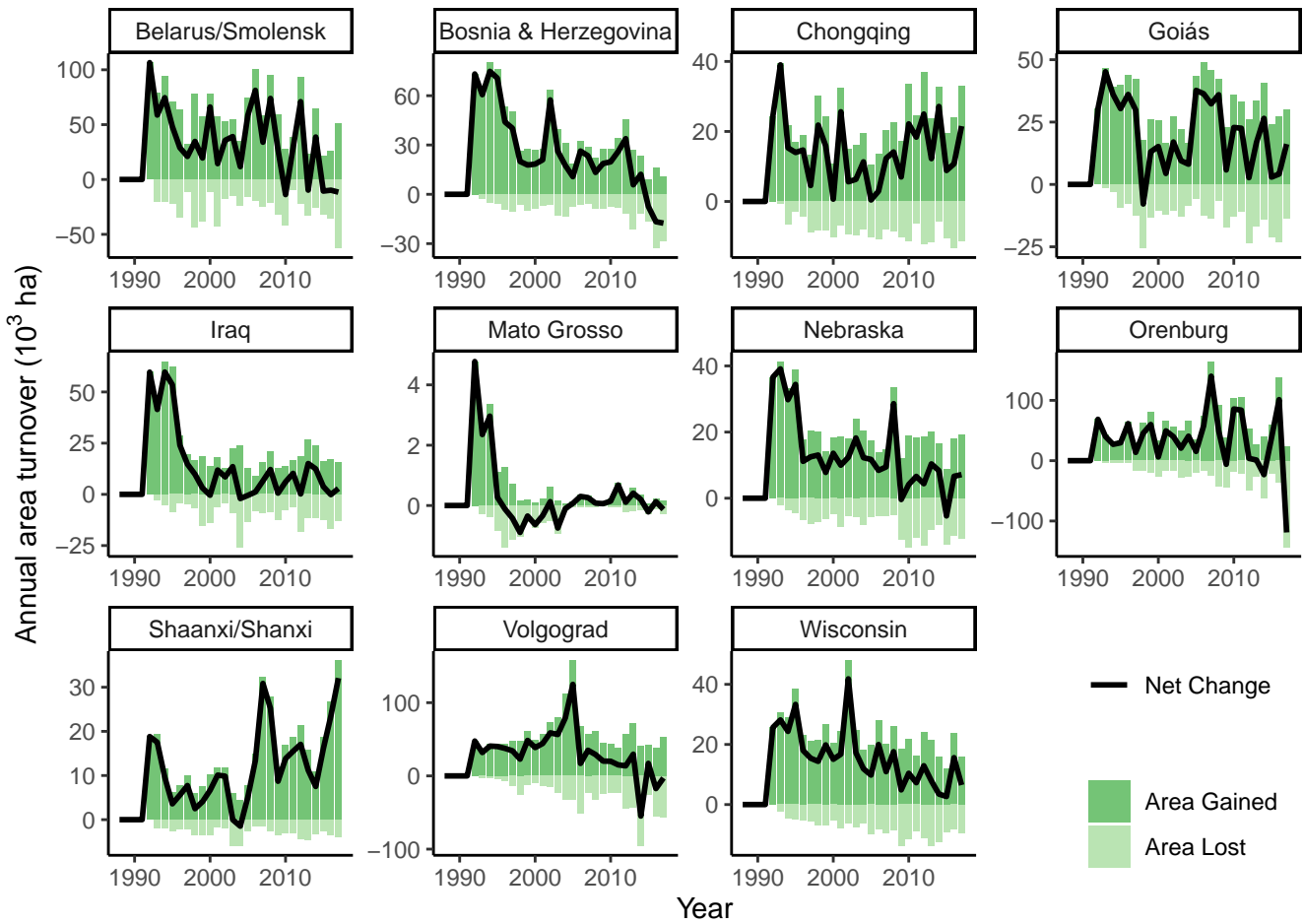


Fig. S5. Annual turnover of abandoned croplands at each site, showing the annual gain (dark green) and annual loss (i.e., recultivation, light green) and net change (black line) of abandoned croplands.

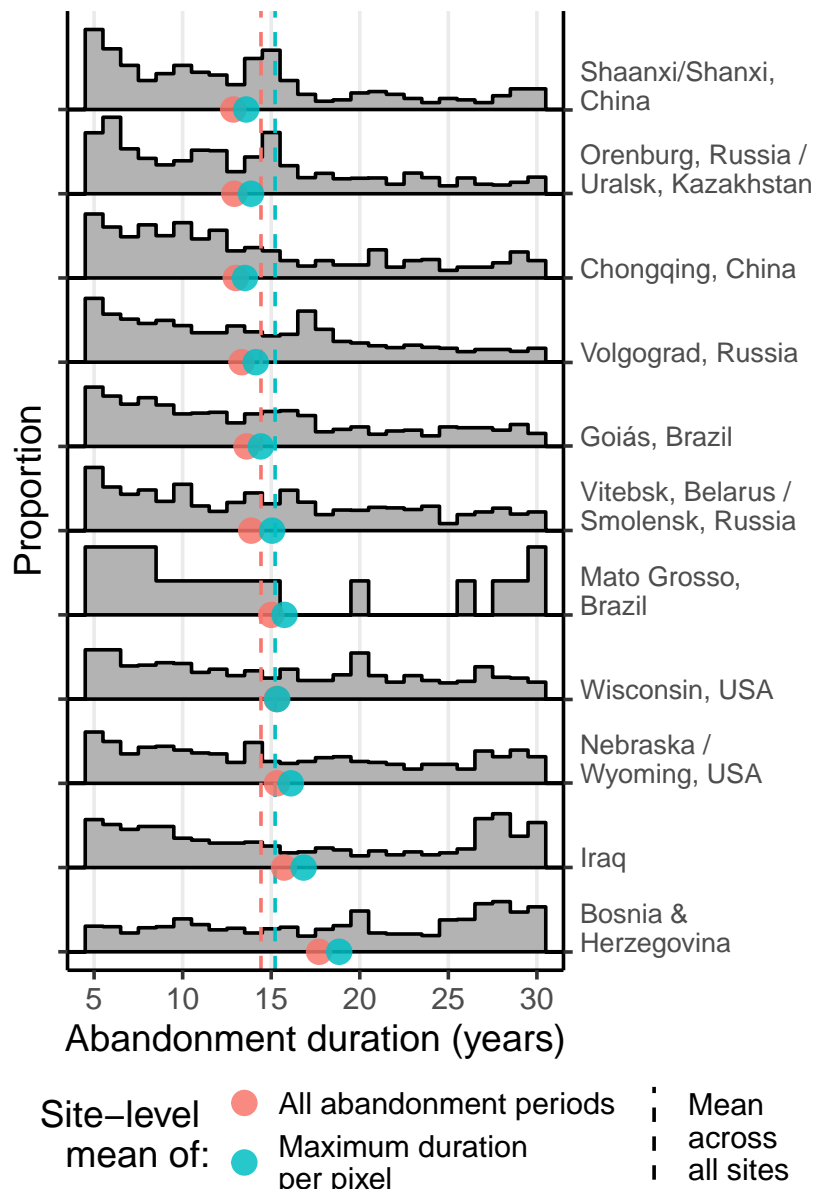


Fig. S6. The distribution of the maximum abandonment duration (in years) for each pixel at each site from 1987 to 2017. The y-scale shows the proportion of pixels with maximum duration values of a given duration at each site. As previously noted, abandonment and recultivation can occur multiple times at a single pixel during our time series, and this figure serves as a companion to the distribution of all abandonment values shown in Figure 2. Site-level mean duration values are shown in the red and blue dots, corresponding to mean values calculated across all periods of abandonment (in red, including multiple periods per pixel) and mean values calculated across only the maximum duration of abandonment at each pixel (in blue). The vertical dashed lines represent the mean of these site-level mean duration values, for all abandonment periods (red) and only the maximum duration at each pixel (blue), respectively.

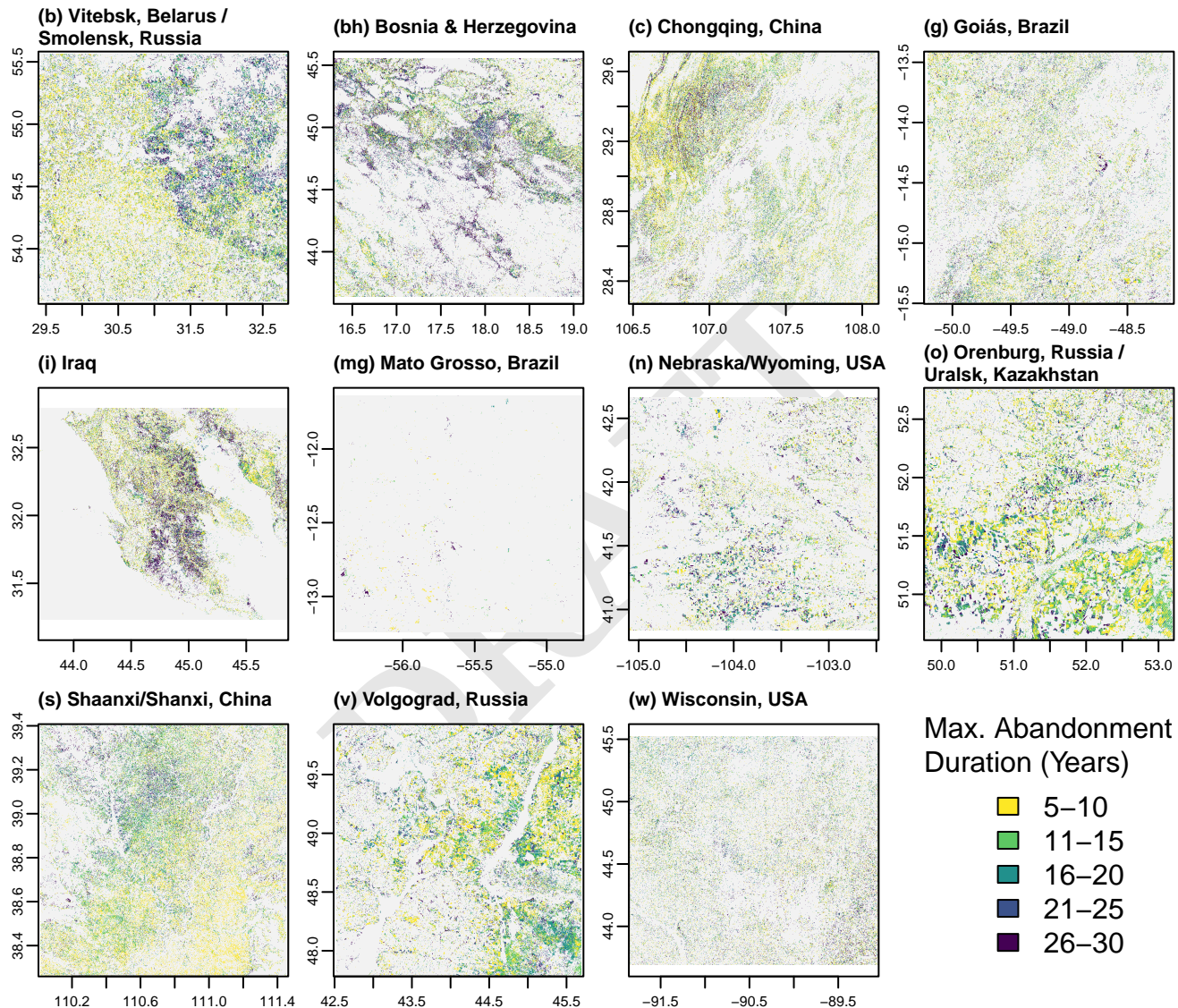


Fig. S7. Maximum duration of cropland abandonment (in years) observed at each pixel between 1987 and 2017 in our eleven study sites. This serves as a companion to maps of the abandonment duration as of 2017 shown in Figure 1. Site locations are shown in Figure S1.

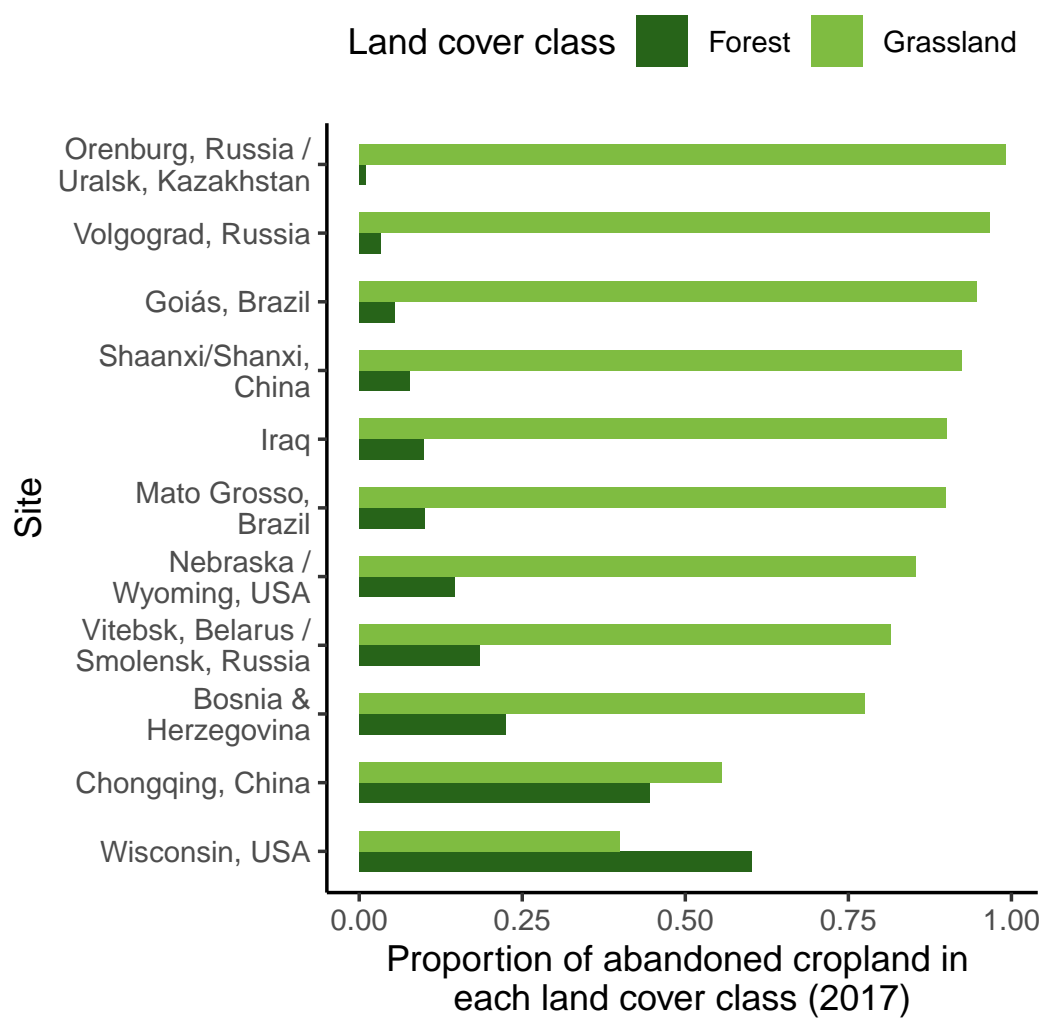


Fig. S8. Proportion of abandoned cropland in each land cover class as of 2017.

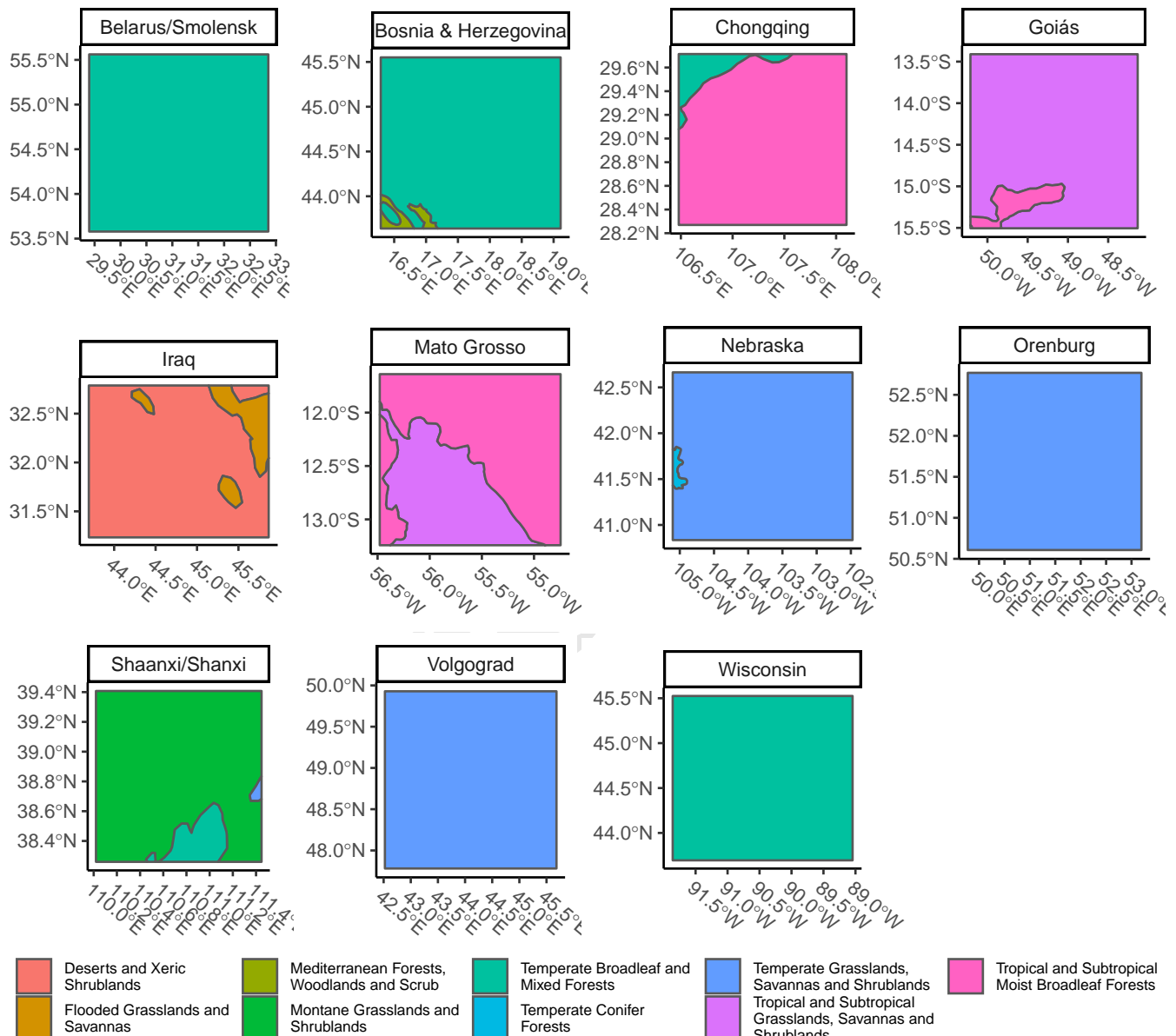


Fig. S9. Site biomes, using biome classifications from The Nature Conservancy's Terrestrial Ecoregions of The World (TEOW) database, derived from Olson et al. (61) and Olson and Dinerstein (62).

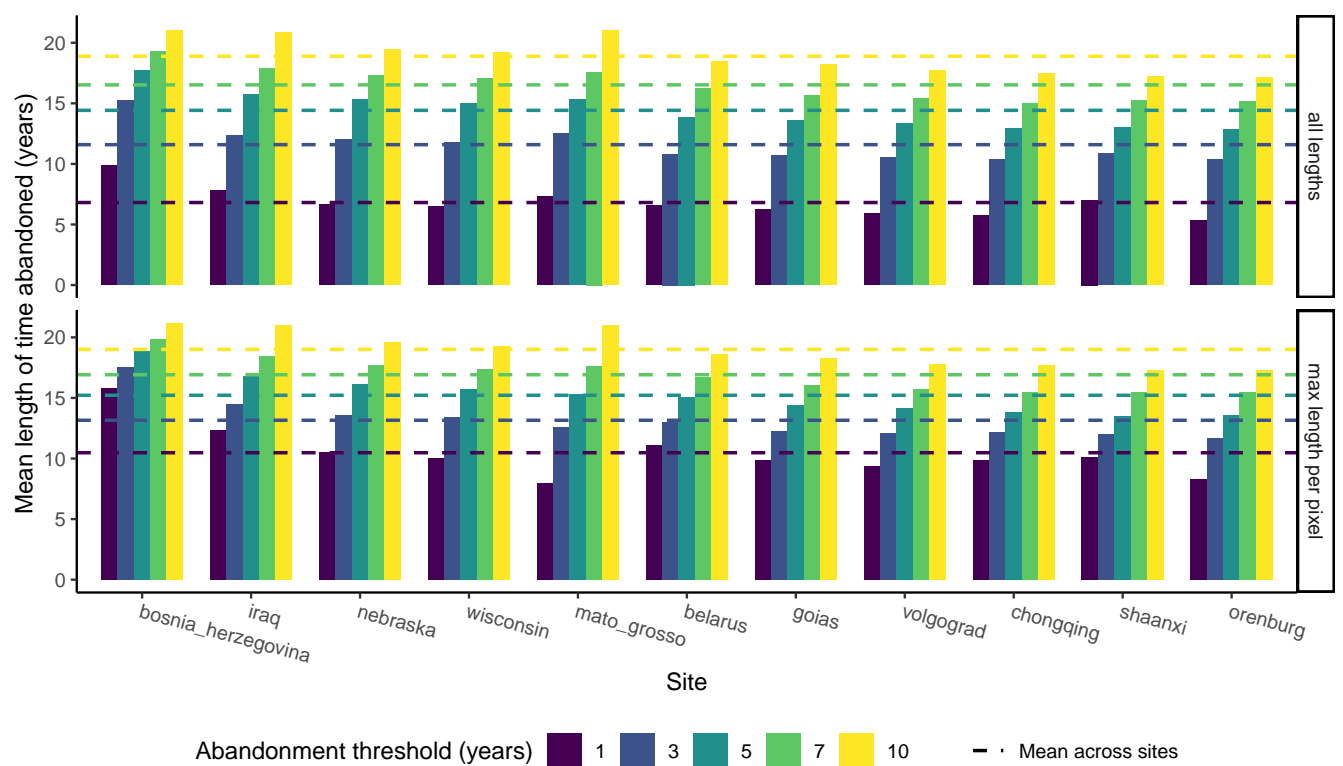


Fig. S10. Mean abandonment lengths shown for various abandonment thresholds.

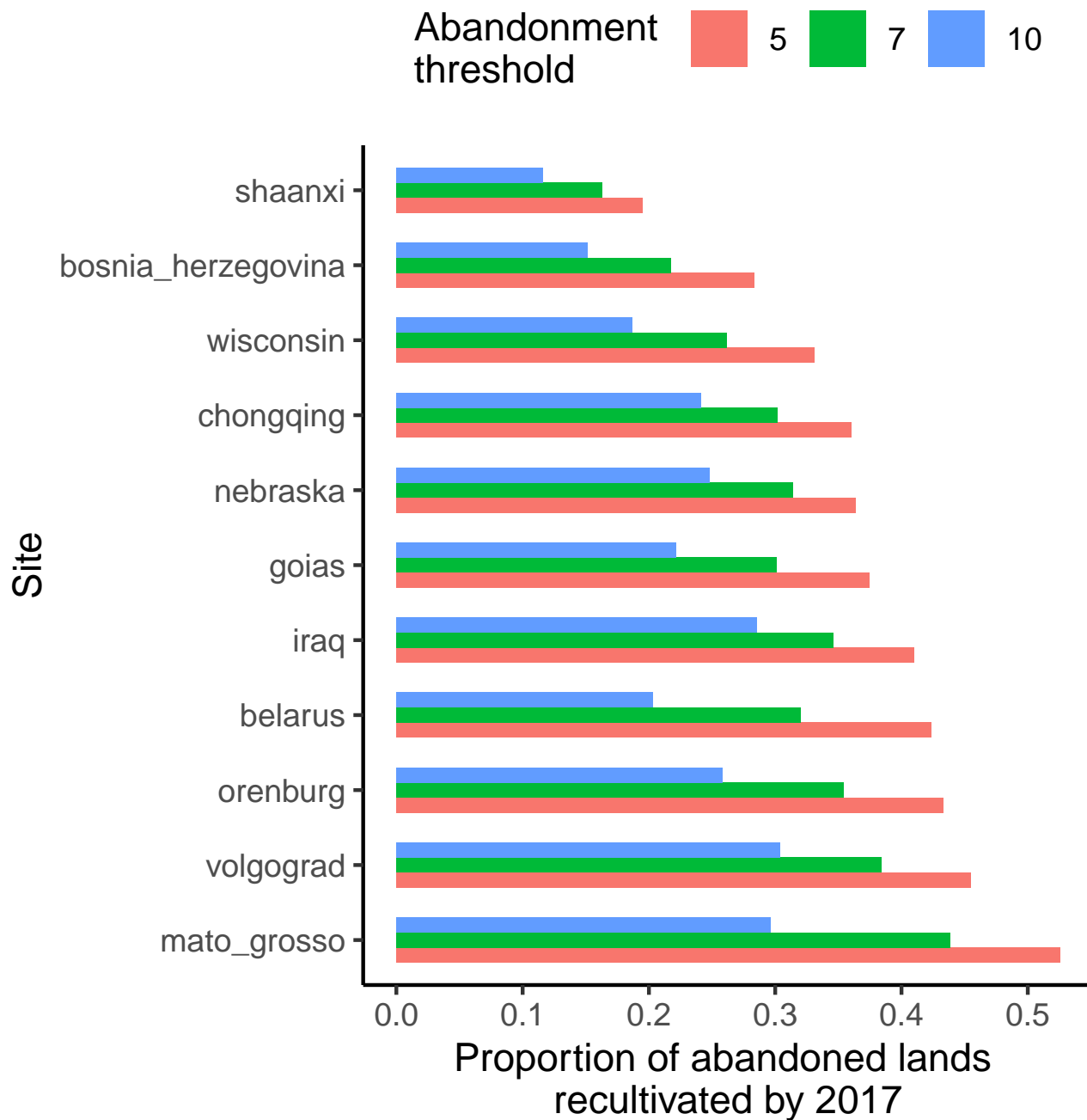


Fig. S11. Recultivation rates shown for various abandonment thresholds.

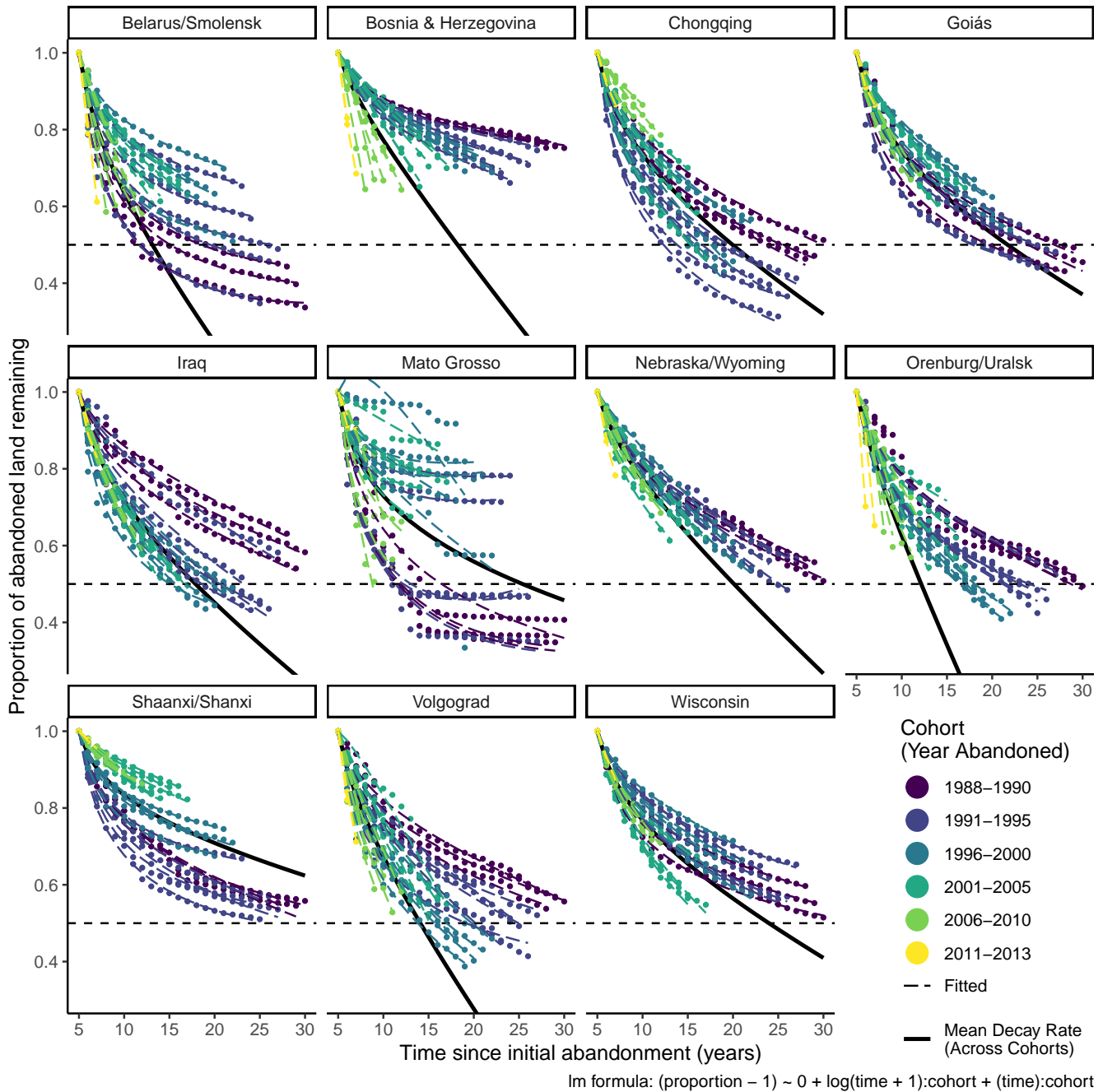


Fig. S12. Decay model results for all sites, showing the proportion of each cohort of abandoned land (i.e., all pixels abandoned in a given year) remaining abandoned over time for each of our eleven sites. Points represent actual observations by cohort, dashed lines represent linear model predictions (fitted values) for each cohort as a function of time (including a linear and logarithmic term of time), and the solid black line represents the site-level mean trend across all cohorts (calculated by taking the mean of each time coefficient values across all cohorts, respectively, and using those two mean values to plot a mean trend). Colors of both points and dashed lines correspond to roughly five-year group of cohorts, ranging from dark purple (oldest cohorts) to green and yellow (most recent cohorts). The horizontal black dashed line shows a proportion of 0.5, indicating the point where half of a cohort has been recultivated. Model diagnostic plots are shown in Figures S14 and S15.

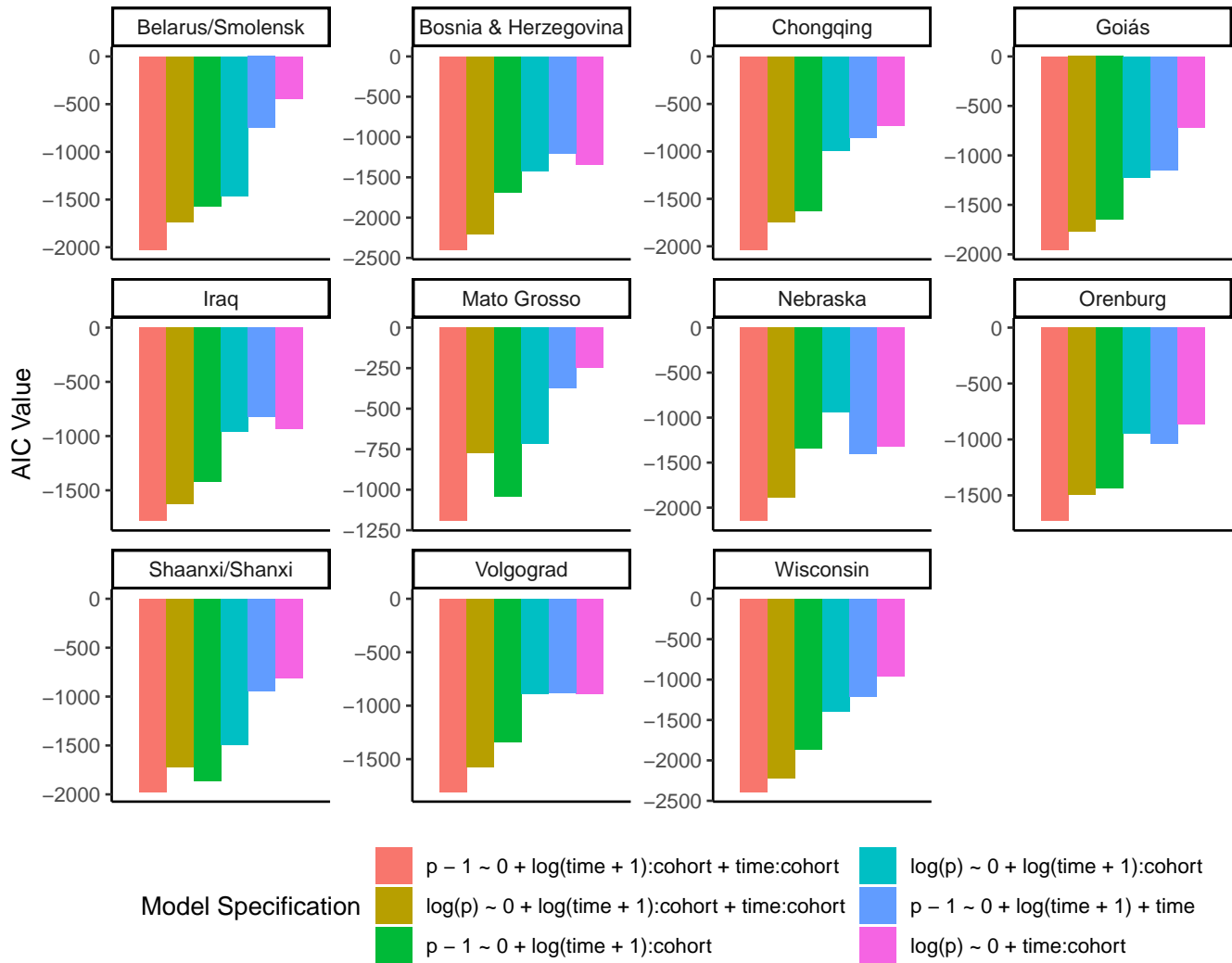


Fig. S13. Akaike Information Criterion (AIC) values for various recultivation ("decay") model specifications for each site. More negative AIC values indicate a better model fit.

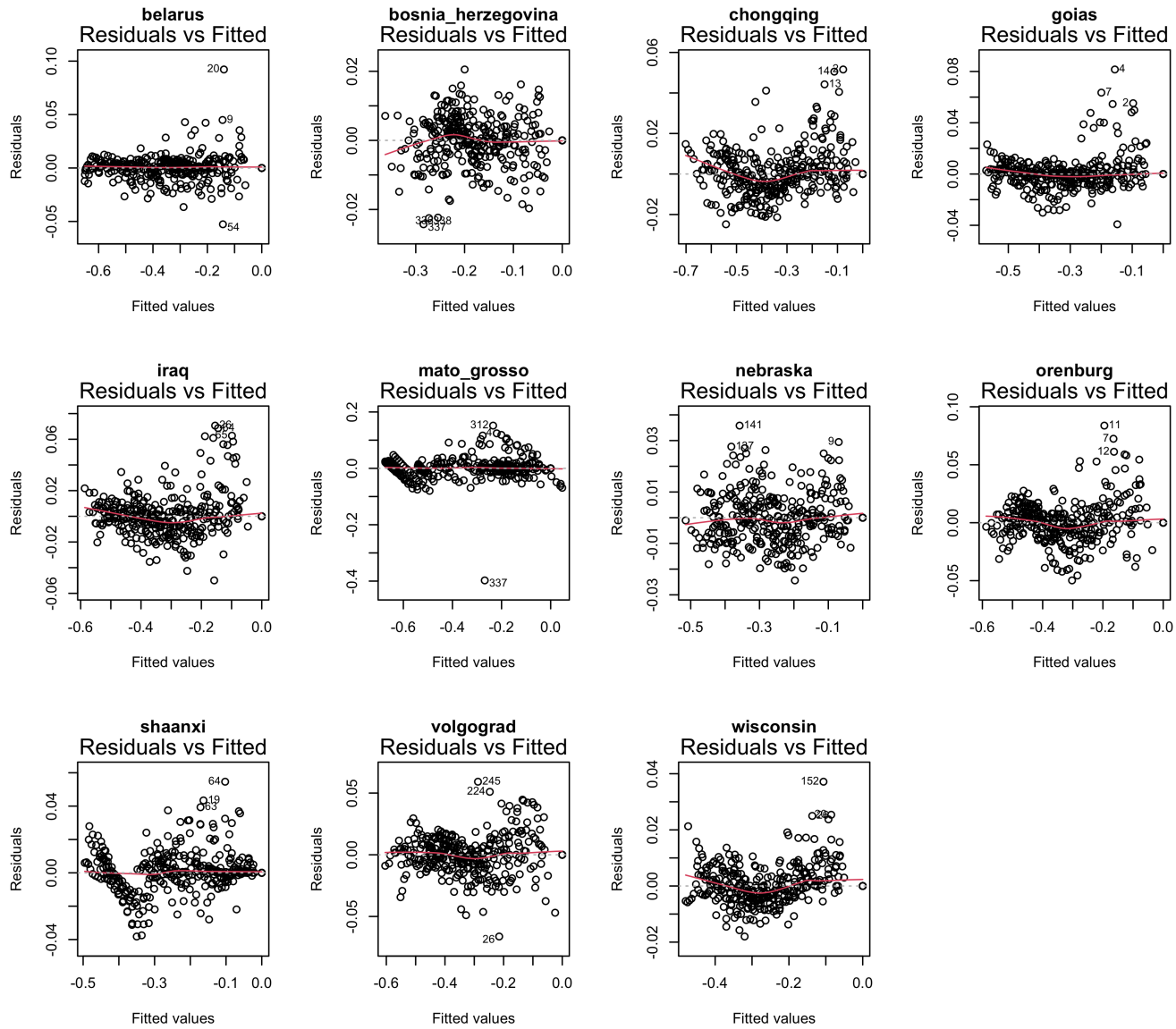


Fig. S14. Residuals vs. fitted diagnostic plots for our linear models of the recultivation ("decay") of abandonment at each site. These models take the form shown in Equation Eq. (S2), and are shown in Figure S12.

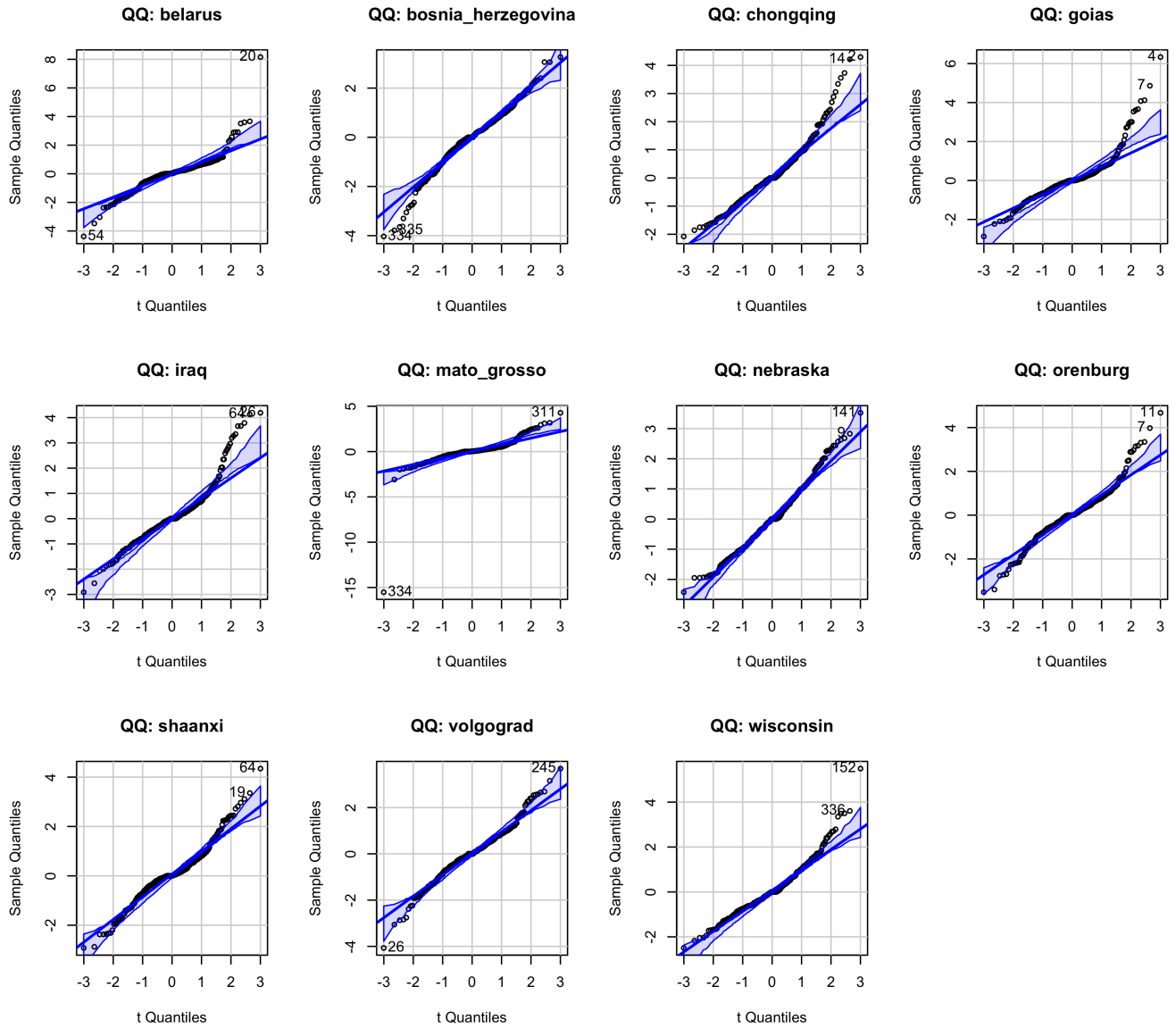


Fig. S15. QQ plots calculated using the `{car}` package (63) for our linear models of the recultivation (“decay”) of abandonment at each site. These models take the form shown in Equation Eq. (S2), and are shown in Figure S12.

Mean Decay Rates By Site

Im formula: $(\text{proportion} - 1) \sim 0 + \log(\text{time} + 1):\text{cohort} + (\text{time}):\text{cohort}$

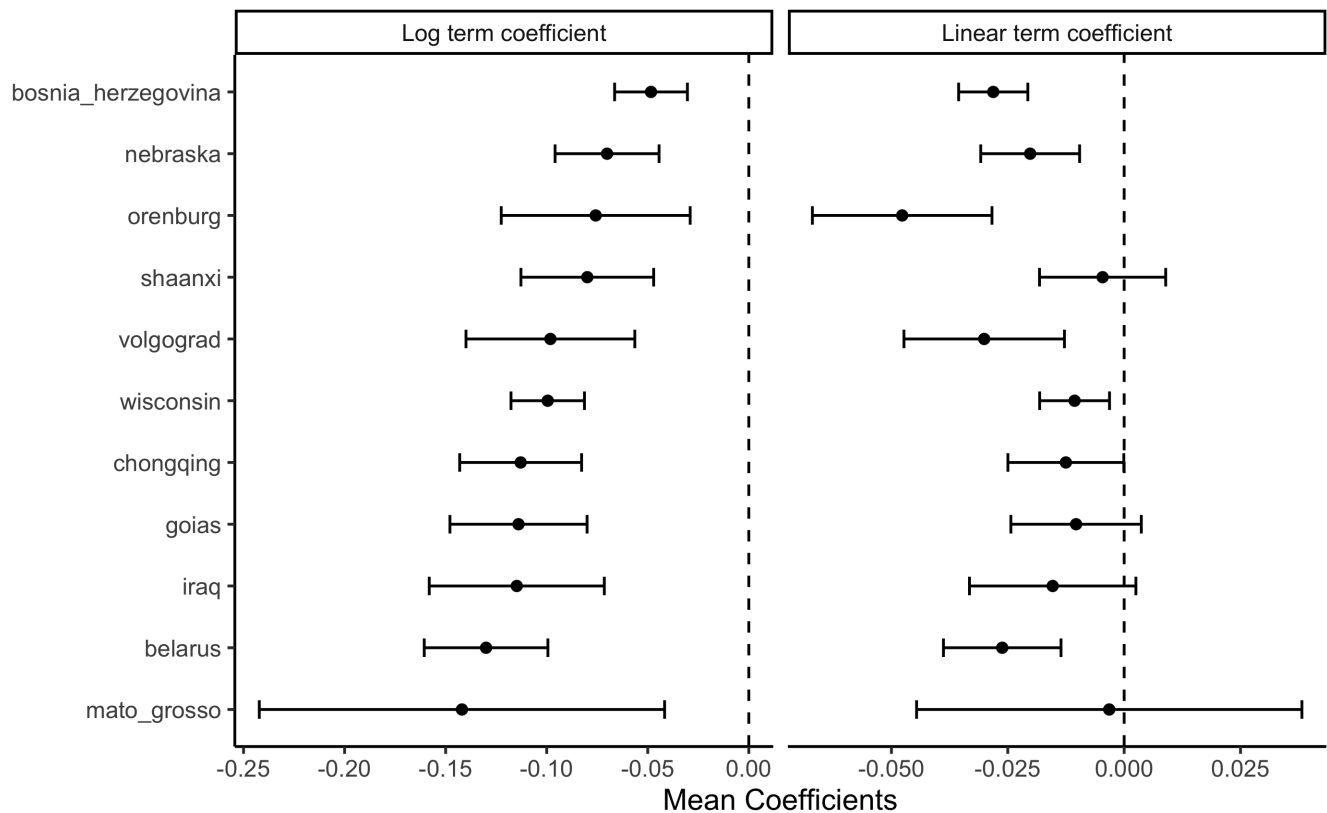


Fig. S16. Mean decay model coefficients across cohorts at each site. The left panel shows the mean coefficient on the $\log(\text{time})$ terms and the right shows the site mean coefficient on the linear time terms. These mean coefficients are used to plot the mean decay trajectories shown in Figure 3.

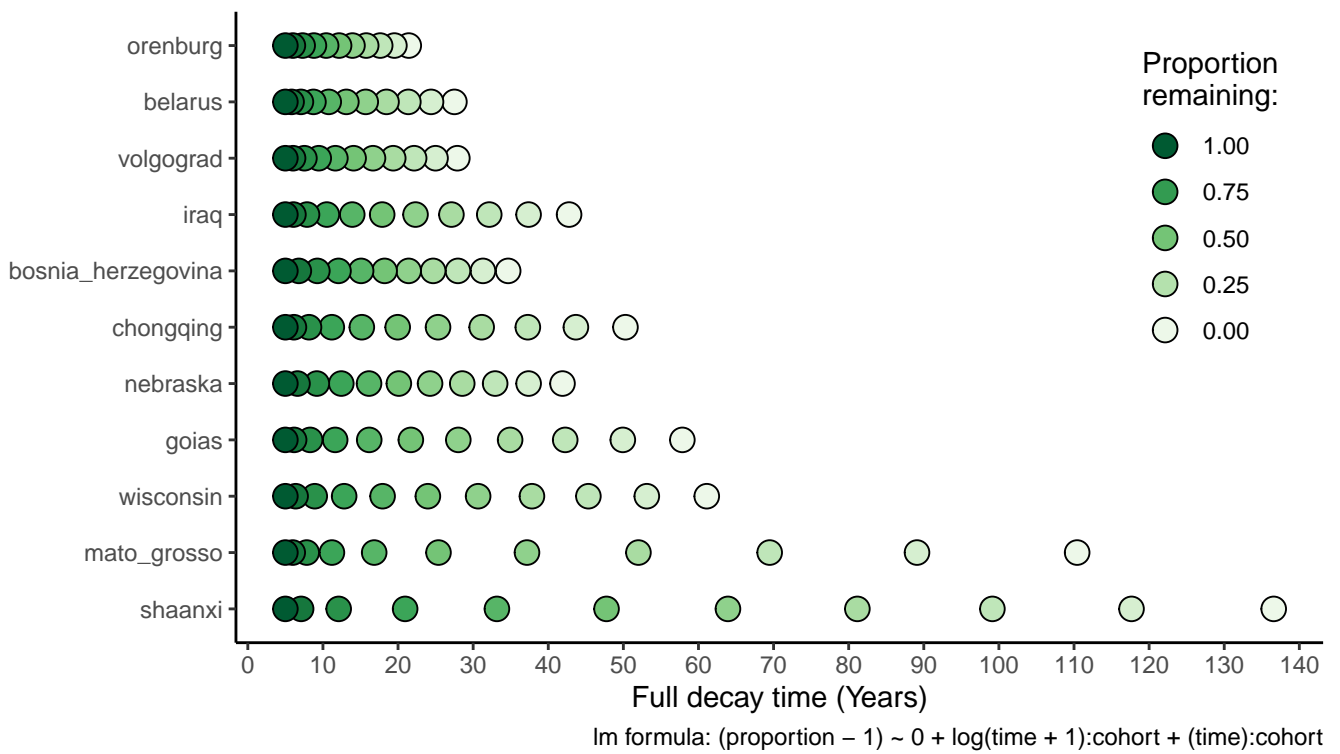


Fig. S17. An alternative representation of the mean decay rate for each site (also shown in Figure 3). The color of each point corresponds to the proportion remaining after a given amount of time.

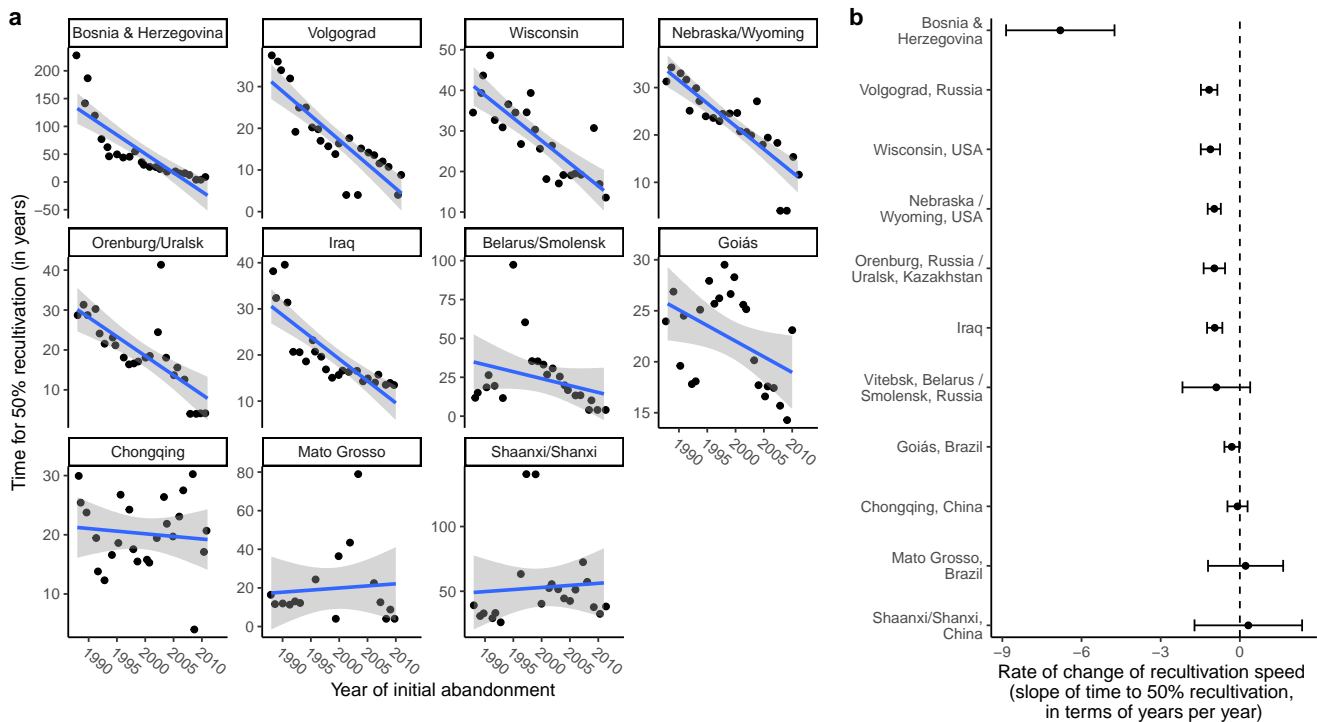


Fig. S18. The rate of change of decay rates (measured as the half-life, or the time required for 50% of each cohort to be recultivated) at each site over the course of the time series. Individual site trends are shown in panel a. Solid lines show simple linear regressions, the slopes of which are shown in panel b. Gray bands around the linear trends in panel a and the error bars on slope estimates in panel b both represent 95% confidence intervals. These models are described by Eq. Eq. (S3). Model diagnostic plots are shown in Figures S19 and S20.

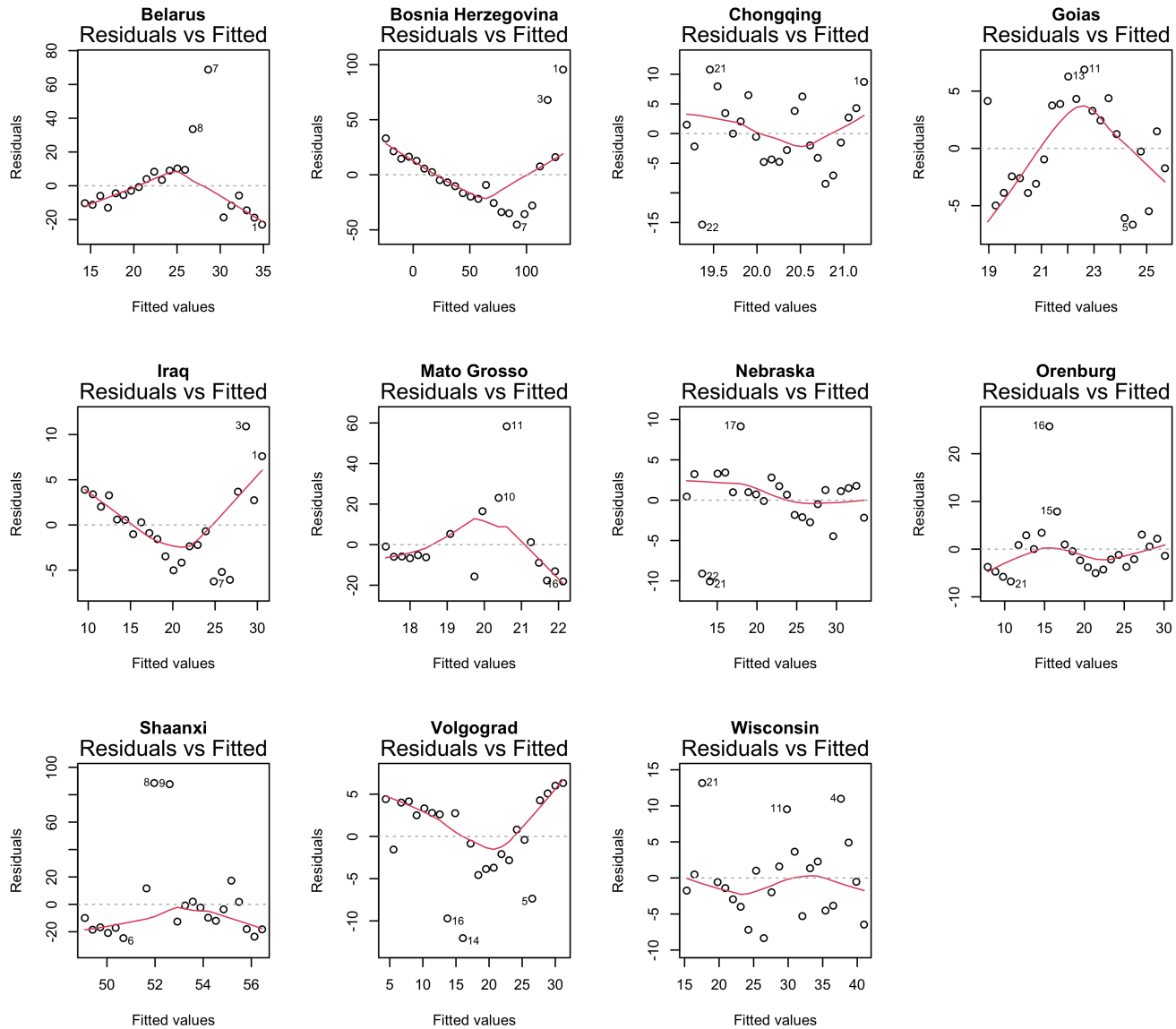


Fig. S19. Residuals vs. fitted diagnostic plots for each site, for a simple 1m call corresponding to Eq. Eq. (S3), in which the half-life (i.e., the time required for half (50%) of a given cohort of abandoned cropland to be recultivated) is modeled as a function of the year of initial abandonment at each site.

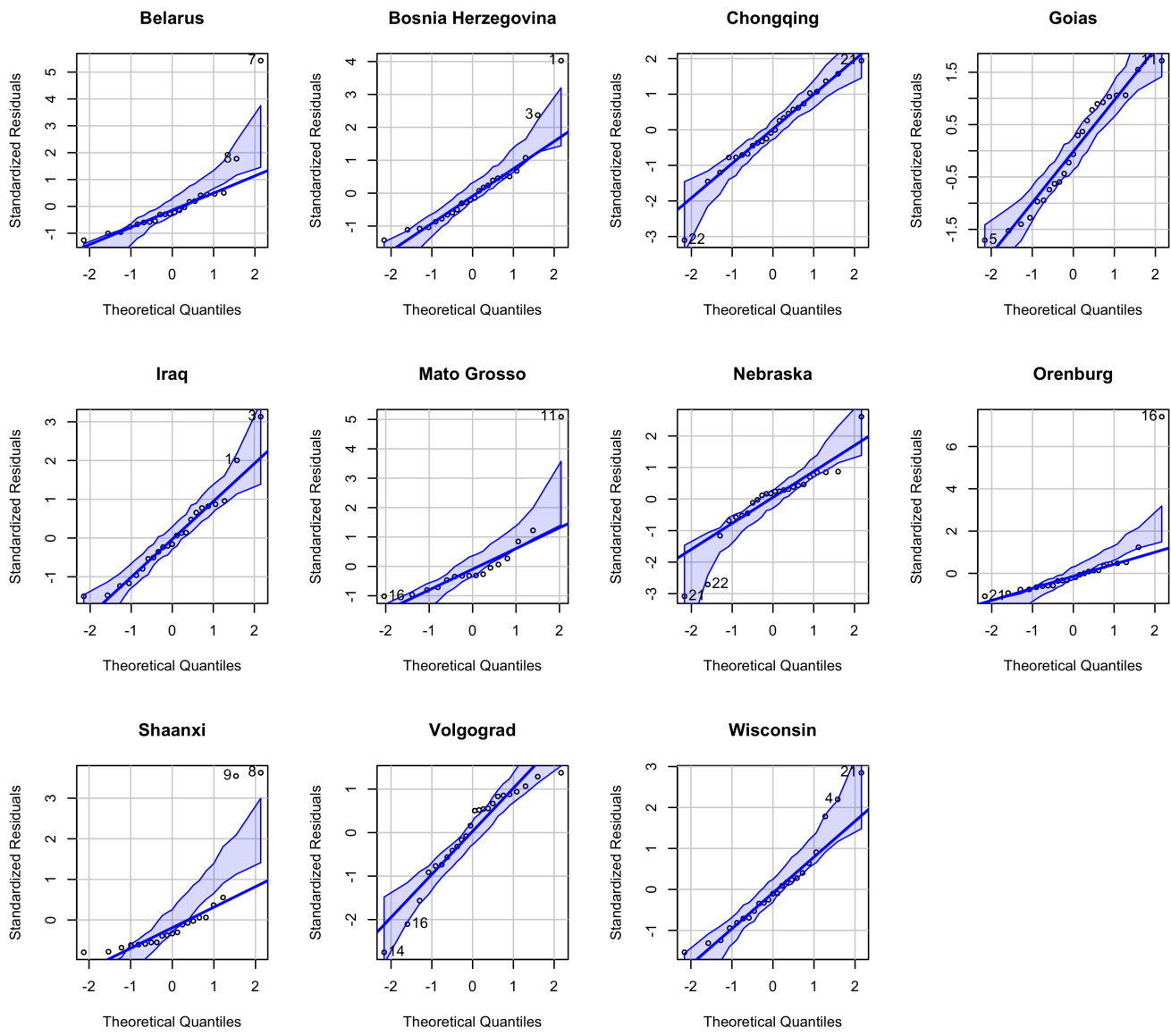


Fig. S20. QQ plots calculated using the `car` package ((63)), for a simple `1m` call corresponding to Eq. Eq. (S3), in which the half-life (i.e., the time required for half (50%) of a given cohort of abandoned cropland to be recultivated) is modeled as a function of the year of initial abandonment at each site.

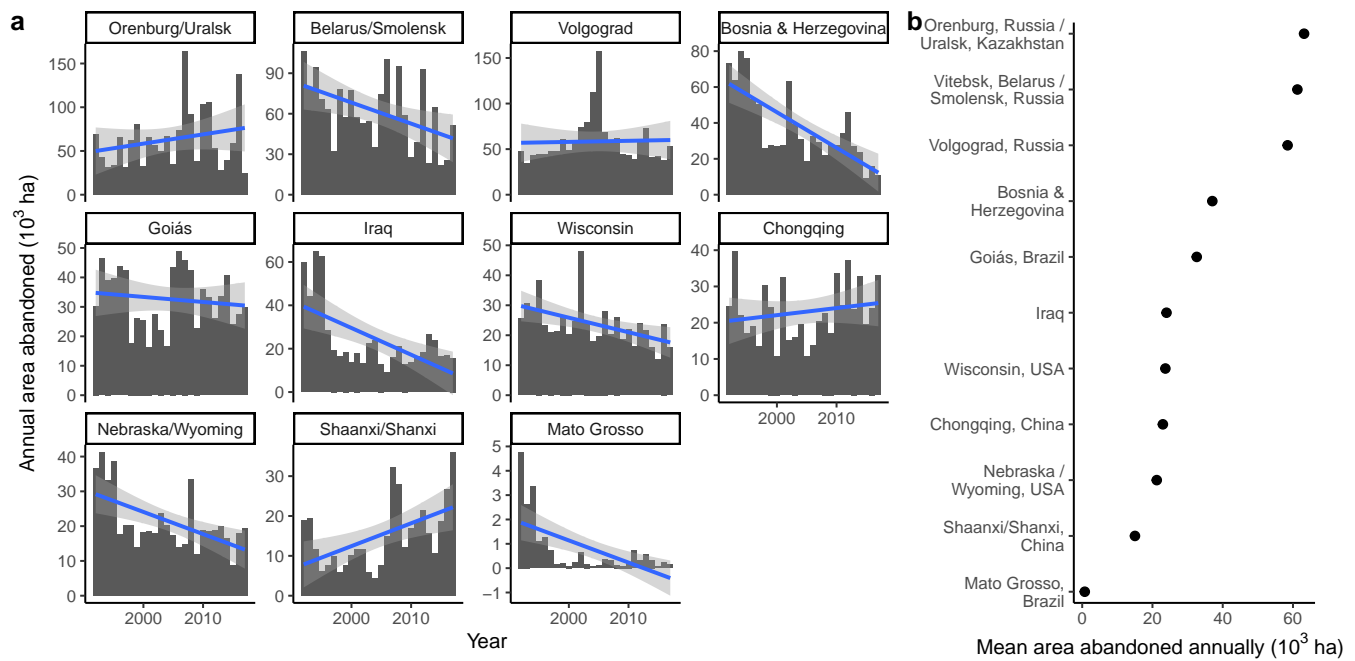


Fig. S21. Annual gain in newly abandoned cropland at our eleven sites. Panel a shows the trend in annual abandonment over time at each site (in 10^3 ha), and Panel b shows the mean annual abandonment (in 10^3 ha) at each site. The mean values in panel b feed into the extrapolations. Note that the annual gain in abandonment corresponds to the dark green bars in Figure S5.

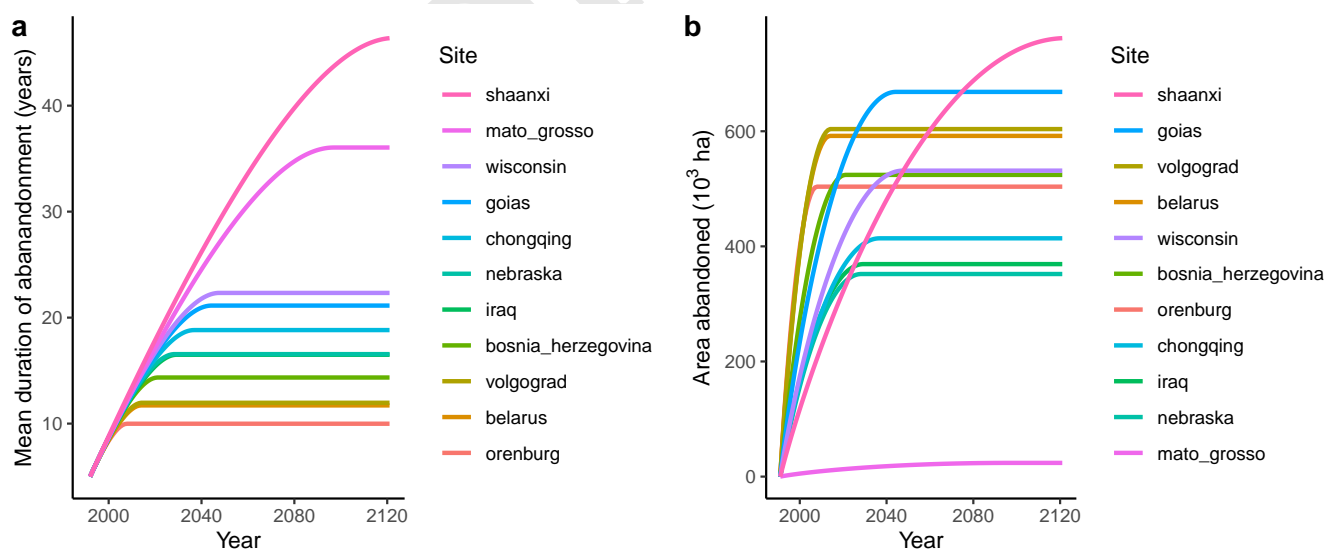


Fig. S22. The results of our simple extrapolation, including a) the mean age of abandonment, and b) the total area abandoned into the future. Colors corresponding to each site are consistent across the three panels. These extrapolations assume recultivation based on the mean decay trend for each site Figure 3 and annual new abandonment based on the mean annual gain in abandonment shown in Figure S5 (dark green bars).

Extrapolation 1

Assuming i) mean decay rates and ii) constant area abandoned each year.

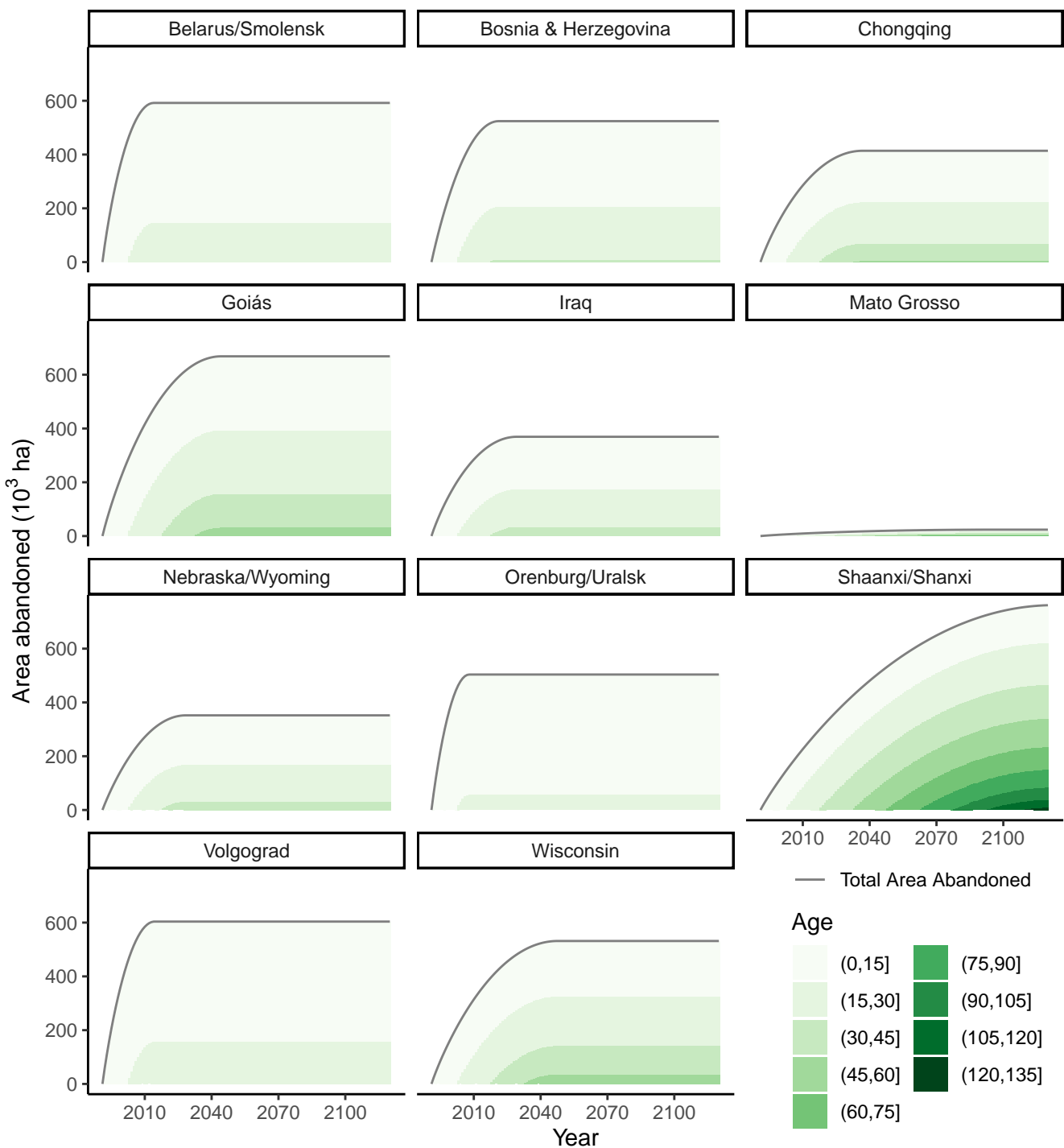


Fig. S23. Extrapolating area by age bin, assuming a 1) each site follows the mean recultivation ("decay") rate, and 2) a constant area abandoned each year (based on the mean annual area abandoned at each site).

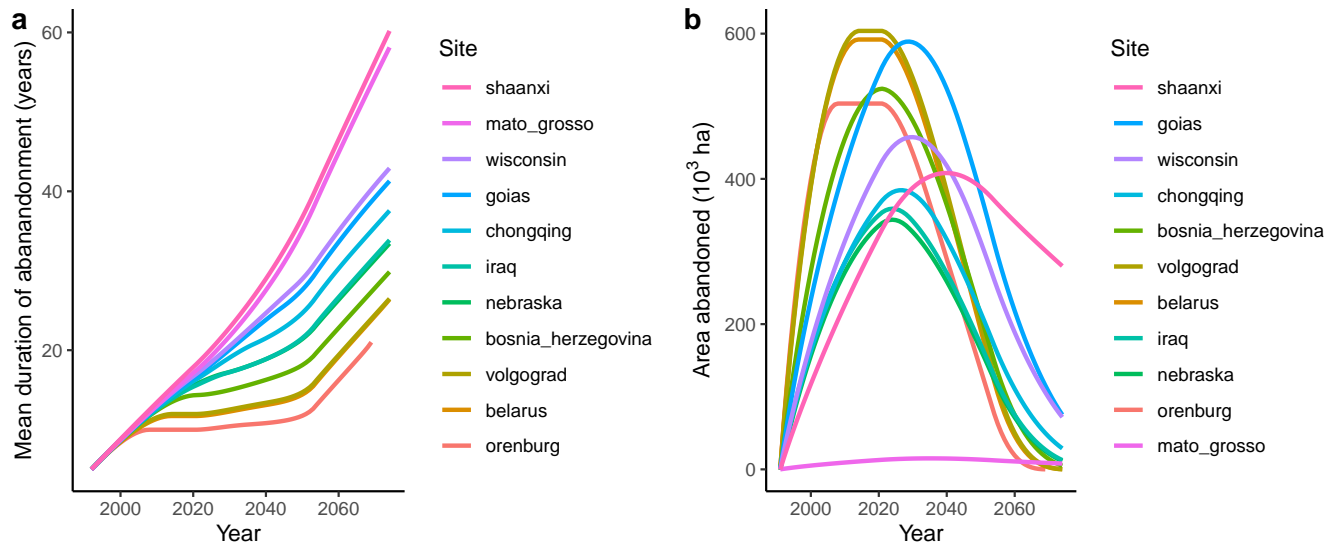


Fig. S24. The results of our second extrapolation, including a) the mean age of abandonment, and b) the total area abandoned into the future. Colors corresponding to each site are consistent across the three panels. These extrapolations assume recultivation based on the mean decay trend for each site (Figure 3) and annual new abandonment based on the mean annual gain in abandonment shown in Figure S5 (dark green bars).

Extrapolation 2

Assuming i) mean decay rates and ii) constant area abandoned each year until 2017, then linear decline in area abandoned each year until reaching 0 in 2050.

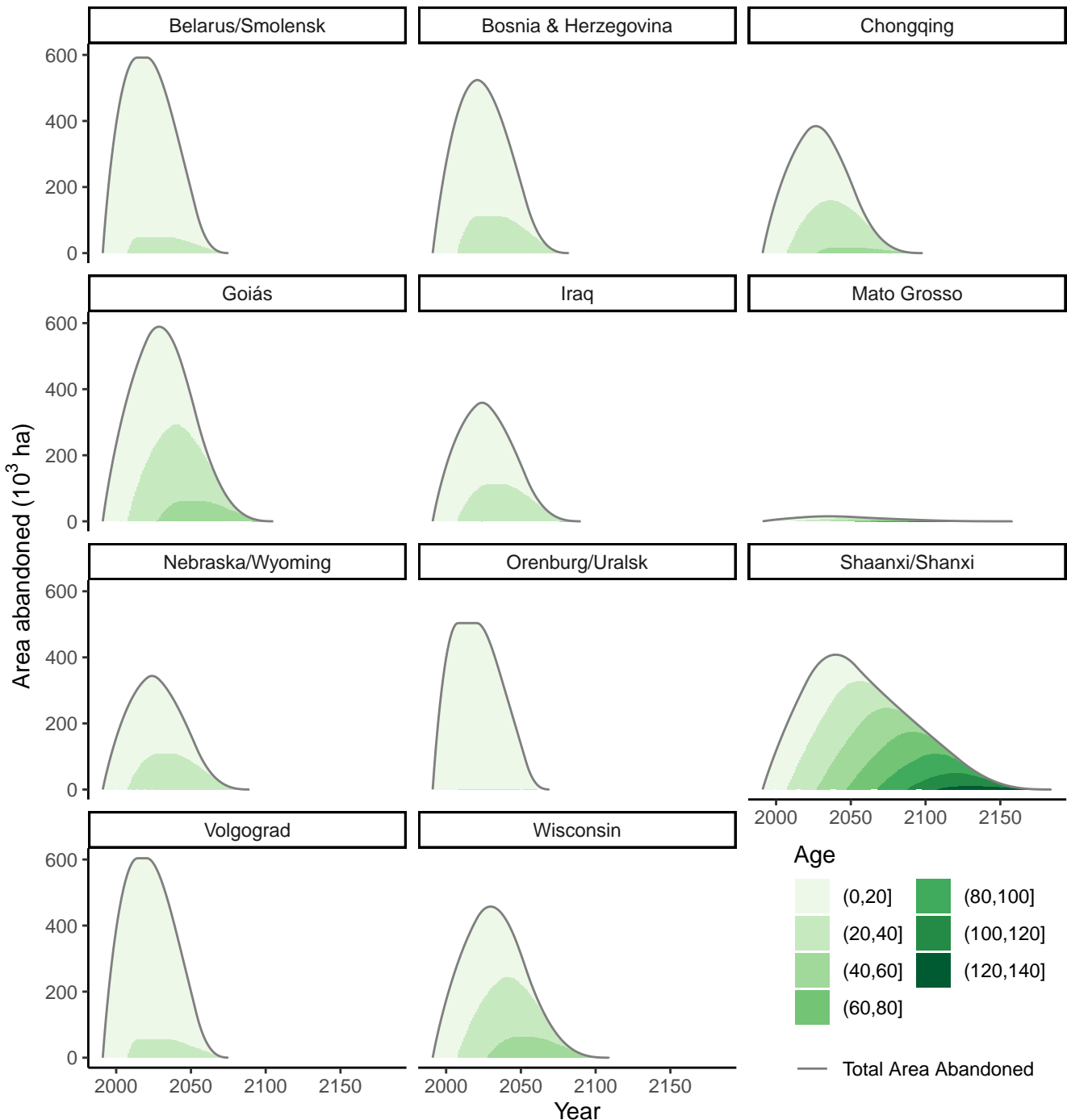


Fig. S25. Extrapolating area by age bin, assuming a 1) each site follows the mean recultivation ("decay") rate, and 2) a constant area abandoned each year until 2017 (based on the mean annual area abandoned at each site), followed by a linearly declining area abandoned each year until reaching 0 in 2050.

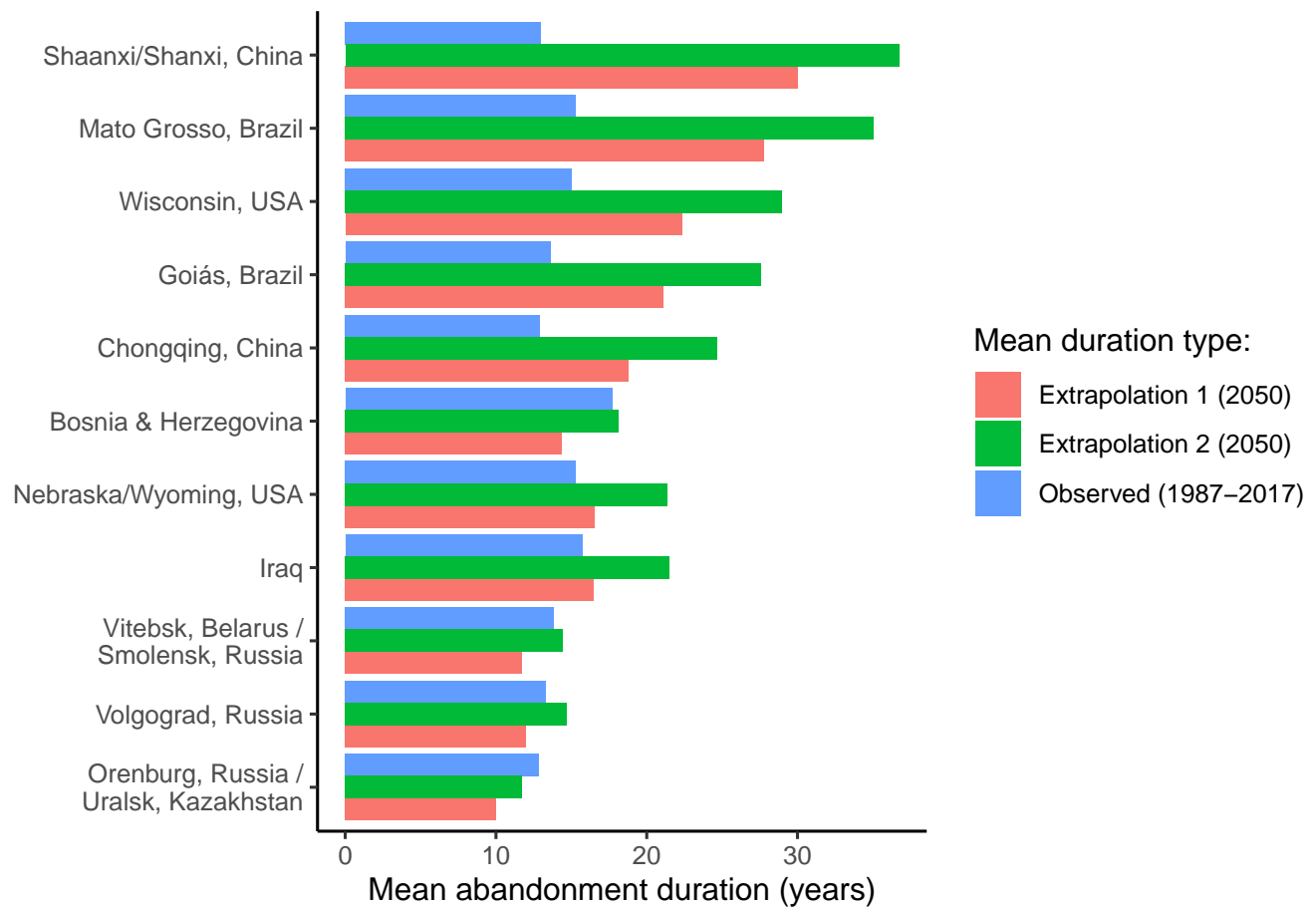


Fig. S26. Comparing the mean duration of abandonment at our 11 sites observed between 1987 and 2017 with the extrapolated mean duration as of 2050 for our two extrapolations.

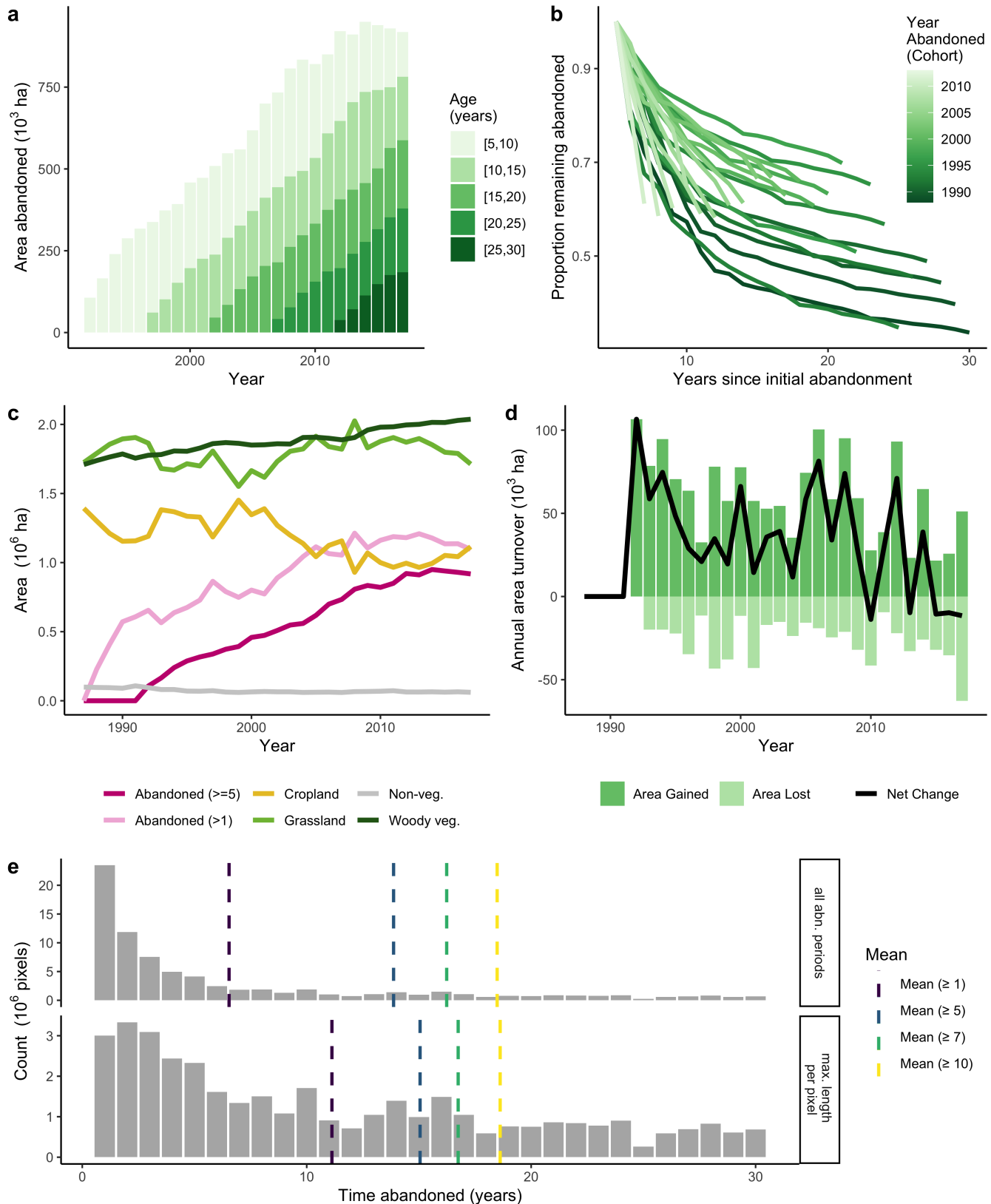


Fig. S27. Abandonment patterns for Vitebsk, Belarus / Smolensk, Russia, showing a) accumulation of abandoned land by age class, b) decay of abandoned land by year abandoned, c) the area in each land cover class through time (including both land that has been abandoned for five or more years, as well as any land abandoned for 1 or more years, therefore including short-term fallows), d) the annual turnover of abandoned land through time, and e) the distribution of abandonment duration for all periods of cropland abandonment (top) and the maximum duration of abandonment at each pixel (bottom).

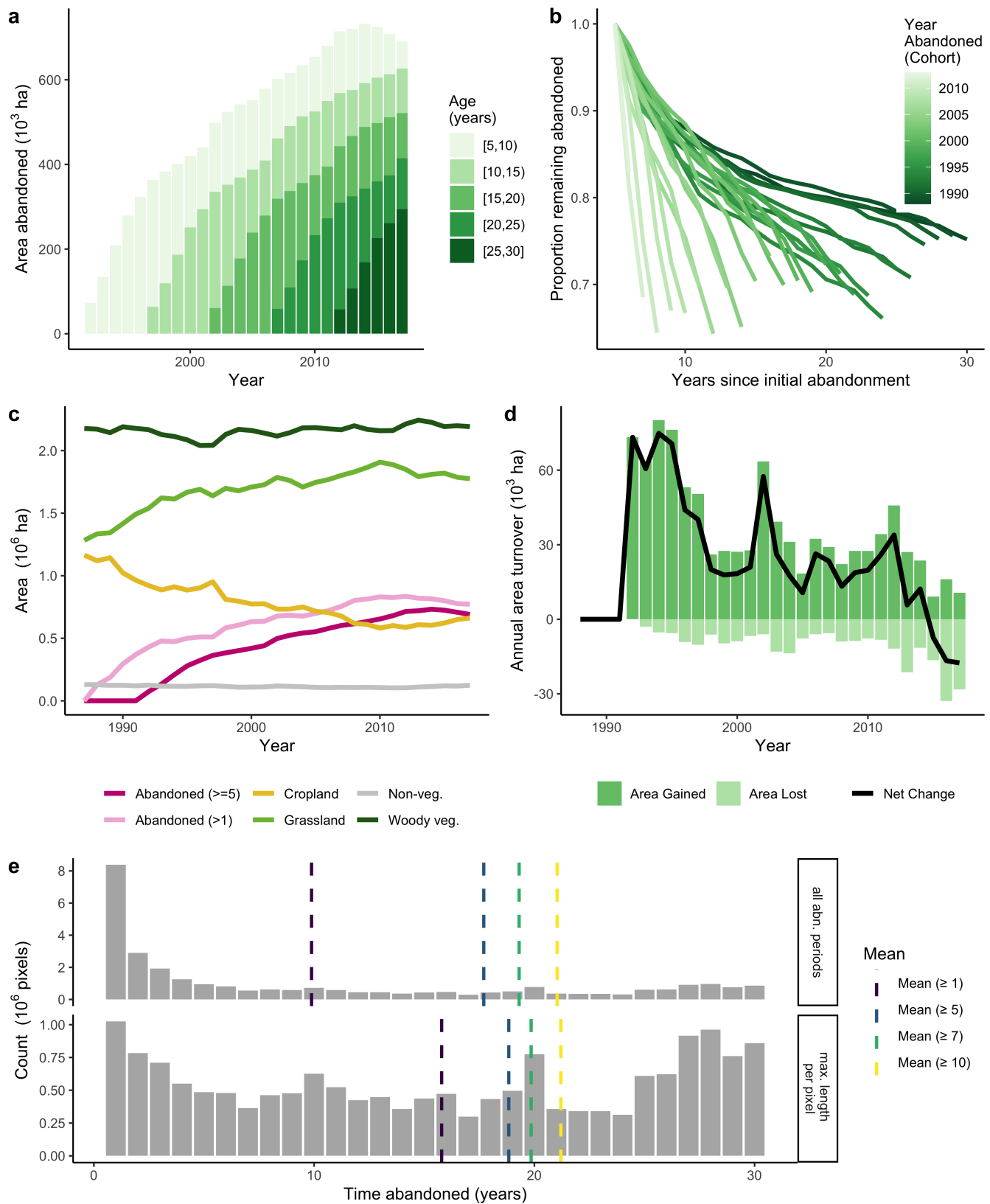


Fig. S28. Abandonment patterns for Bosnia & Herzegovina, following Figure S27.

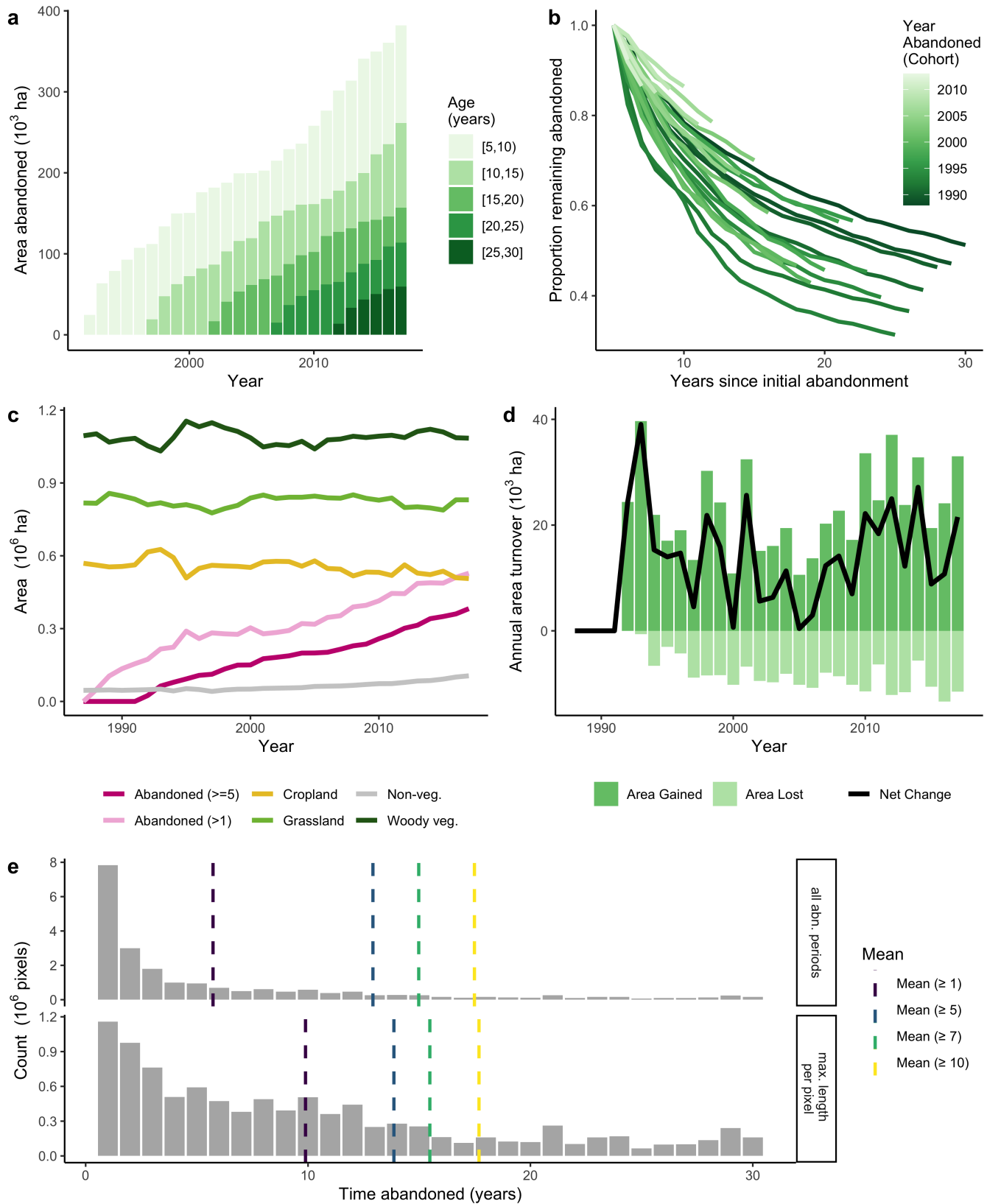


Fig. S29. Abandonment patterns for Chongqing, China, following Figure S27.

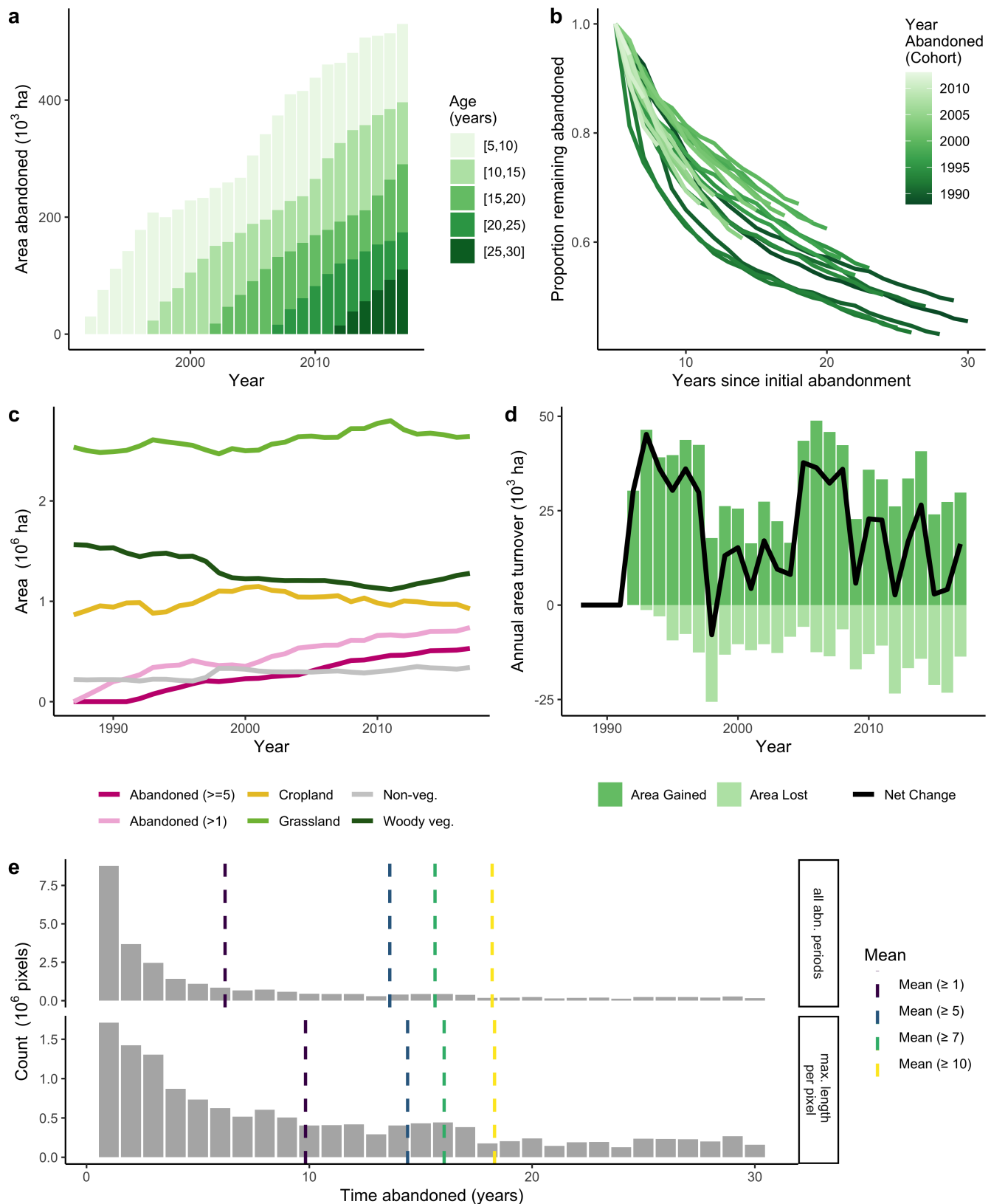


Fig. S30. Abandonment patterns for Goiás, Brazil, following Figure S27.

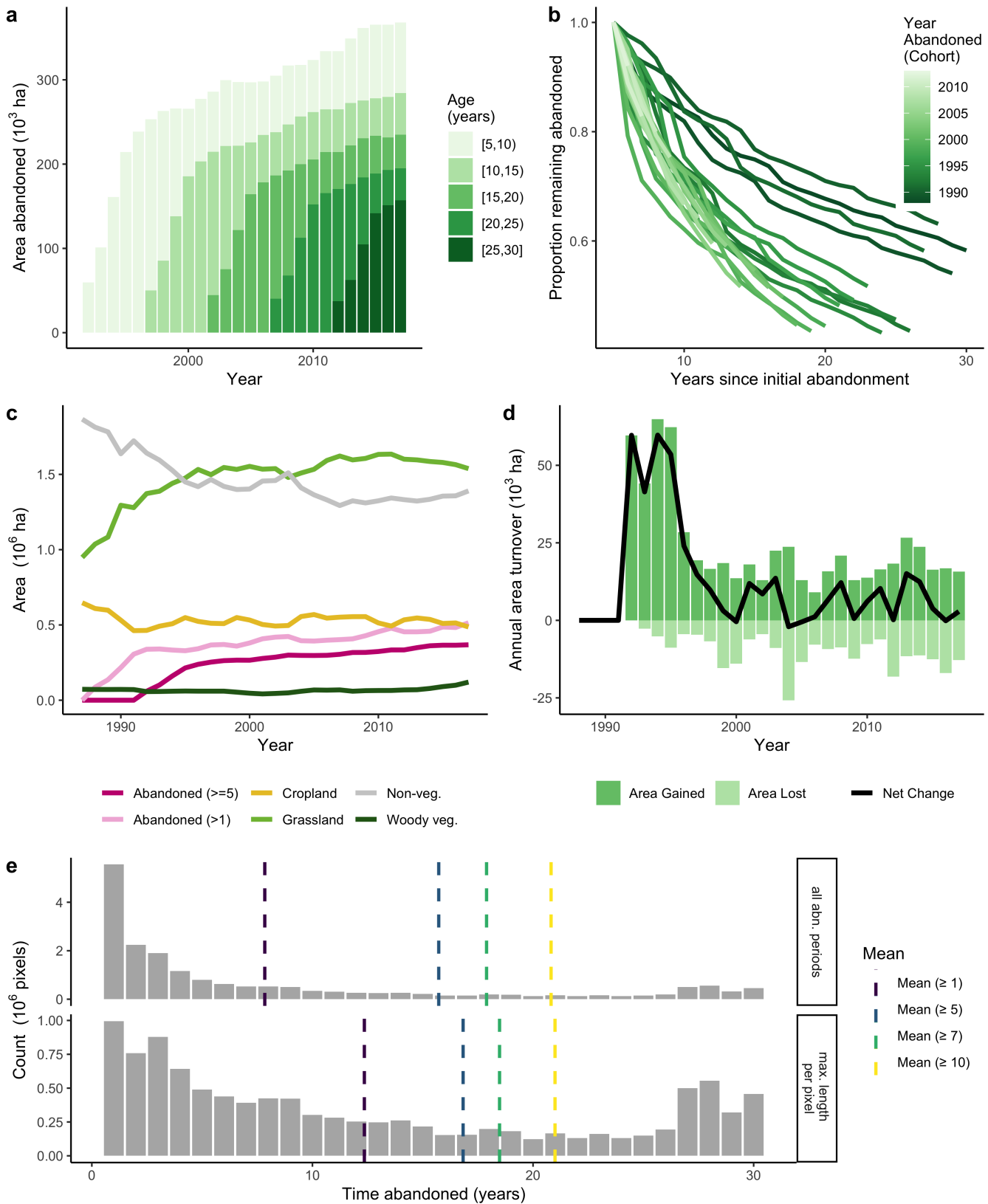


Fig. S31. Abandonment patterns for Iraq, following Figure S27.

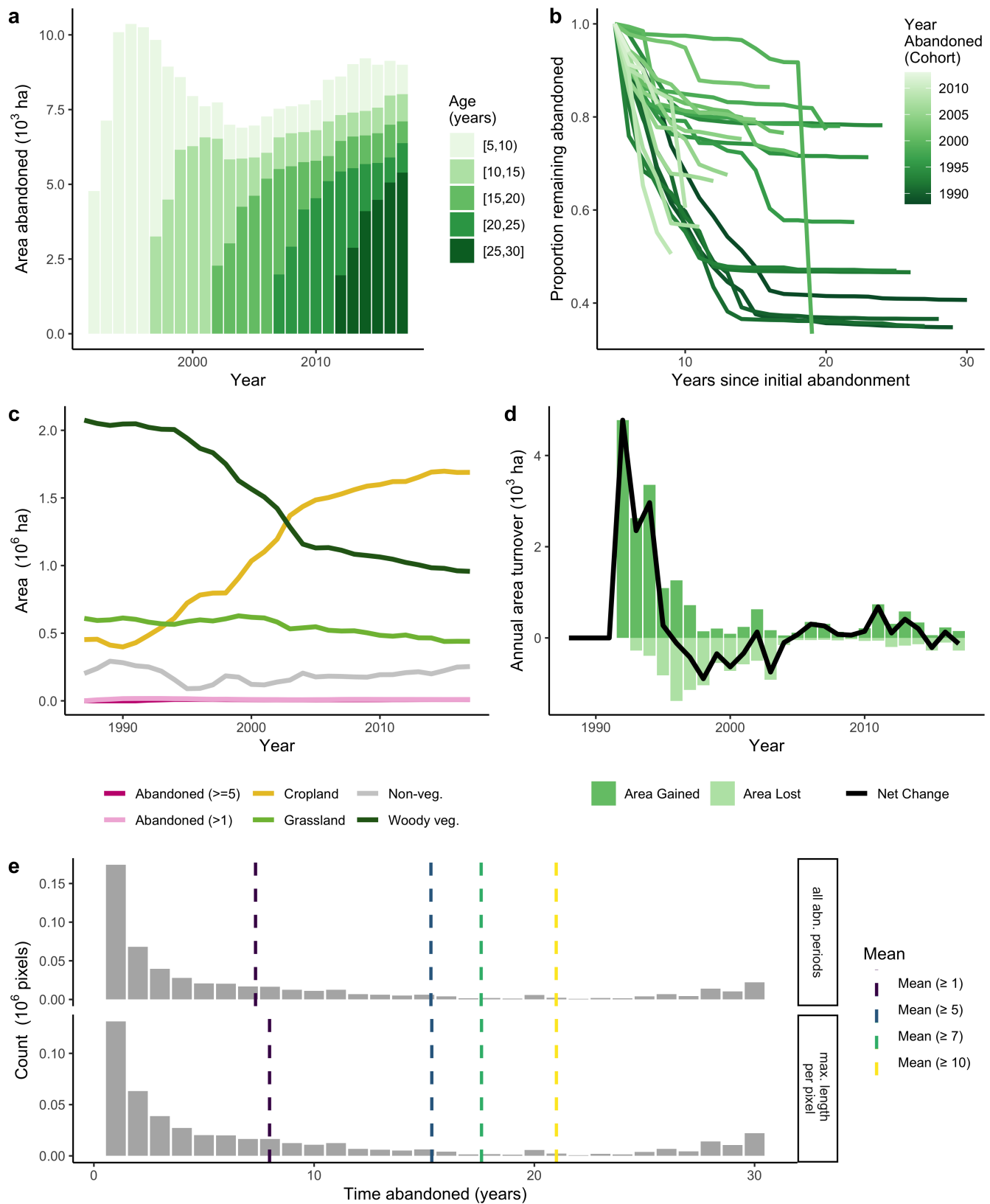


Fig. S32. Abandonment patterns for Mato Grosso, Brazil, following Figure S27.

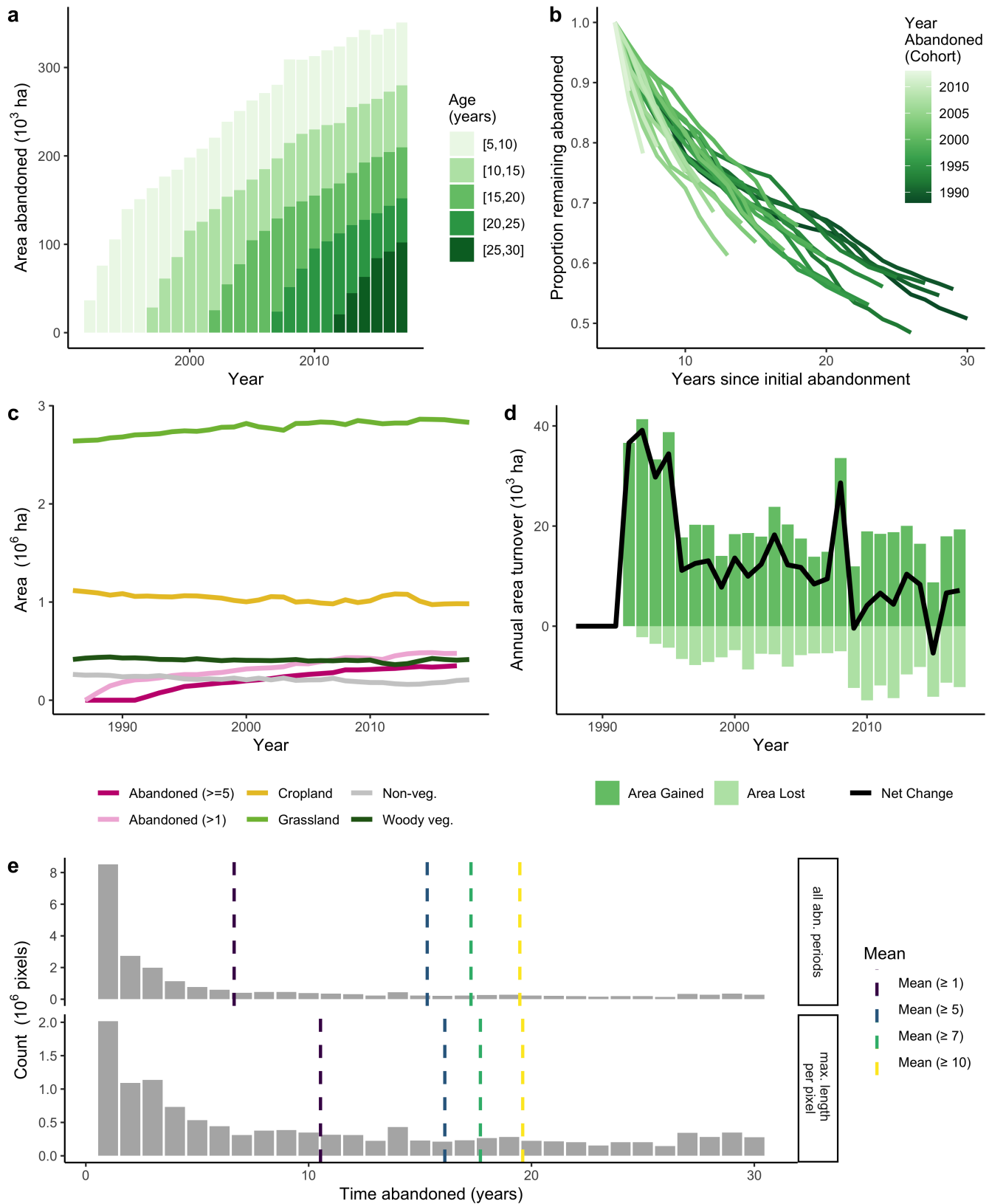


Fig. S33. Abandonment patterns for Nebraska/Wyoming, USA, following Figure S27.

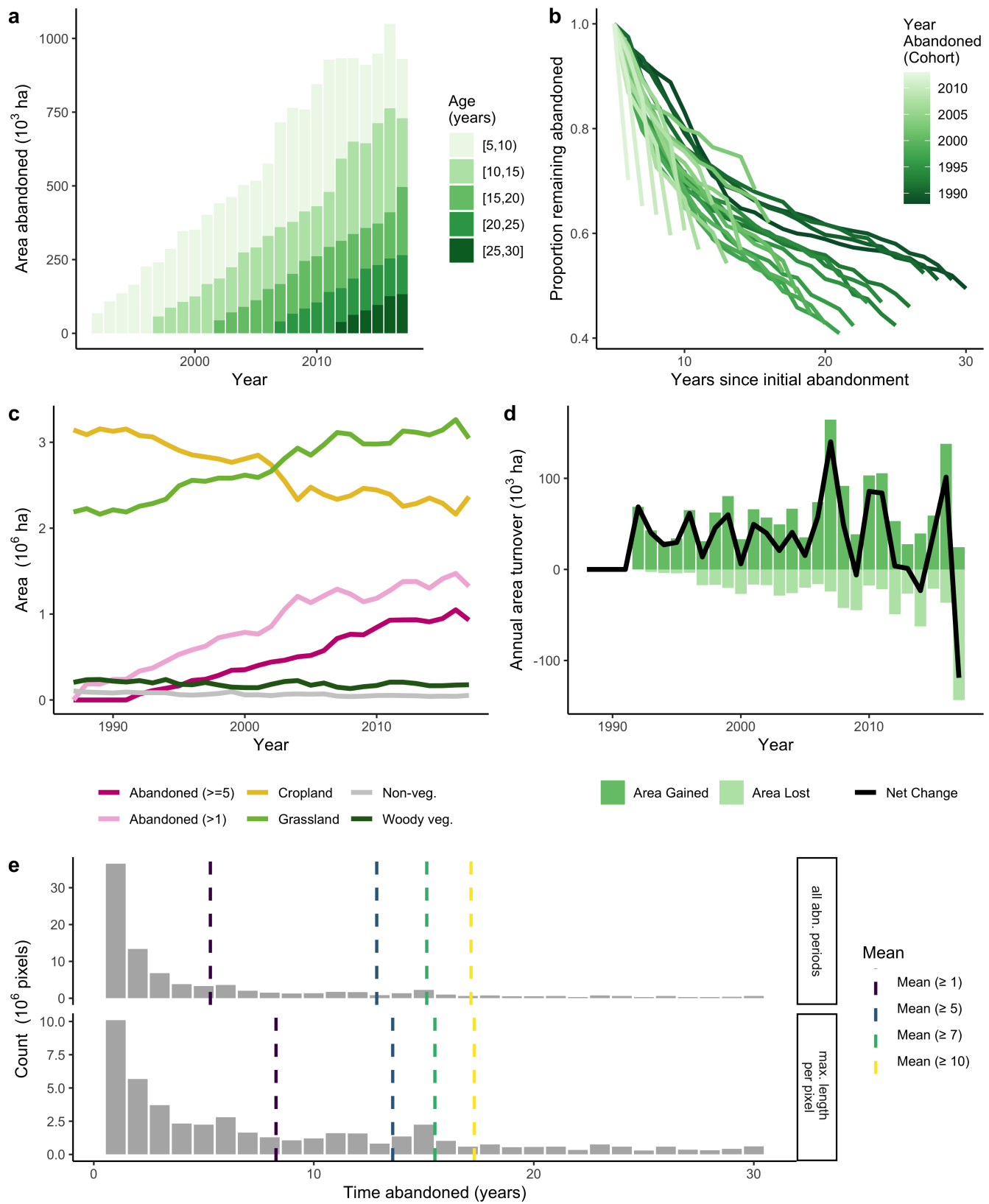


Fig. S34. Abandonment patterns for Orenburg, Russia / Uralsk, Kazakhstan, following Figure S27.

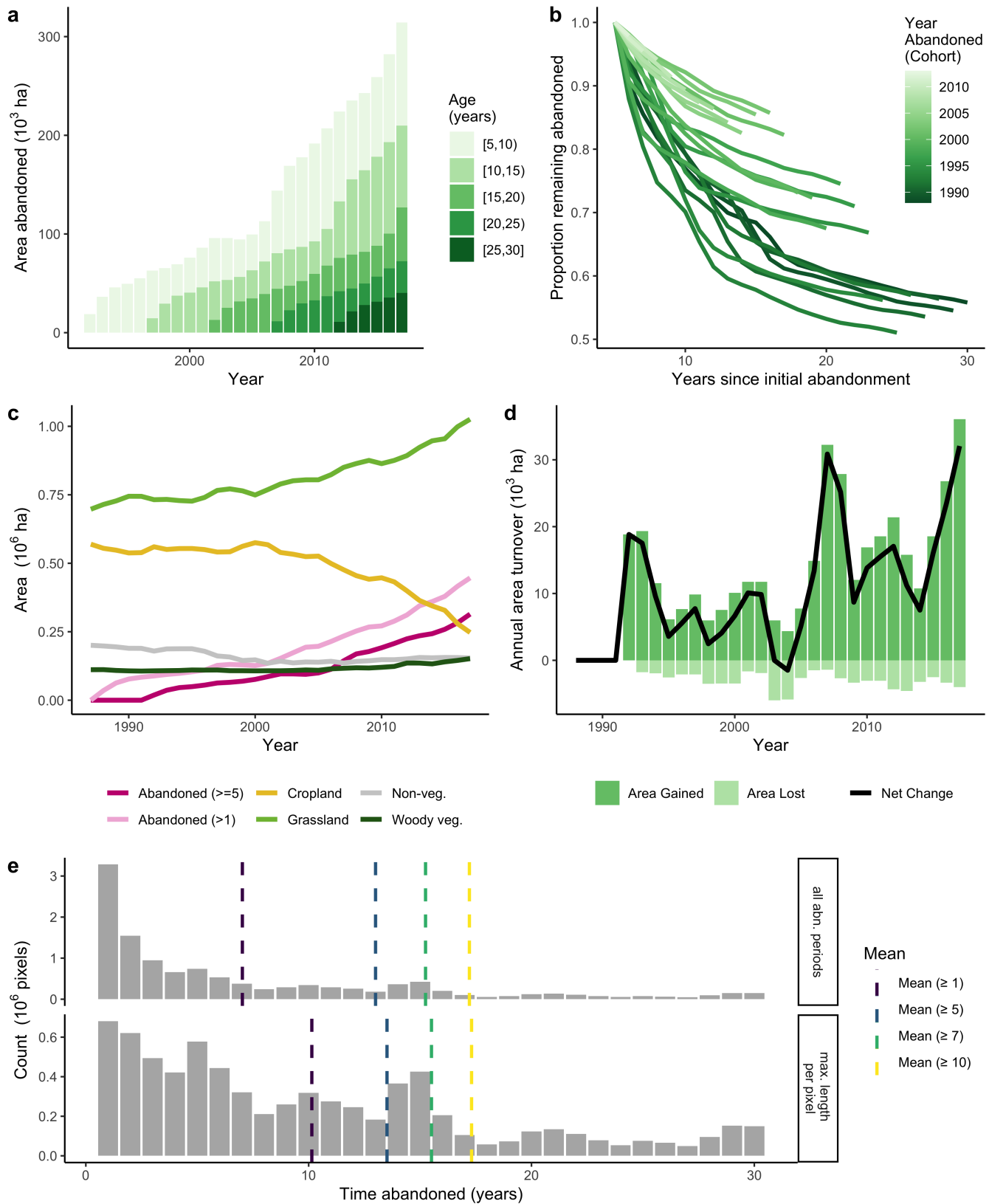


Fig. S35. Abandonment patterns for Shaanxi/Shanxi, China, following Figure S27.

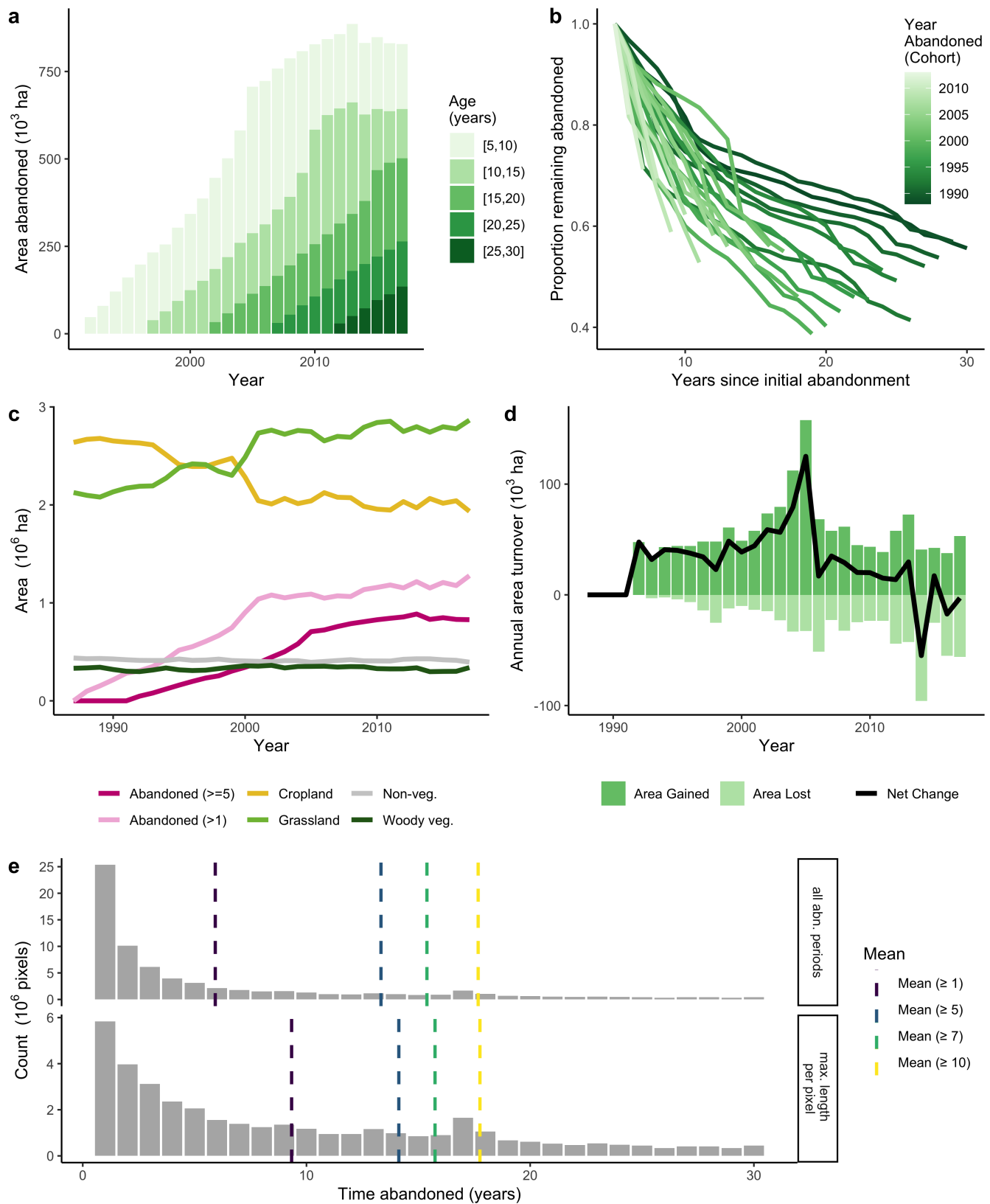


Fig. S36. Abandonment patterns for Volgograd, Russia, following Figure S27.

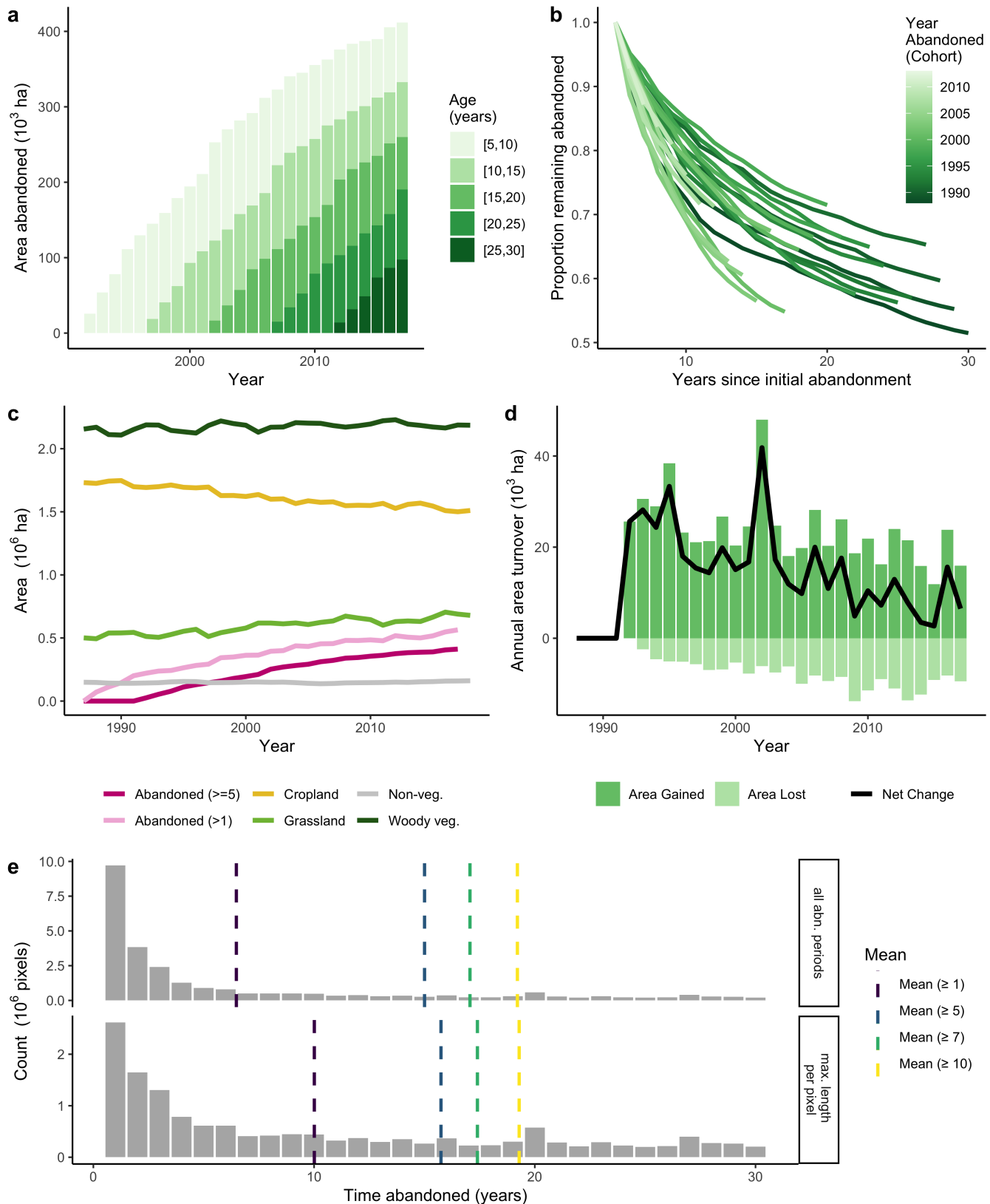


Fig. S37. Abandonment patterns for Wisconsin, USA, following Figure S27.